Electron Ion Collider Detectors

with some history, physics …

Zhenyu Ye (yezhenyu@lbl.gov)
Lawrence Berkeley National Laboratory

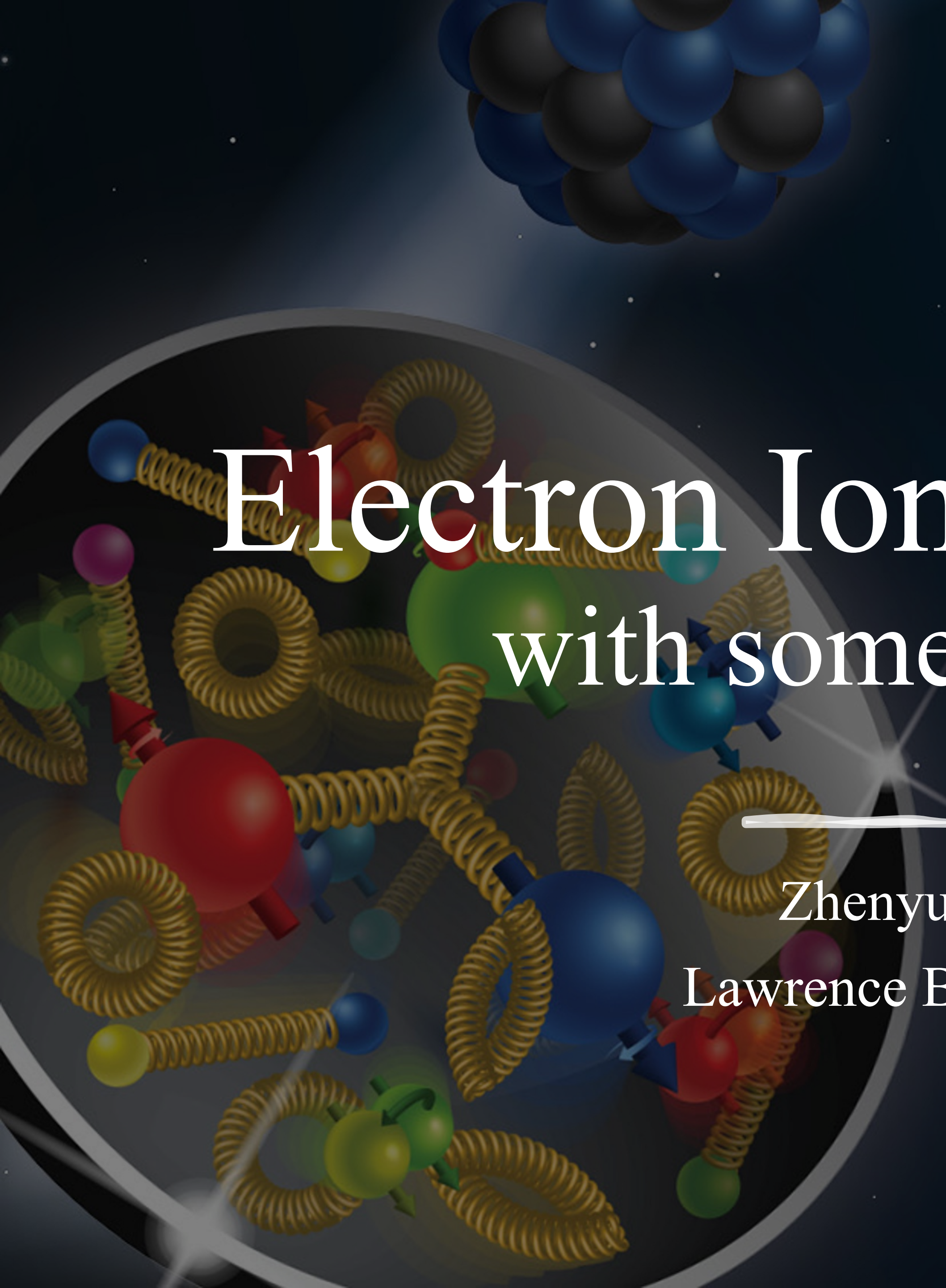

Electron-Ion Collider

BROOKHAVEN NATIONAL LABORATORY

Jefferson Lab

U.S. DEPARTMENT OF ENERGY | Office of Science

Motivation: Properties of Nuclear Matter and Why So?

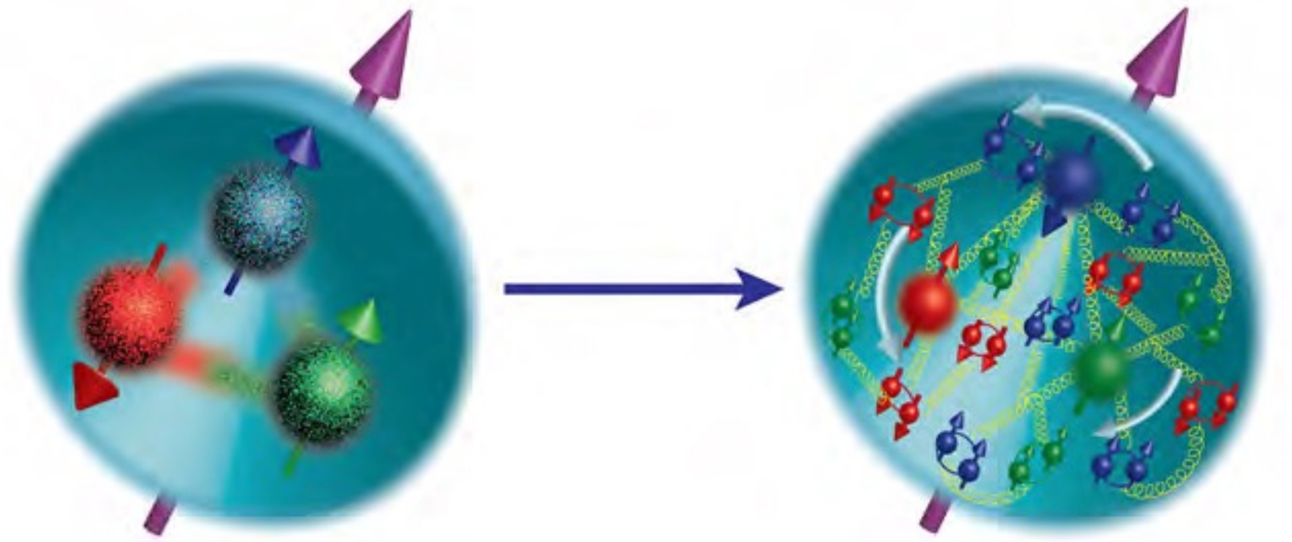

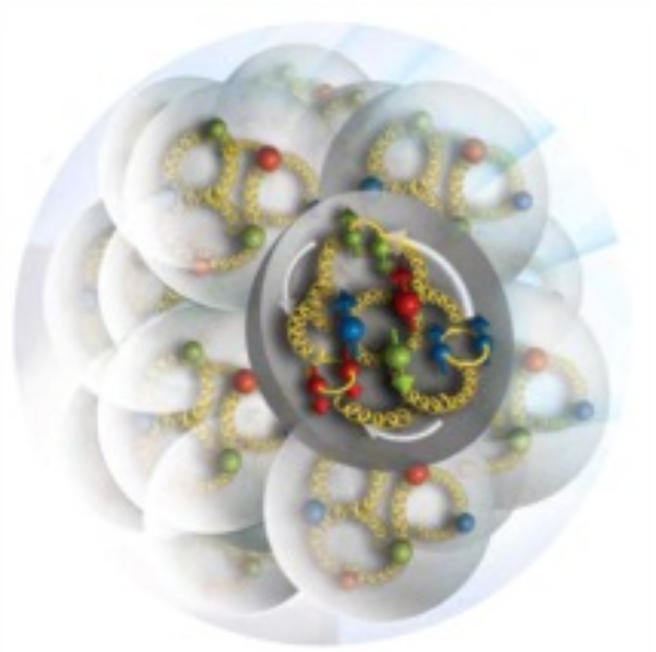

Electron-Nucleus Scatterings

- In e-N scattering, the nature of the interaction of the virtual photon with the nucleon depends strongly on wavelength
  - At very low electron energies, $\lambda \gg r_p$: the scattering is equivalent to that from a "point-like" spin-less object
  - At low electron energies, $\lambda \sim r_p$: the scattering is equivalent to that from an extended charged object
  - At high electron energies, $\lambda < r_p$: the wavelength is sufficiently short to resolve sub-structure. Scattering from constituent quarks
  - At very high electron energies, $\lambda \ll r_p$: the nucleon appears to be a sea of quarks and gluons

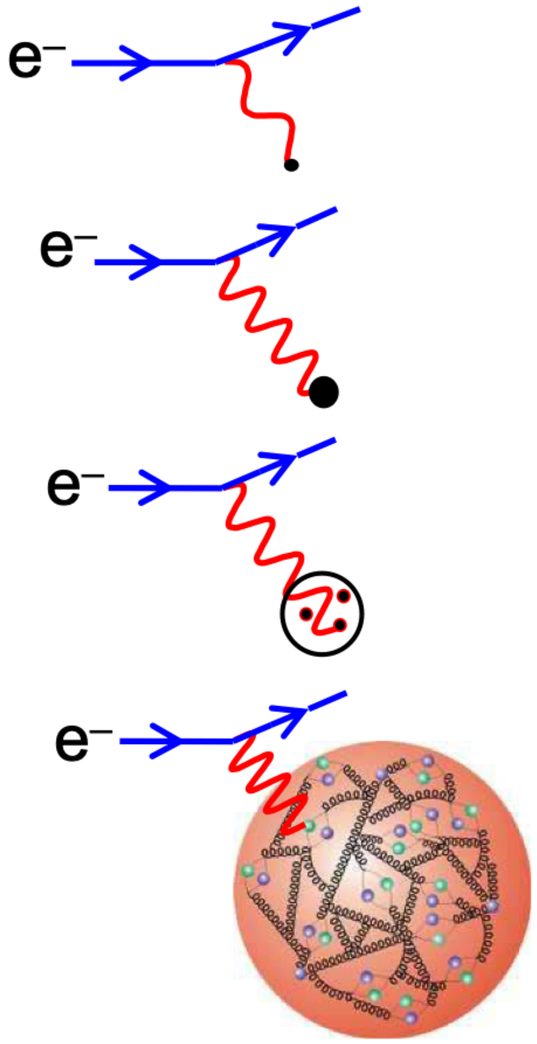

Electron-Nucleus Scatterings: kinematic variables

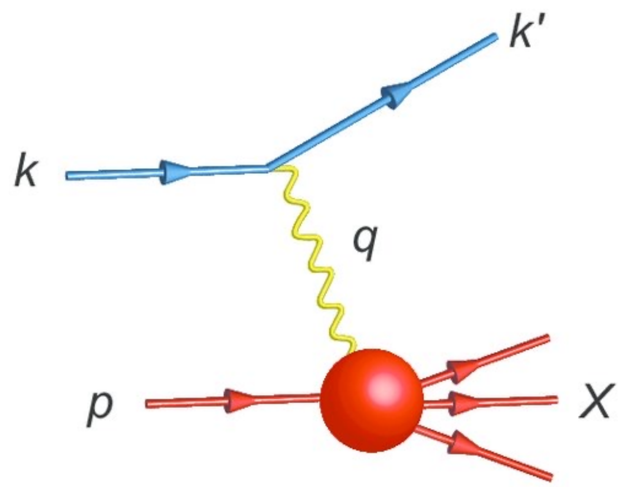

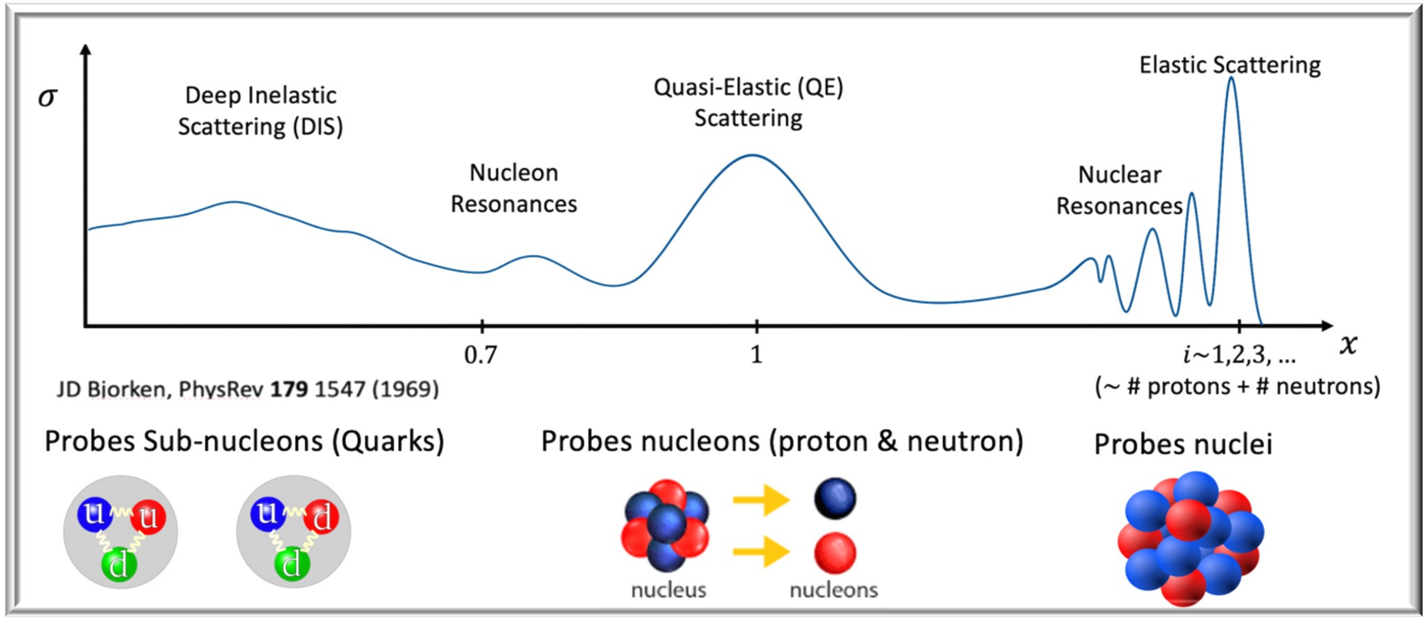

$$Q^2 = -q^2 = -(k-k')^2 \approx 4E_0E'sin^2(\frac{\theta}{2})$$

Four-momentum transfer squared to the target

$$v = \frac{q \cdot p}{M} = E_0 - E'$$

Energy loss by the incident lepton in the target rest frame

$$x = \frac{Q^2}{2q \cdot p} = \frac{Q^2}{2Mv}$$

Bjorken x (at the leading order x is the fraction of the target nucleus momentum carried by the struck object)

$$W^2 = (p+q)^2 = M^2 + 2Mv - Q^2$$

Mass squared of the system X

History of Lepton-Nucleus Scattering Experiments

- Measurements of **nucleon form factors** in **elastic electron-nucleon scatterings** by Hofstadter et al. in the 1960's demonstrated for the 1st time that the nucleon has about 1 fm spatial extension.

Extended proton with spin (Rosenbluth formula):

$$\frac{d\sigma}{d\Omega} = \frac{d\sigma^{\text{Mott}}}{d\Omega}\frac{E'}{E}\left[\frac{G_E^2 + \tau G_M^2}{1+\tau} + 2\tau G_M^2 \tan^2(\theta/2)\right]$$

$\tau = \frac{Q^2}{4M^2}$ G_E and G_M: proton form factors

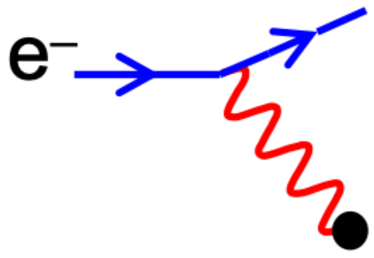

$$\sigma(\theta_e) = \sigma_{Mott} \cdot |F(q)|^2$$

$$\sigma_{Mott} = \left(\frac{\alpha}{2E_0}\right)^2 \frac{\cos^2\left(\frac{\theta}{2}\right)}{\sin^4\left(\frac{\theta}{2}\right)}$$

Mott cross-section for a spin-½ lepton scattering on spin-0 particle

$E_e \sim$ a few 100 MeV

$$|F(q)|^2 = \left|\int_{volume} \rho(\vec{r}) e^{i\vec{q}\cdot\vec{r}} d^3\vec{r}\right|^2$$

Nucleon form factor squared with internal charge density $\rho(r)$

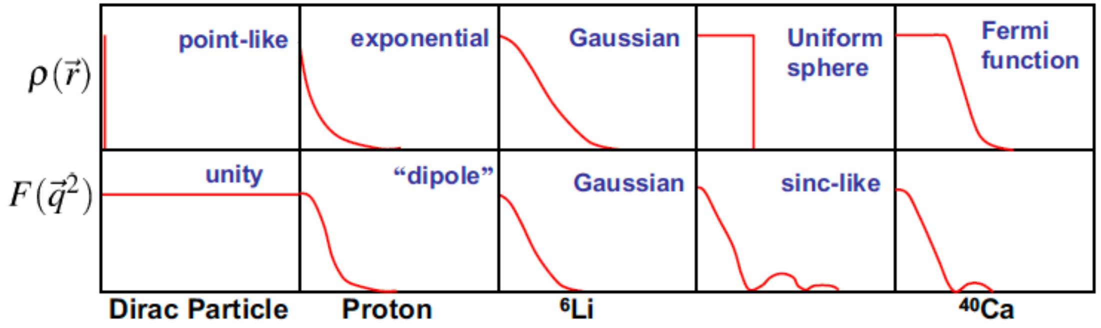

History of Lepton-Nucleus Scattering Experiments

- Measurements of **nucleon form factors** in **elastic electron-nucleon (e-N) scatterings** by Hofstadter et al. in the 1960's demonstrated for the 1st time that the nucleon has about 1 fm spatial extension.

Hofstadter, R., Rev. Mod. Phys. 28, 214 (1956)

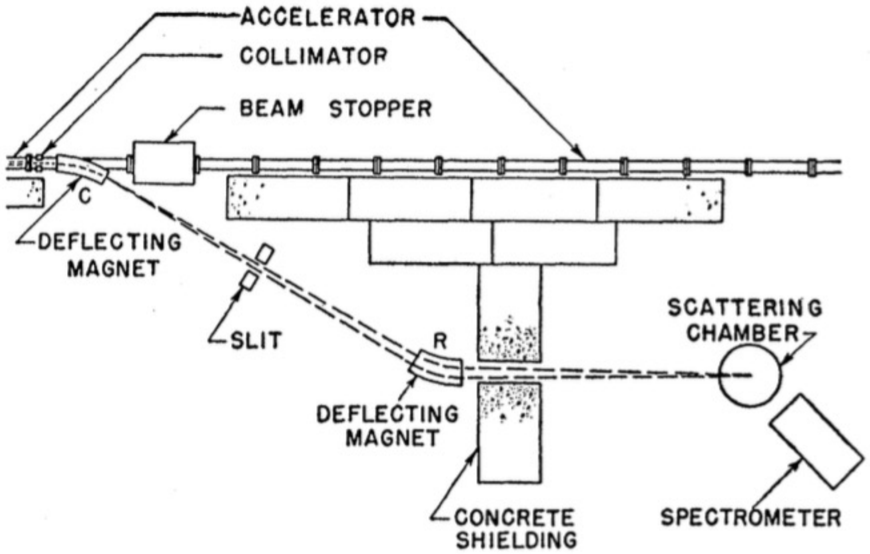

FIG. 14. The general layout of the equipment at the halfway point and the accelerator. Experiments, limited by the spectrometer to 190 Mev, are carried out in this area.

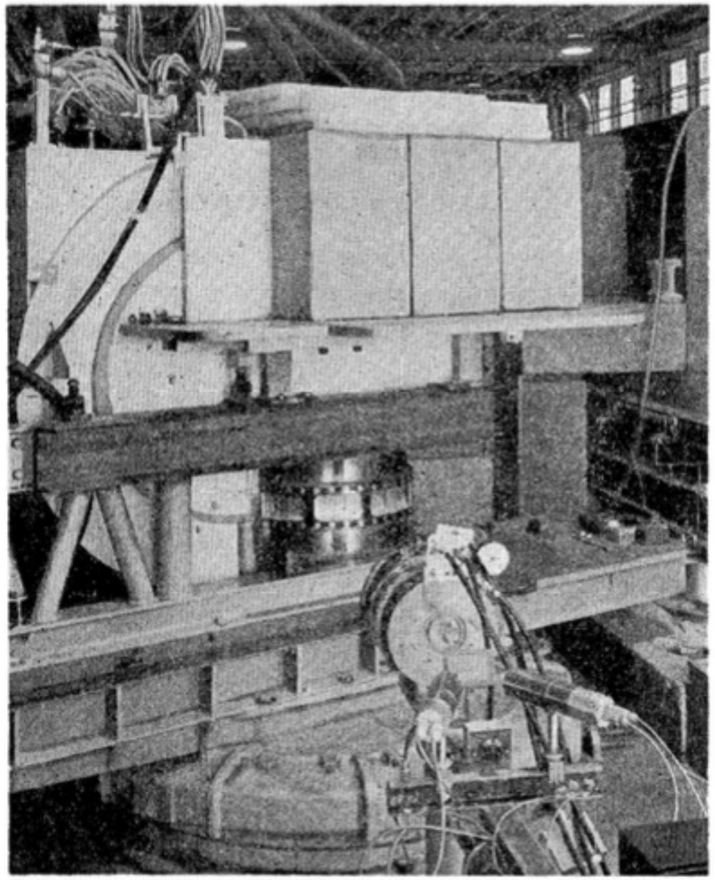

FIG. 15. The semicircular 190-Mev spectrometer, to the left, is shown on the gun mount. The upper platform carries the lead and paraffin shielding that encloses the Čerenkov counter. The brass scattring chamber is shown below with the thin window encircling it. Ion chamber monitors appear in the foreground.

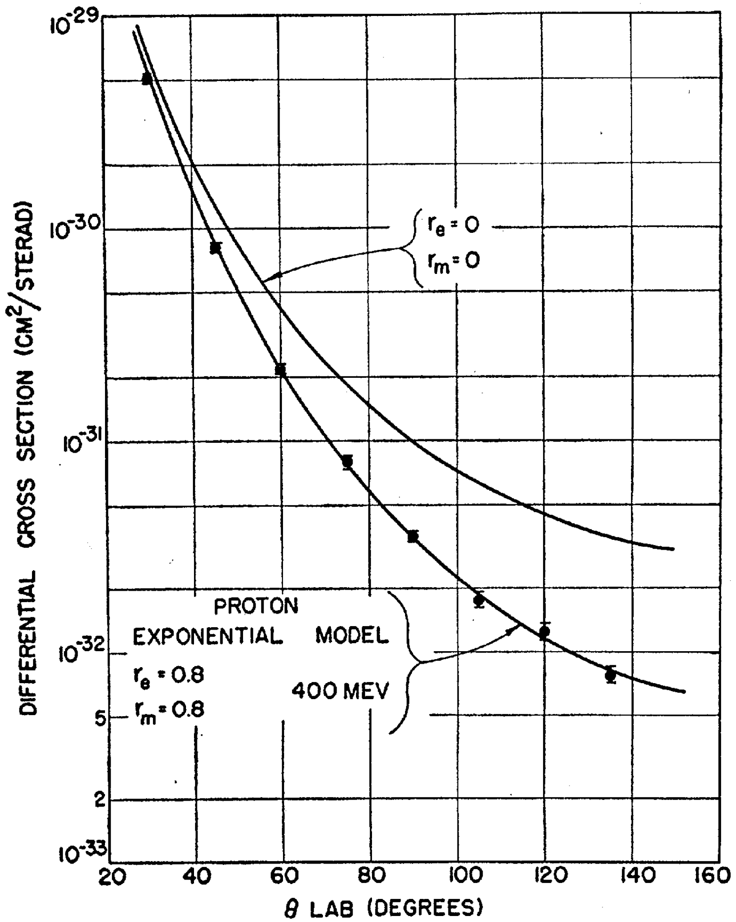

History of Lepton-Nucleus Scattering Experiments

- Measurements of **nucleon structure functions** in **deep inclusive deep inelastic e-N scatterings** that were pioneered by Friedman, Kendall, Taylor et al. in the 1970's suggested the existence of **point-like constituents in the nucleon** and **asymptotic freedom of the strong force**.

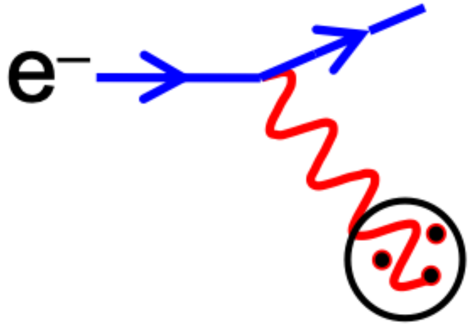

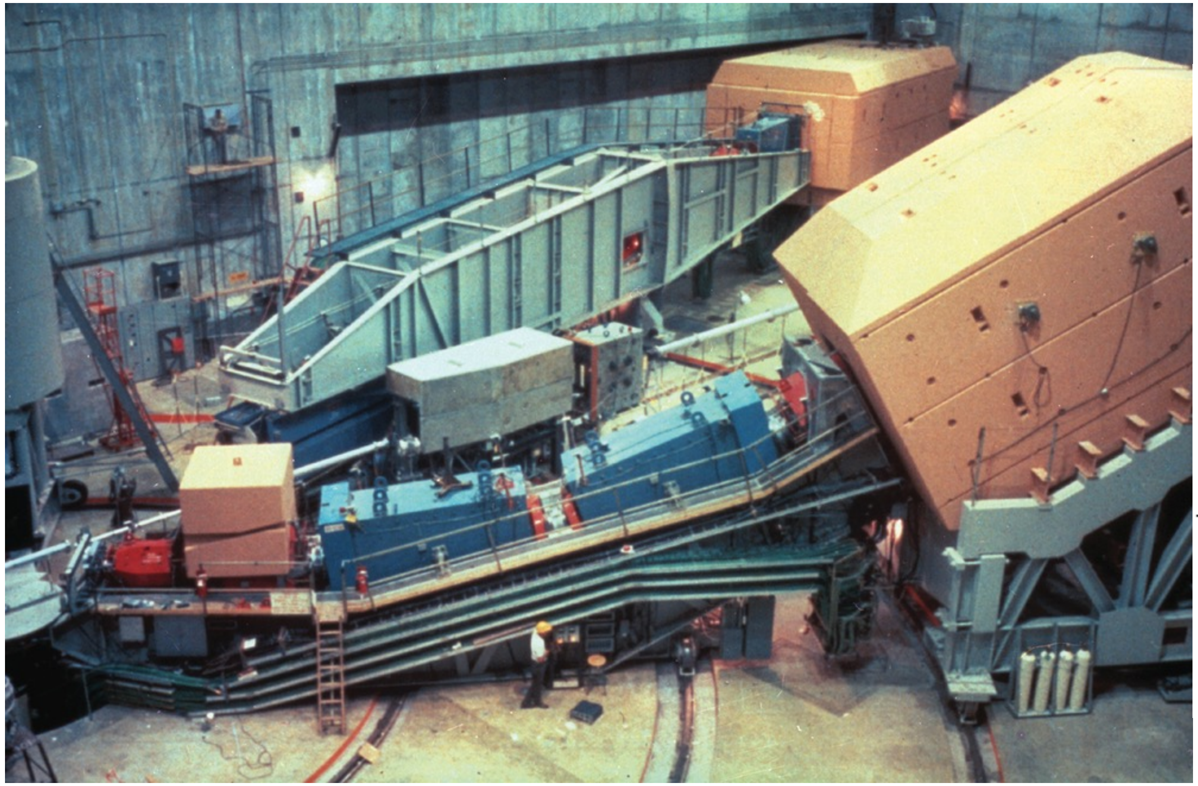

E_e=7-17 GeV

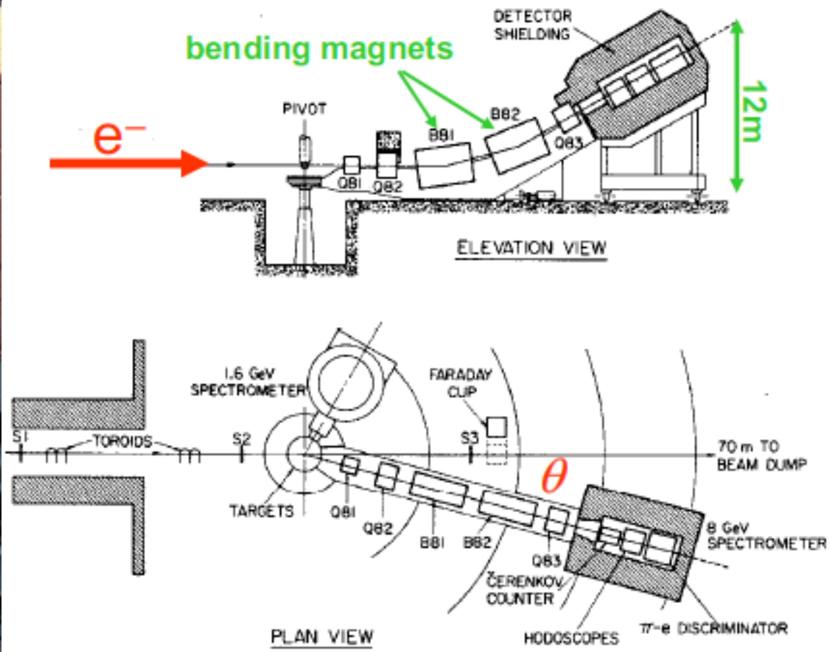

History of Lepton-Nucleus Scattering Experiments

- Measurements of **nucleon structure functions** in **deep inclusive deep inelastic e-N scatterings** that were pioneered by Friedman, Kendall, Taylor et al. in the 1970's suggested the existence of **point-like constituents in the nucleon** and **asymptotic freedom of the strong force**.

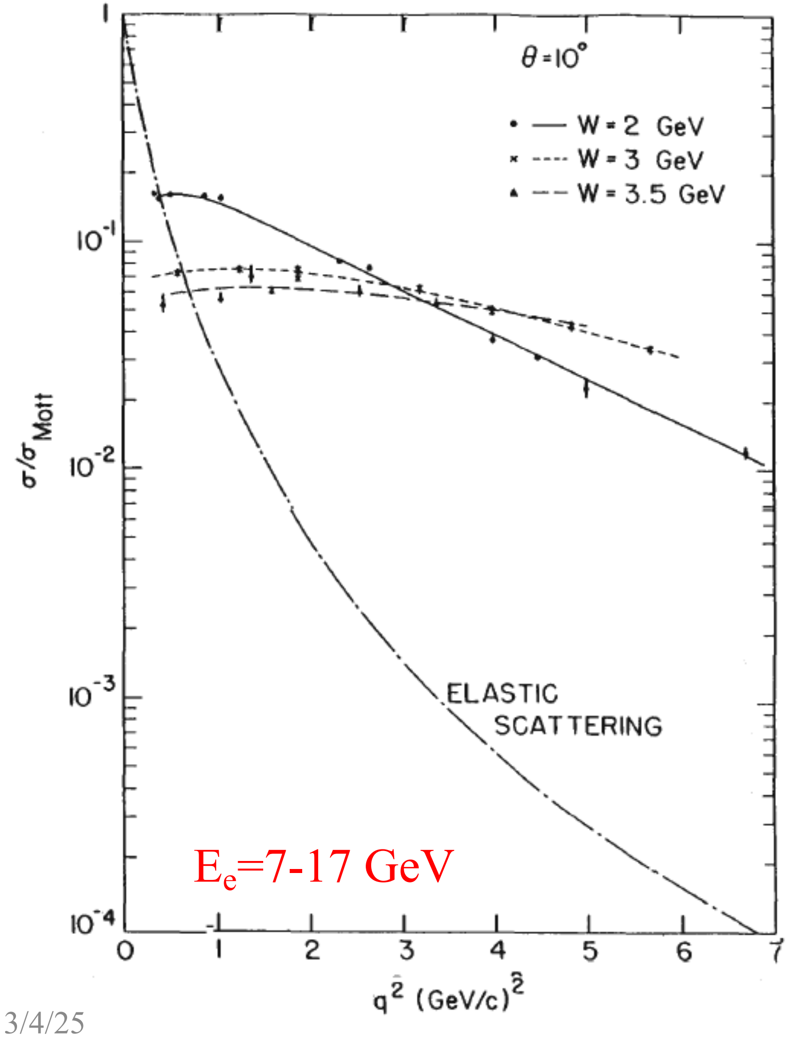

$$\frac{d^2\sigma}{dQ^2dx} = \frac{4\pi\alpha^2}{Q^4}\frac{1}{x}\left[xy^2F_1(x,Q^2) + \left(1 - y - \frac{Mxy}{2E}\right)F_2(x,Q^2)\right]$$

$$F_1(x,Q^2) = \frac{1}{2x}\sum_i e_i^2 x q_i(x,Q^2),$$

$$F_2(x,Q^2) = 2xF_1(x,Q^2) = \sum_i e_i^2 x q_i(x,Q^2)$$

} structure functions

$q_i(x, Q^2)$ is the probability distribution of partons of flavor i, depending on x and weakly on Q^2

History of Lepton-Nucleus Scattering Experiments

- DIS measurements on a collider (large c.m.s.) with the HERA accelerator at DESY (1992-2007)

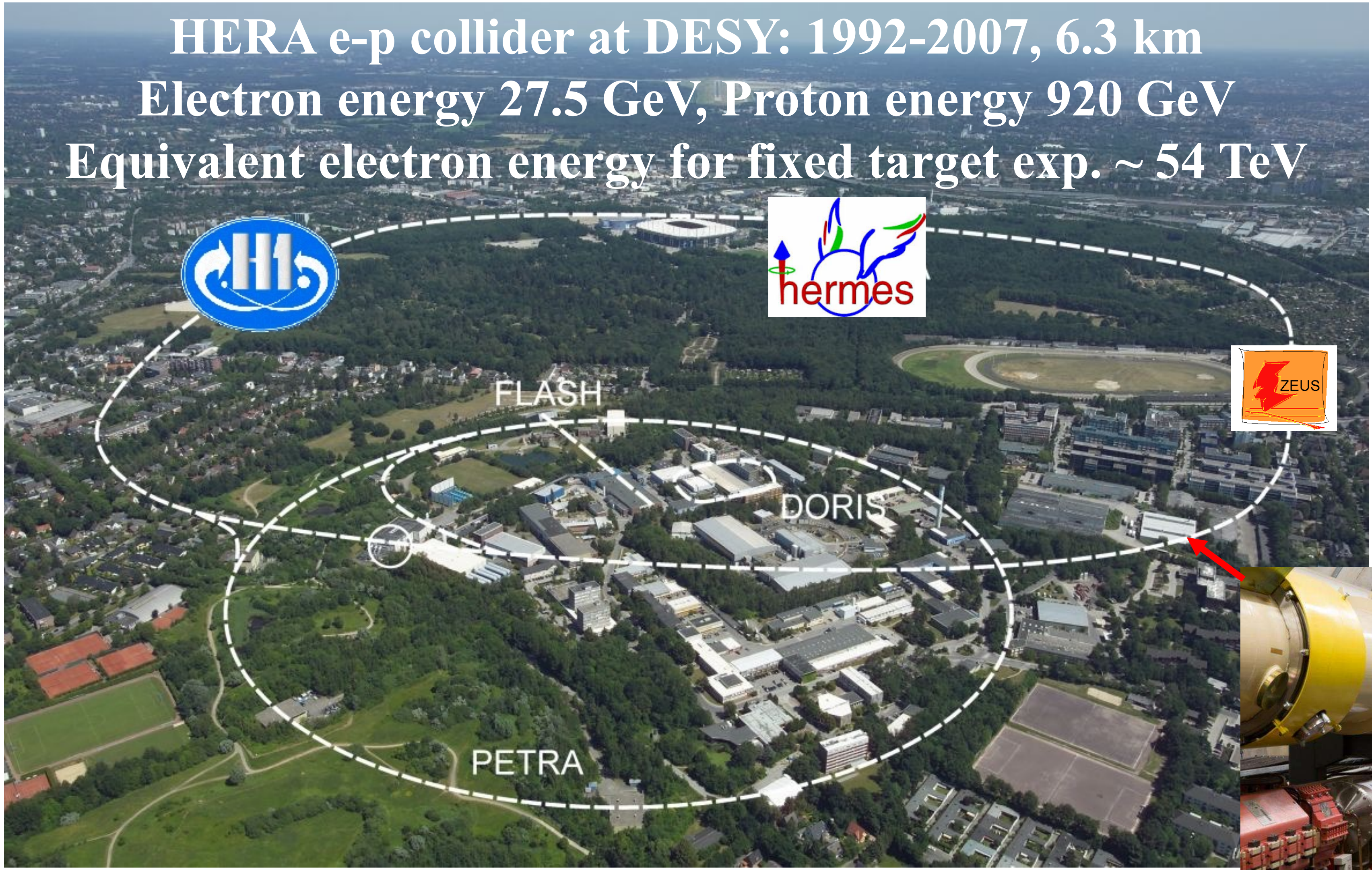

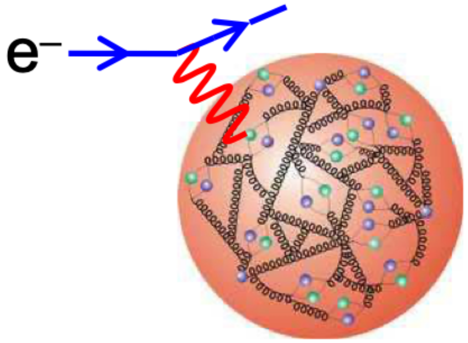

History of Lepton-Nucleus Scattering Experiments

- DIS measurements on a collider (large c.m.s.) with the HERA accelerator at DESY (1992-2007)

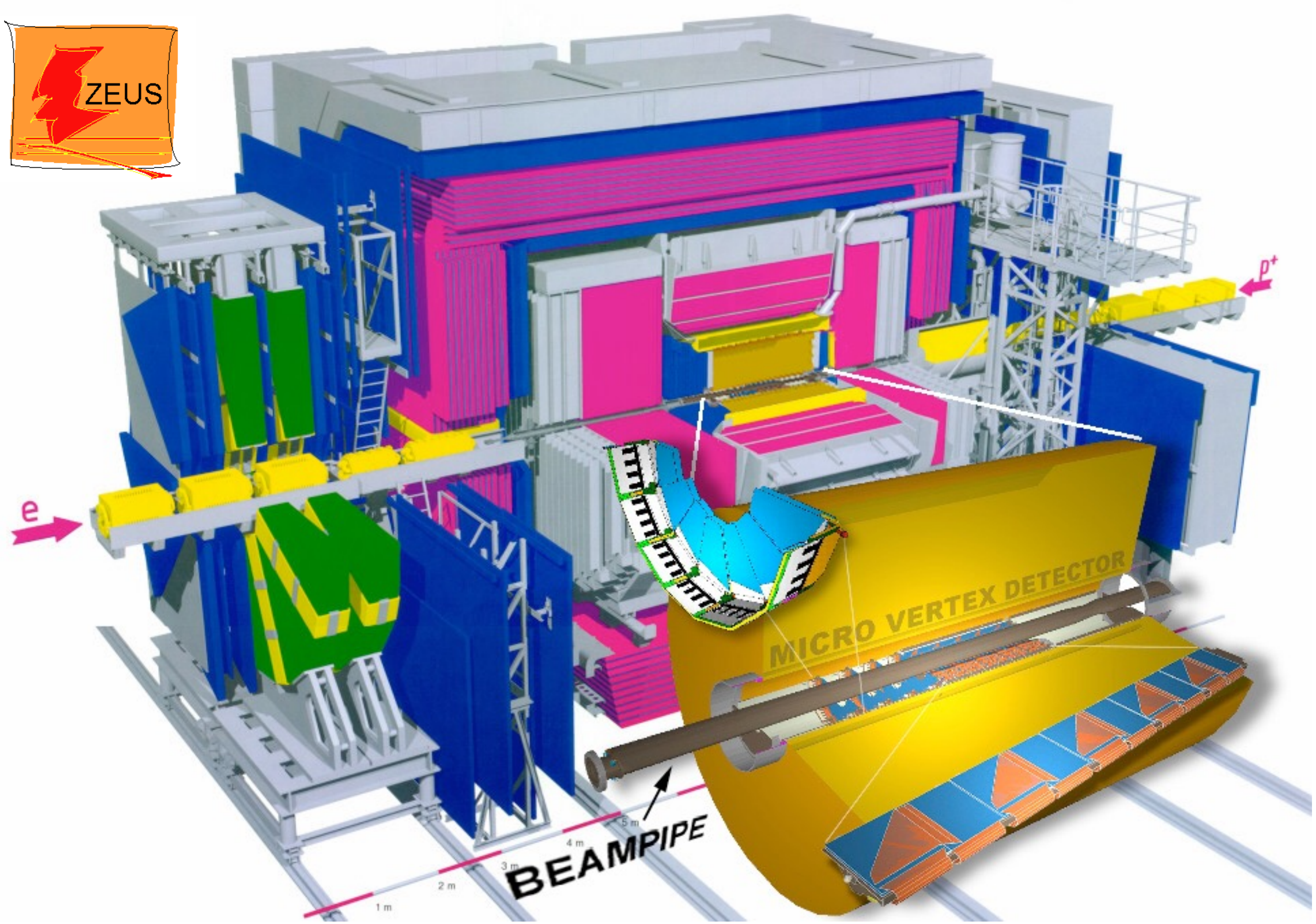

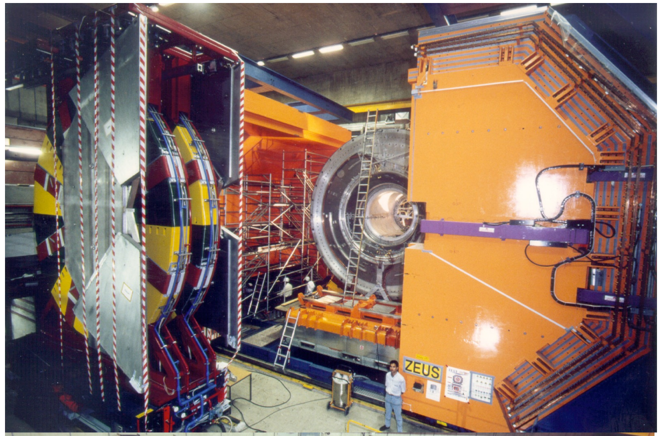

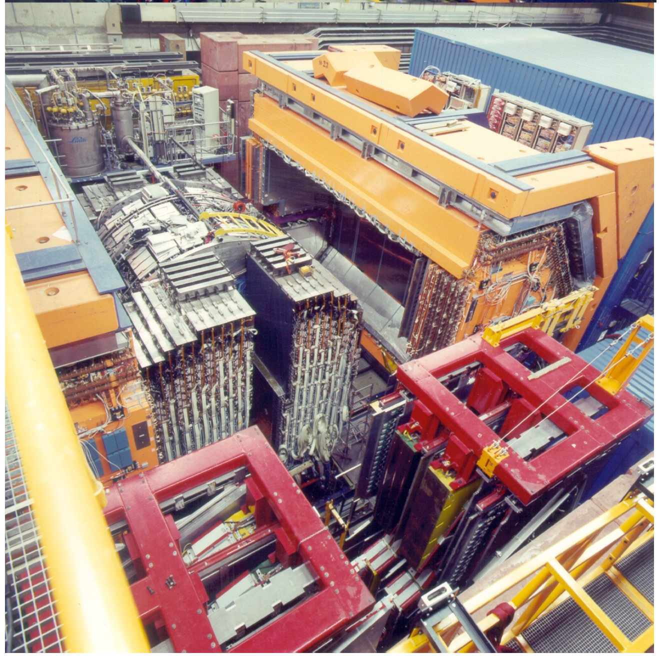

History of Lepton-Nucleus Scattering Experiments

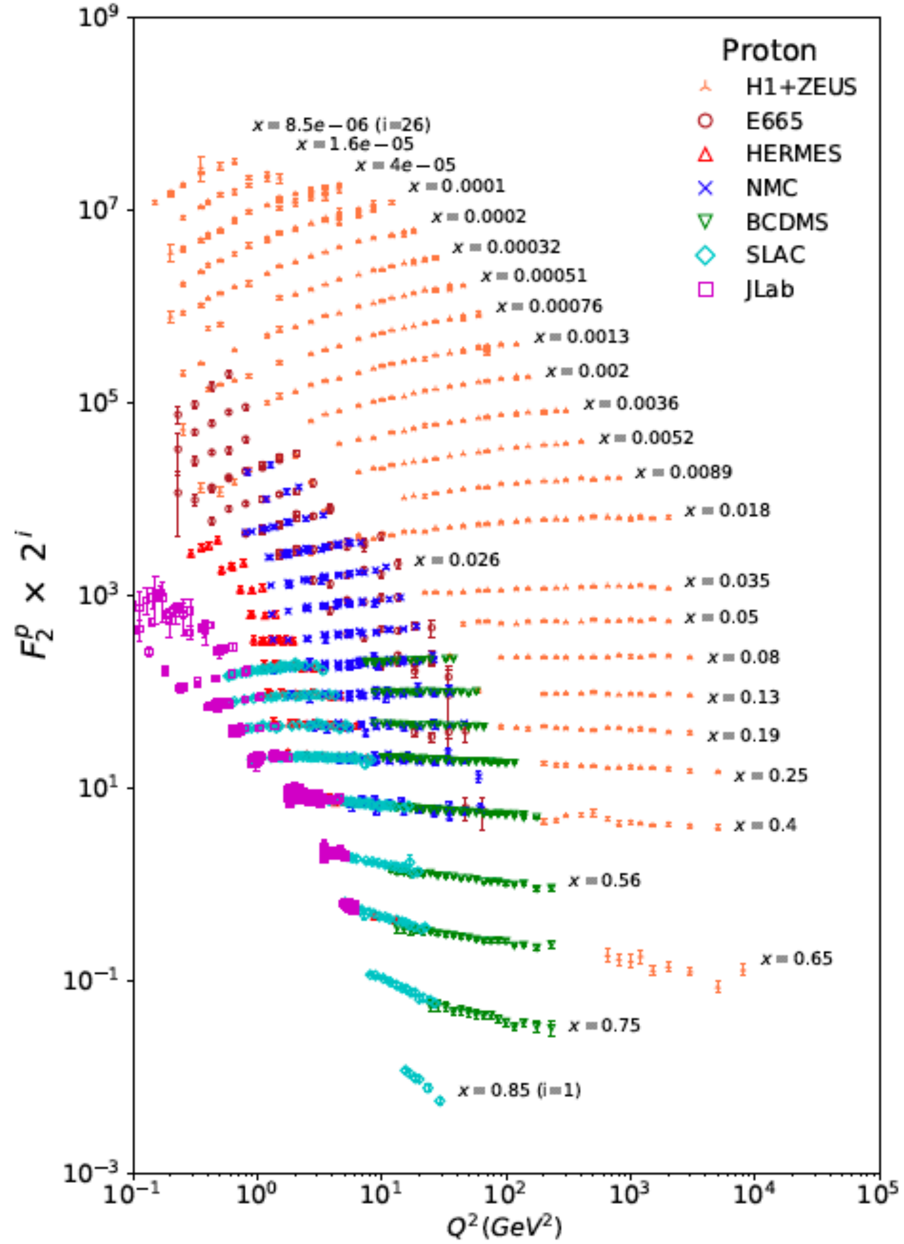

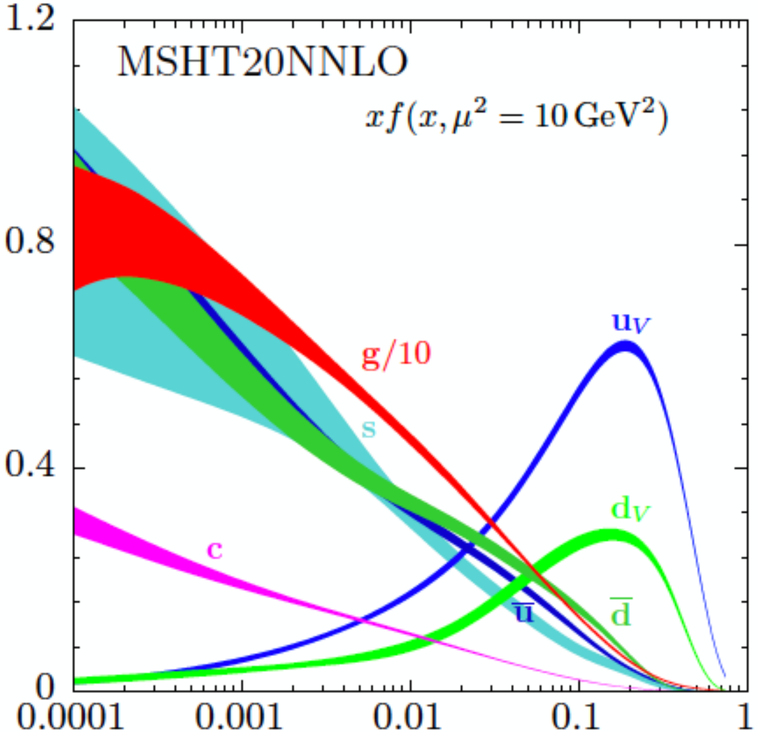

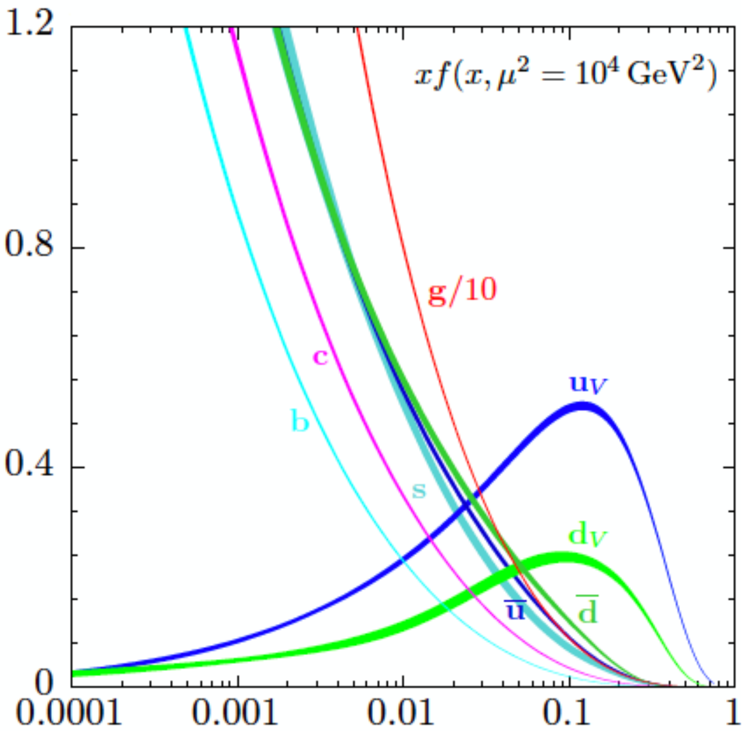

$$F_2(x,Q^2) = 2xF_1(x,Q^2) = \sum_i e_i^2 x q_i(x,Q^2)$$

$q_i(x, Q^2)$ is the probability distribution of partons of flavor *i,* depending on longitudinal momentum fraction x and (weakly) on scaling variable Q^2

History of Lepton-Nucleus Scattering Experiments

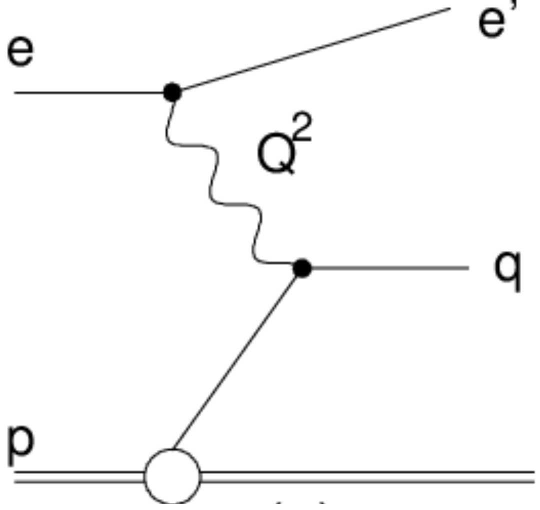

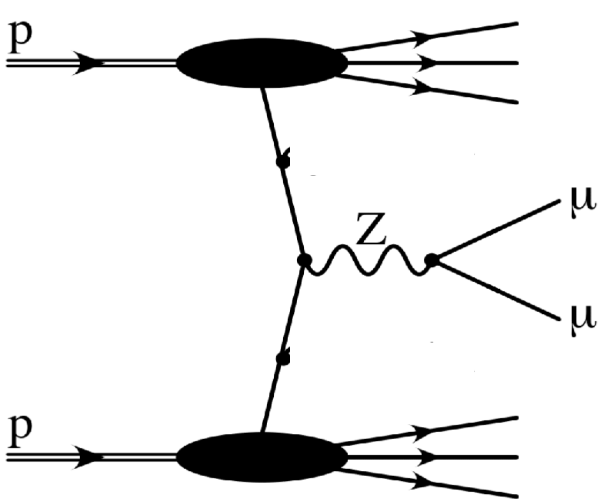

$$\sigma(e + p \to jet + X) = \int_{x=0}^{1} dx\, q(x, Q^2) \otimes \hat{\sigma}_{\gamma^* q \to q}$$

$$\sigma(p + p \to Z + X)$$
$$= \iint_{x_1, x_2} dx_1 dx_2\, q_1(x_1, Q^2) \otimes q_2(x_2, Q^2) \otimes \hat{\sigma}_{q_1 q_2 \to Z}$$

PDFs are universal. Precise knowledge of the PDFs is crucial for precision measurements to search Beyond-Standard Model physics.

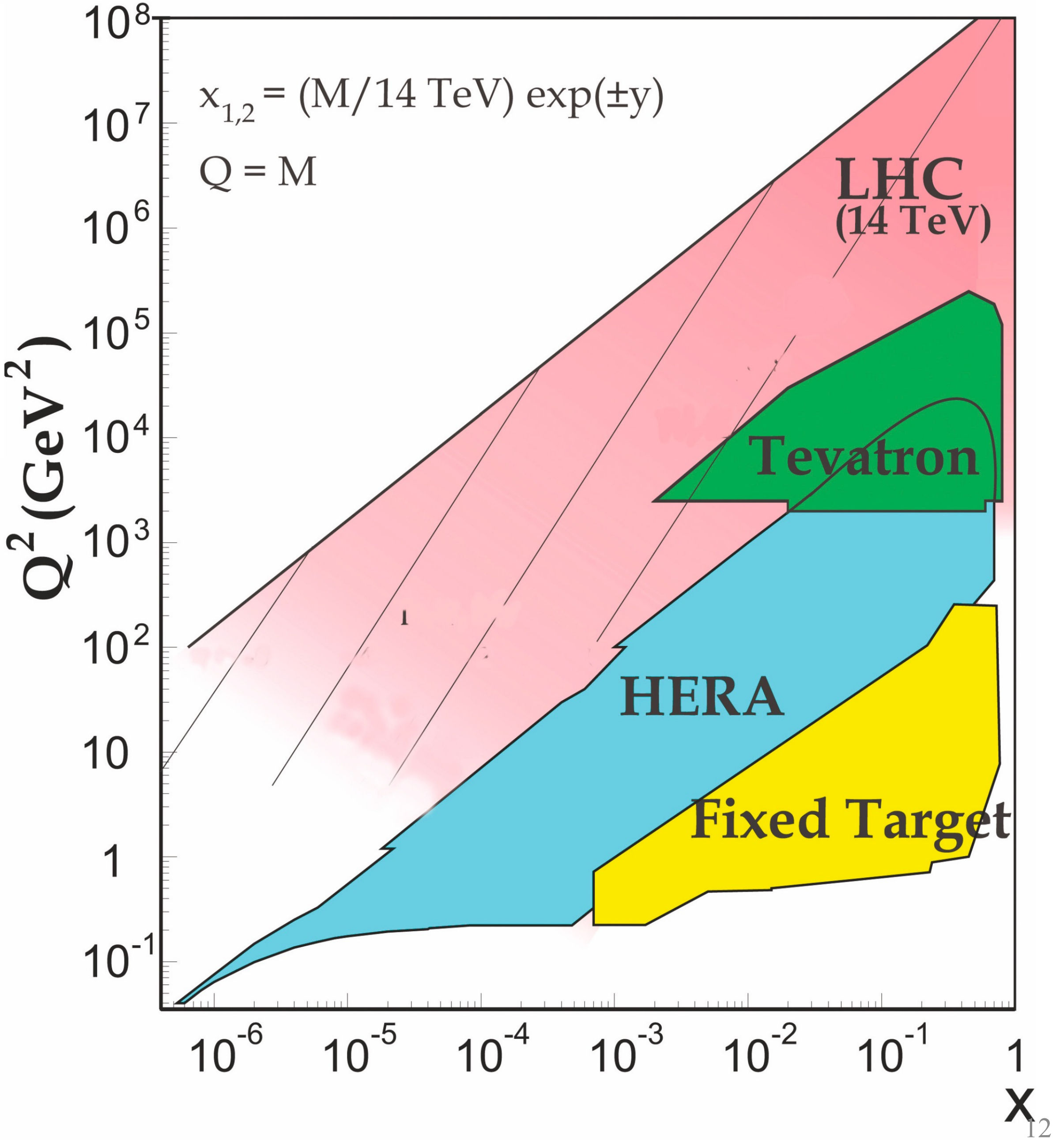

History of Lepton-Nucleus Scattering Experiments

"You think you understand something? Now add spin…" -- R. Jaffe

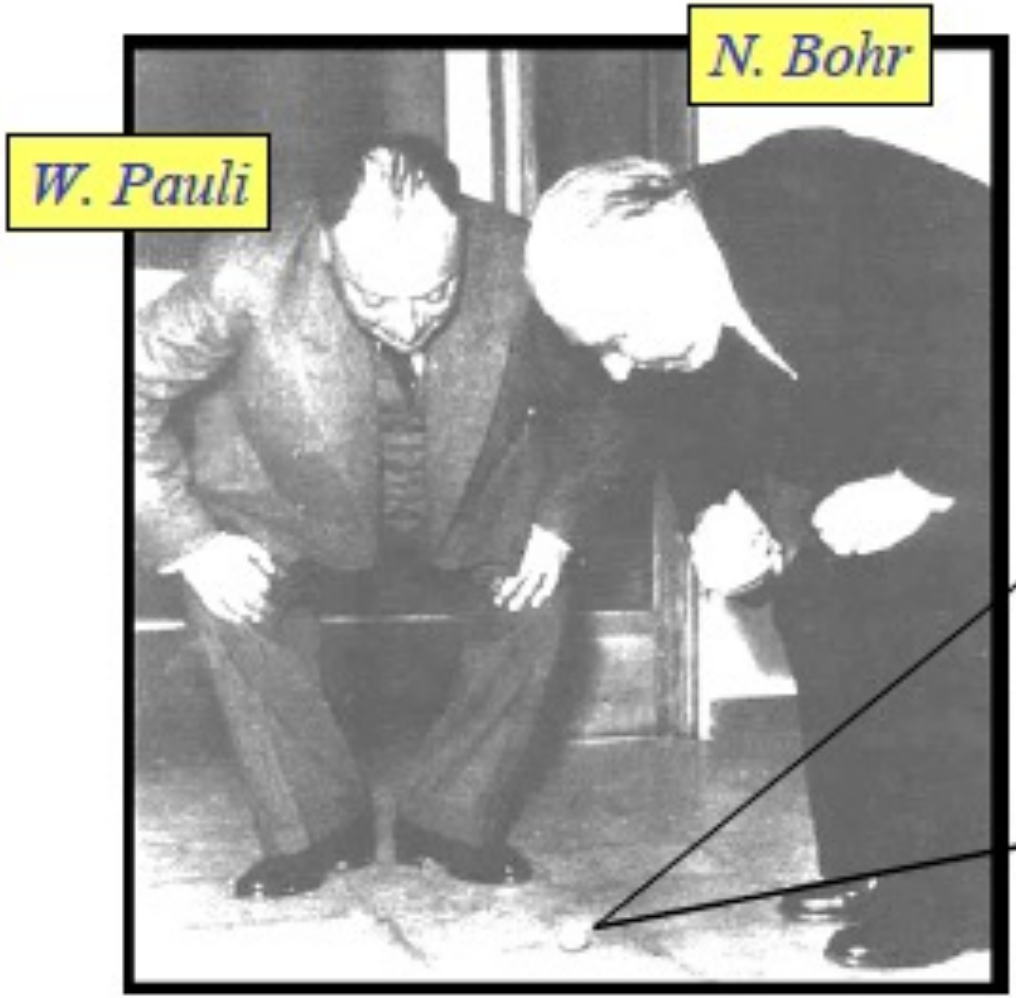

History of Lepton-Nucleus Scattering Experiments

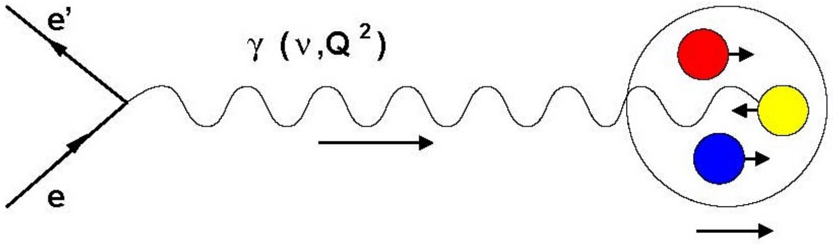

q-

Photon and nucleon spins aligned

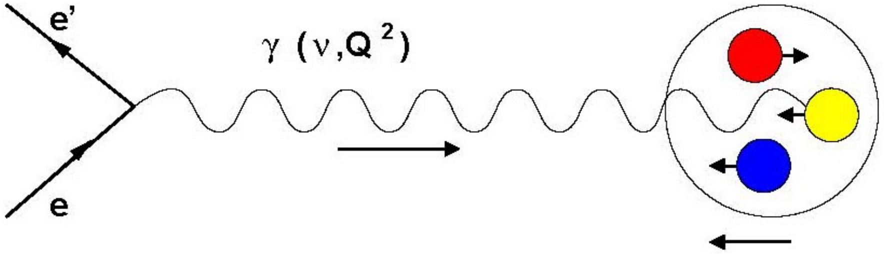

q+

Photon and nucleon spins anti-aligned

- Virtual photon can only couple to quarks of opposite helicity
- Select quark helicity by changing target polarization direction
- Different targets give sensitivity to different quark flavors

$$A_{\parallel} = \frac{\sigma^{\overset{\rightarrow}{\Leftarrow}} - \sigma^{\overset{\rightarrow}{\Rightarrow}}}{\sigma^{\overset{\rightarrow}{\Leftarrow}} + \sigma^{\overset{\rightarrow}{\Rightarrow}}} = \frac{g_1 - \gamma^2 g_2}{F_1}$$

$$g_1(x) = \frac{1}{2}\sum_f e_f^2 \left(q_f^+(x) - q_f^-(x)\right) = \frac{1}{2}\sum_f e_f^2 \Delta q_f(x)$$

$$F_1 = \frac{1}{2}\sum_f e_f^2 \left(q_f^+(x) + q_f^-(x)\right) = \frac{1}{2}\sum_f e_f^2 q_f(x)$$

$q_f^{\pm}(x, Q^2)$ is the probability distribution of partons of flavor *f with spin (anti-)aligned with the nucleon*

History of Lepton-Nucleus Scattering Experiments

- **Polarized inclusive deep inelastic e-N scatterings** in 1987 discovered "**SPIN CRSIS**"

European Muon Collaboration (EMC) Experiment

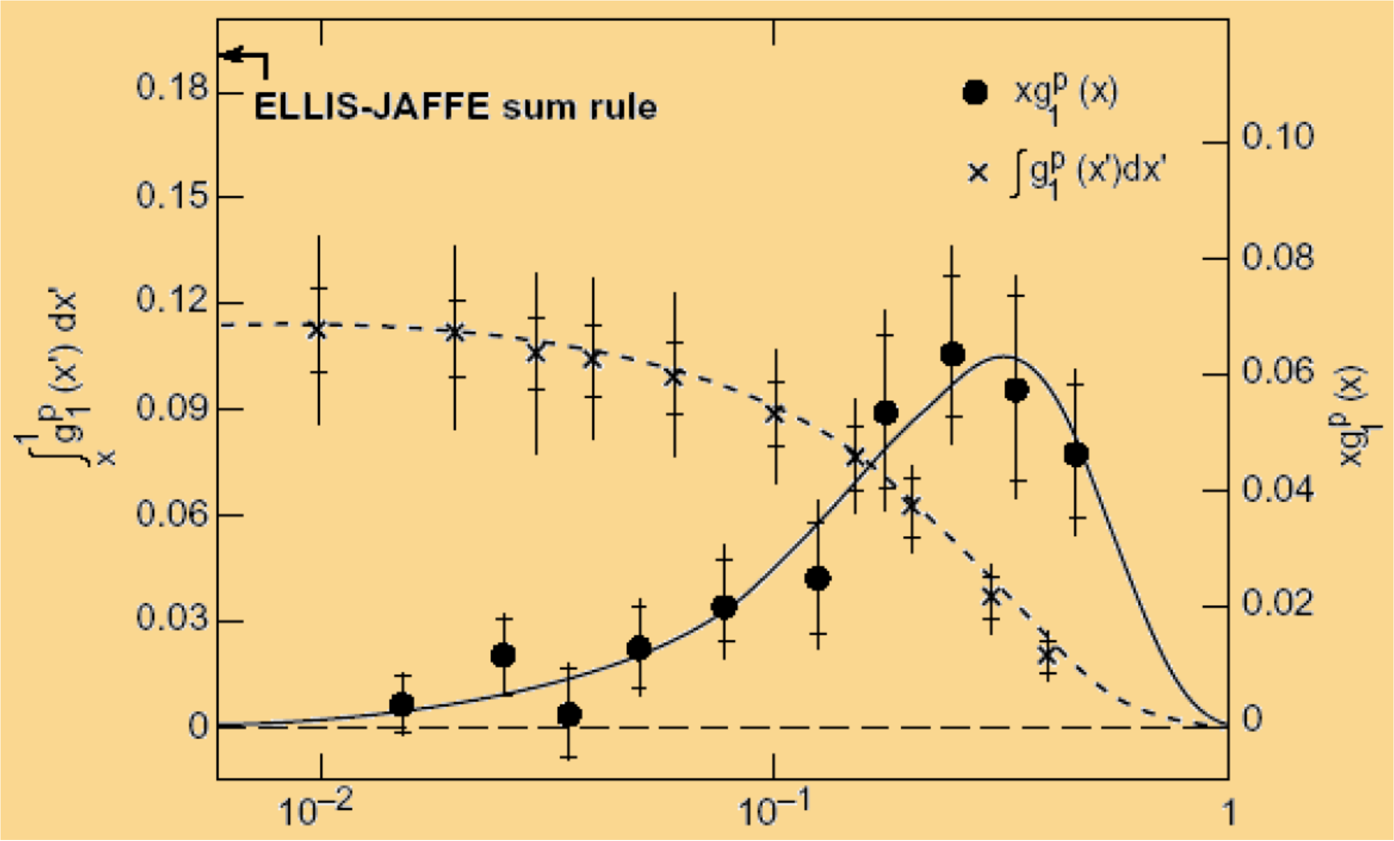

$\Delta\Sigma$ = Quark + Anti-Quark helicity contribution = 0.12 ± 0.17

$\Delta\Sigma$ expected from quark-parton model (Ellis-Jaffe) ~ 0.6

History of Lepton-Nucleus Scattering Experiments

- **Nucleon spin structure** has been studied extensively with **polarized eN/μN** FXT experiments (SLAC 1992-1999, HERMES 1995-2007, COMPASS 2001-2022, CEBAF 1994-present)

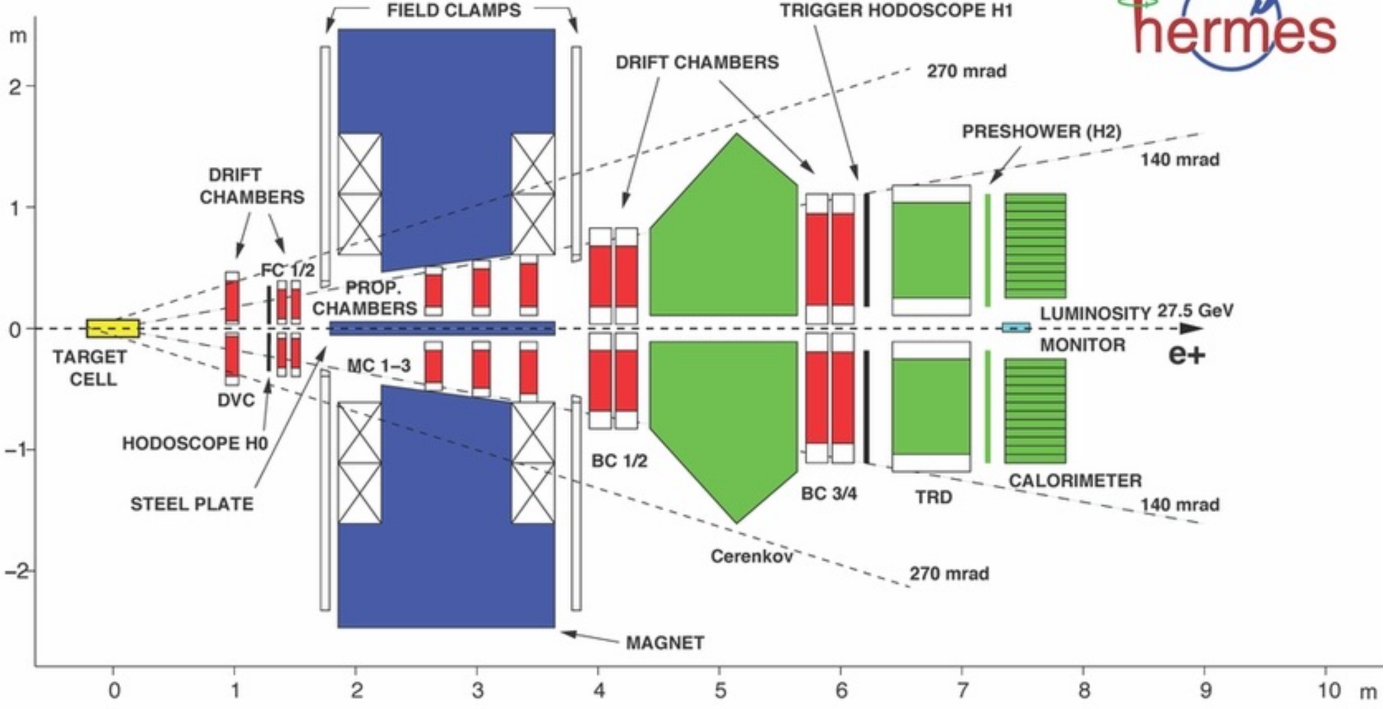

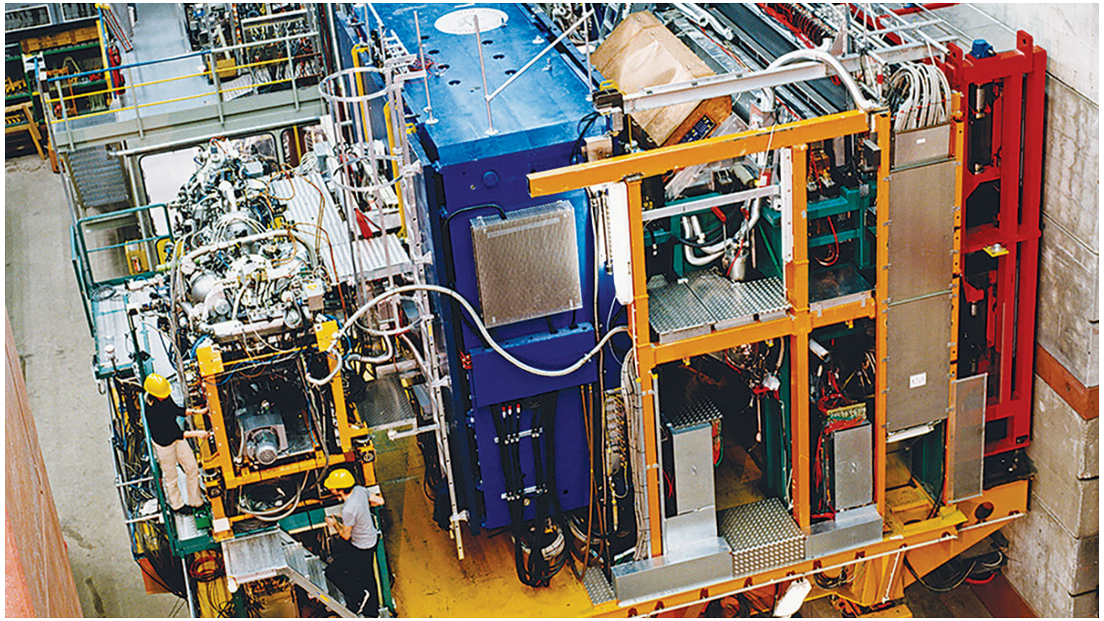

HERMES (polarized FXT exp.) at HERA (1995-2007)

History of Lepton-Nucleus Scattering Experiments

- **Nucleon spin structure** has been studied extensively with **polarized eN/μN** FXT experiments (HERMES 1995-2007, COMPASS 2001-2022, CEBAF 1994-present)

A. Airapetian et al., PRD 75 (2007)

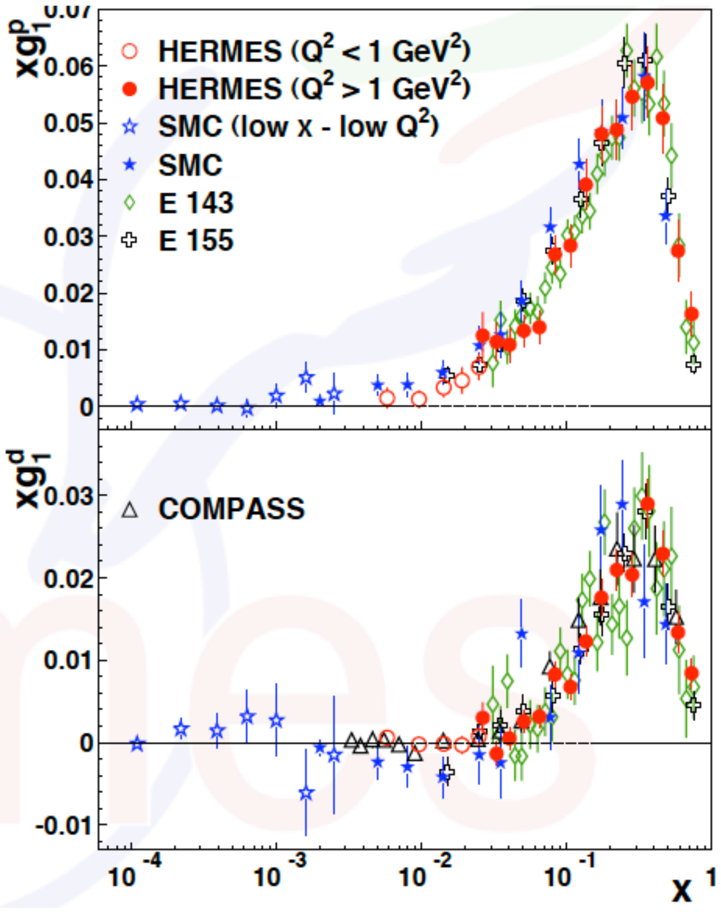

		central value	uncertainties theor.	exp.	evol.
			a_0		
LO	$\mathcal{O}(\alpha_s^0)$	0.278	0.010	0.022	0.025
NLO	$\mathcal{O}(\alpha_s^1)$	0.321	0.011	0.024	0.028
NNLO	$\mathcal{O}(\alpha_s^2)$	0.330	0.011	0.025	0.028
			$\Delta u + \Delta\bar{u}$		
LO	$\mathcal{O}(\alpha_s^0)$	0.825	0.004	0.007	0.008
NLO	$\mathcal{O}(\alpha_s^1)$	0.839	0.004	0.008	0.009
NNLO	$\mathcal{O}(\alpha_s^2)$	0.842	0.004	0.008	0.009
			$\Delta d + \Delta\bar{d}$		
LO	$\mathcal{O}(\alpha_s^0)$	-0.444	0.004	0.007	0.008
NLO	$\mathcal{O}(\alpha_s^1)$	-0.430	0.004	0.008	0.009
NNLO	$\mathcal{O}(\alpha_s^2)$	-0.427	0.004	0.008	0.009
			$\Delta s + \Delta\bar{s}$		
LO	$\mathcal{O}(\alpha_s^0)$	-0.103	0.013	0.007	0.008
NLO	$\mathcal{O}(\alpha_s^1)$	-0.088	0.013	0.008	0.009
NNLO	$\mathcal{O}(\alpha_s^2)$	-0.085	0.013	0.008	0.009

$\Sigma\Delta q \sim 0.3$ => Where is the rest of the nucleon spin?

Nucleon Spin Puzzle

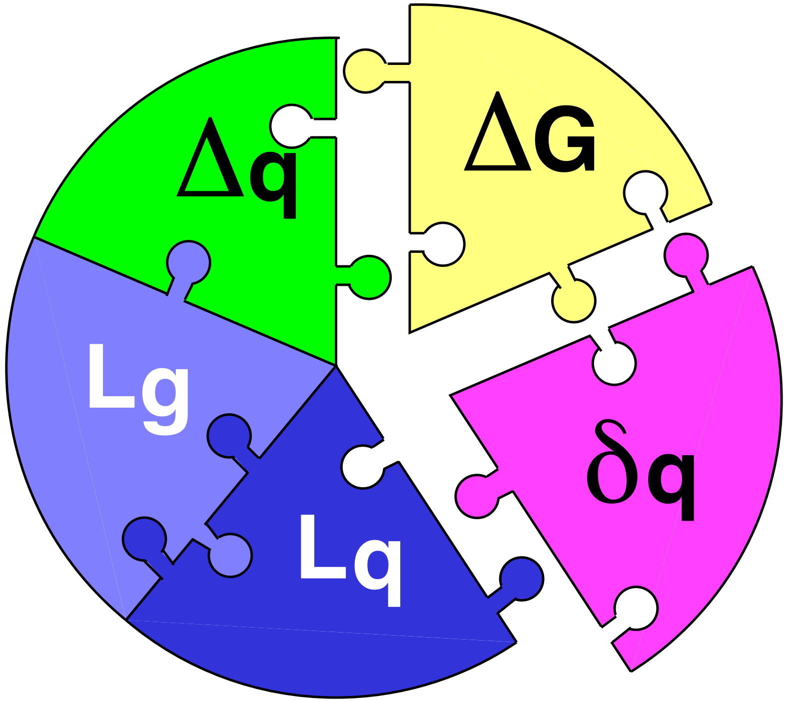

$$\frac{1}{2} = \frac{1}{2}\Delta\Sigma + L_q + \Delta G + L_g$$

Nucleon Spin Puzzle – Gluon Polarization

Gluon polarization accessible in

- polarized inclusive DIS through higher order interaction (gluon splitting)
- polarized pp collisions through e.g. charged hadron and jet production

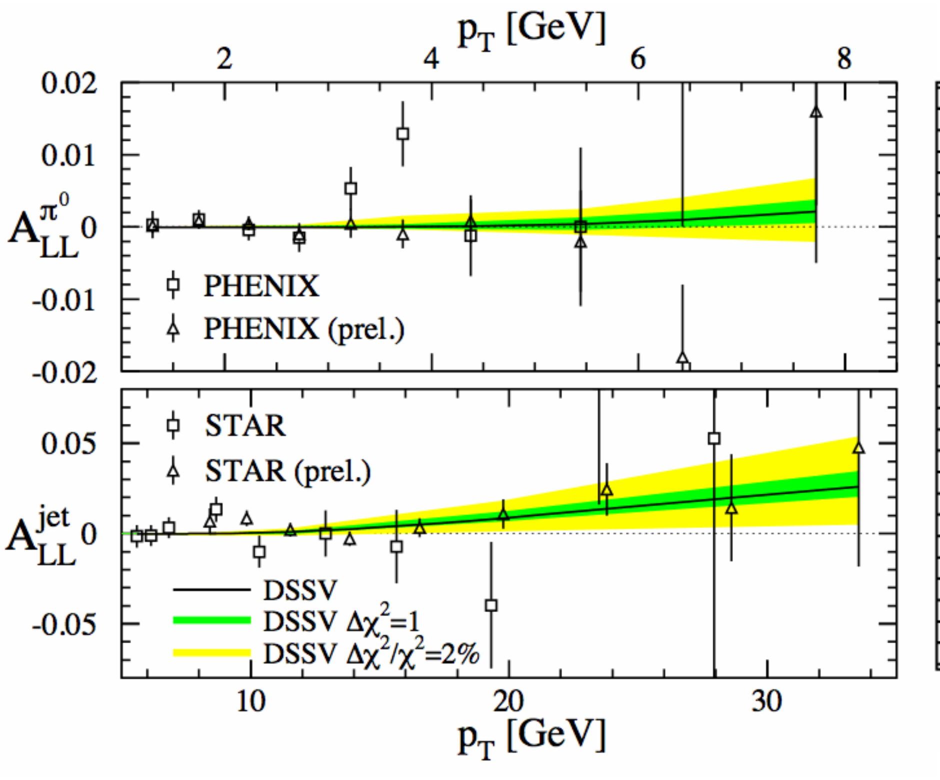

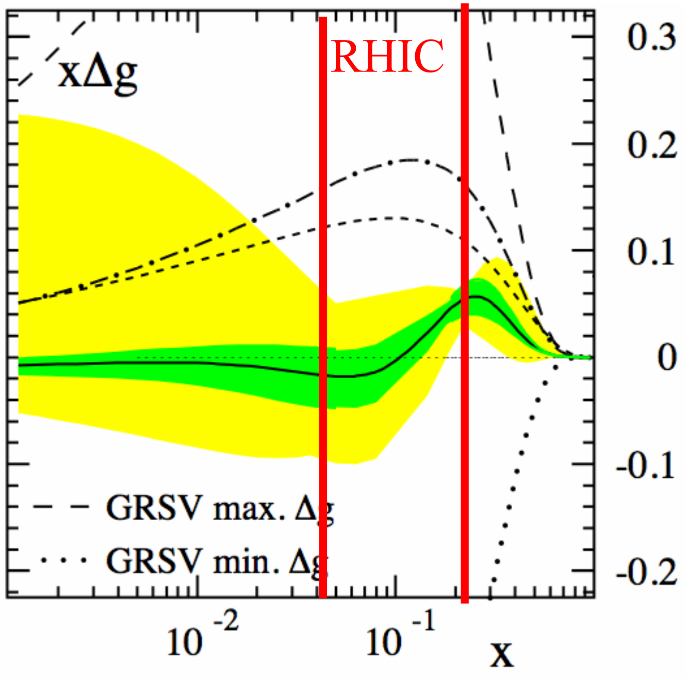

DSSV, PRL 113 (2014)

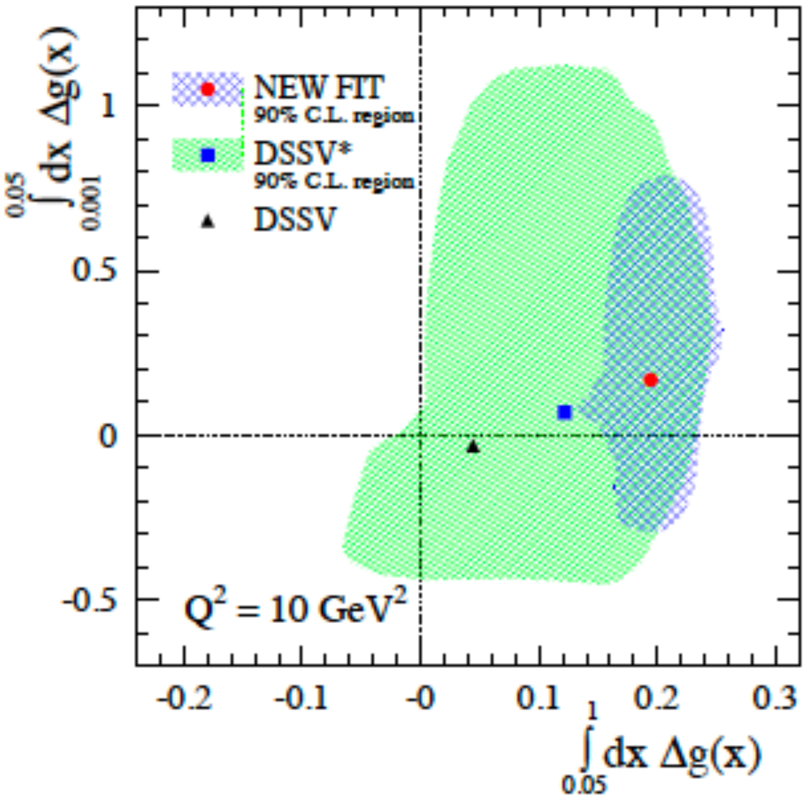

Nucleon Spin Puzzle – Orbital Angular Momenta

Ji's sum rule (1997)

$$J_{g,q} = \frac{1}{2}\lim_{t\to 0}\int dx \cdot x\left[H_{q,g}(x,\xi,t,\mu^2) + E_{q,g}(x,\xi,t,\mu^2)\right]$$

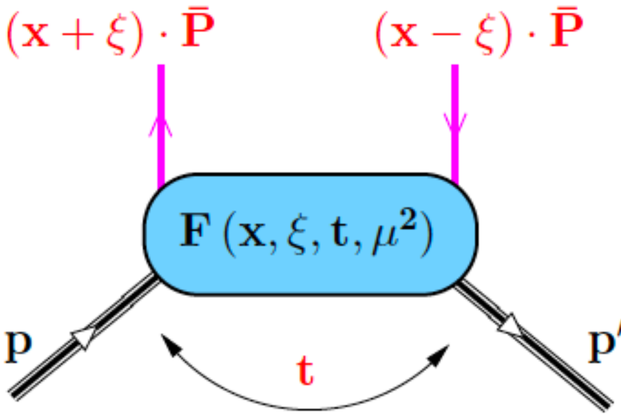

$$F^q = \int dz^- e^{ix\bar{P}^+z^-}\langle p'|\bar{\psi}_q(-z/2)\gamma^+\psi_q(z/2)|p\rangle\Big|_{z^+=\vec{z}_T=0}$$
$$= \frac{1}{\bar{P}^+}\bar{u}(p')\left[H^q(x,\xi,t,\mu^2)\gamma^+ + E^q(x,\xi,t,\mu^2)\frac{i\sigma^{+\alpha}\Delta_\alpha}{2m_N}\right]u(p),$$

$$\widetilde{F}^q = \int dz^- e^{ix\bar{P}^+z^-}\langle p'|\bar{\psi}_q(-z/2)\gamma^+\gamma_5\psi_q(z/2)|p\rangle\Big|_{z^+=\vec{z}_T=0}$$
$$= \frac{1}{\bar{P}^+}\bar{u}(p')\left[\widetilde{H}^q(x,\xi,t,\mu^2)\gamma^+\gamma_5 + \widetilde{E}^q(x,\xi,t,\mu^2)\frac{\gamma_5\Delta^+}{2m_N}\right]u(p)$$

- GPDs are related to known quantities (FFs, PDFs).

FFs	$\int_{-1}^{1} dx\, H_q(x,\xi,t,\mu^2) = F_1^q(t)$ $\int_{-1}^{1} dx\, \widetilde{H}_q(x,\xi,t,\mu^2) = g_V^q(t)$	$\int_{-1}^{1} dx\, E_q(x,\xi,t,\mu^2) = F_2^q(t)$ $\int_{-1}^{1} dx\, \widetilde{E}_q(x,\xi,t,\mu^2) = g_A^q(t)$
PDFs	$H_q(x,0,0,\mu^2) = q(x,\mu^2)$ $\widetilde{H}_q(x,0,0,\mu^2) = \Delta q(x,\mu^2)$	E_q and $\widetilde{E}_q$ decouple in the forward limit

- Constrained by symmetries:

  time-reversal F(x; ξ) = F(x; -ξ)

- GPDs enter in hard exclusive reactions, e.g., DVCS

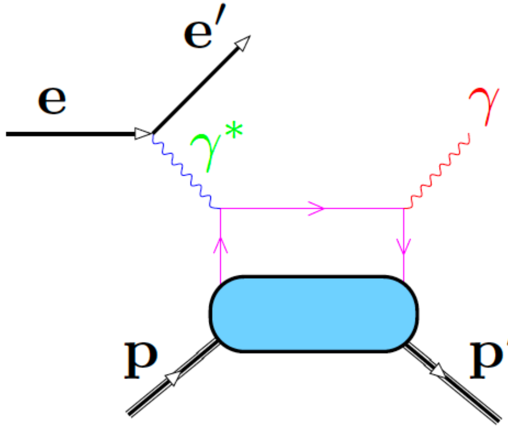

Nucleon Spin Puzzle – Orbital Angular Momenta

A. Airapetian et al., JHEP 0806 (2008)

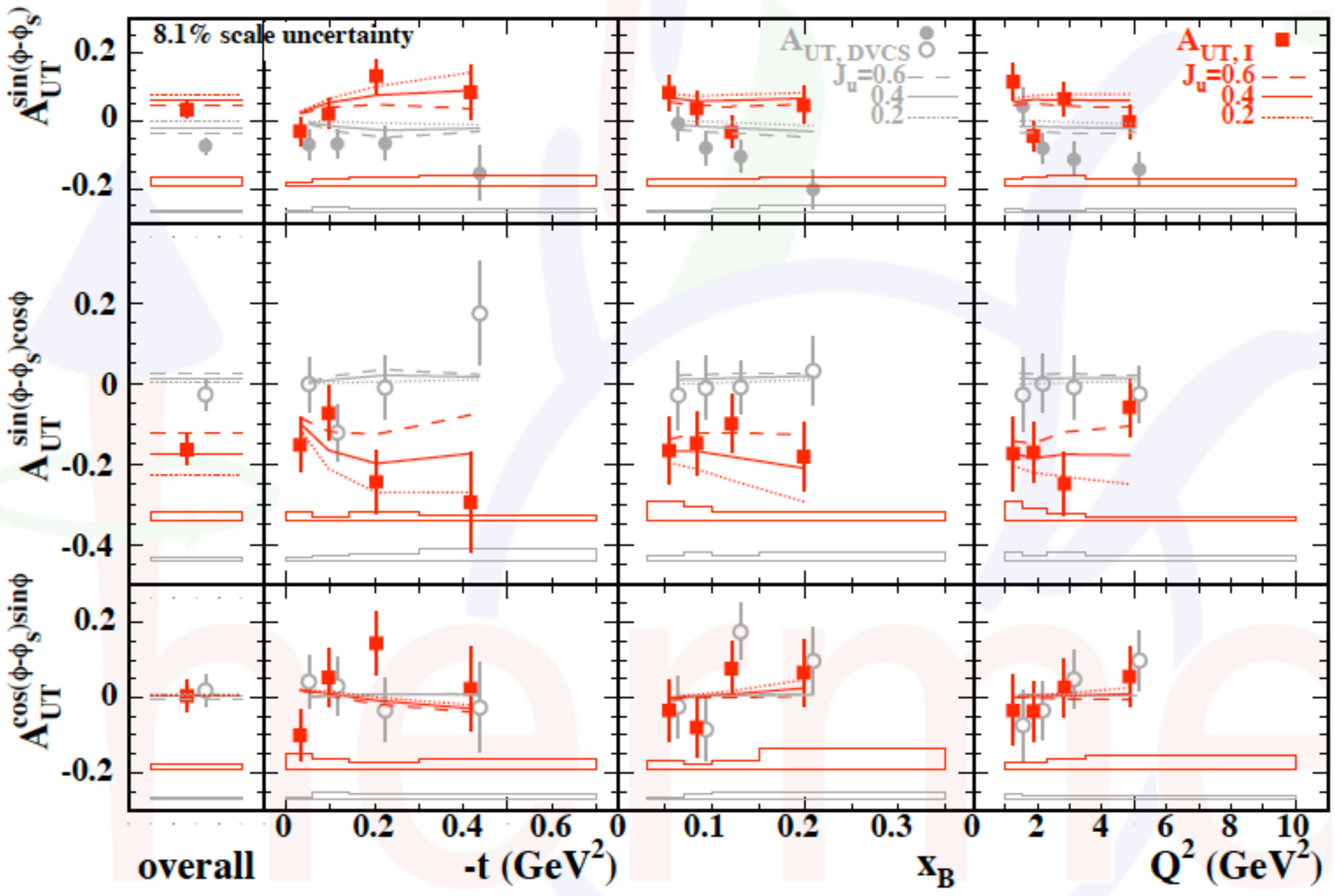

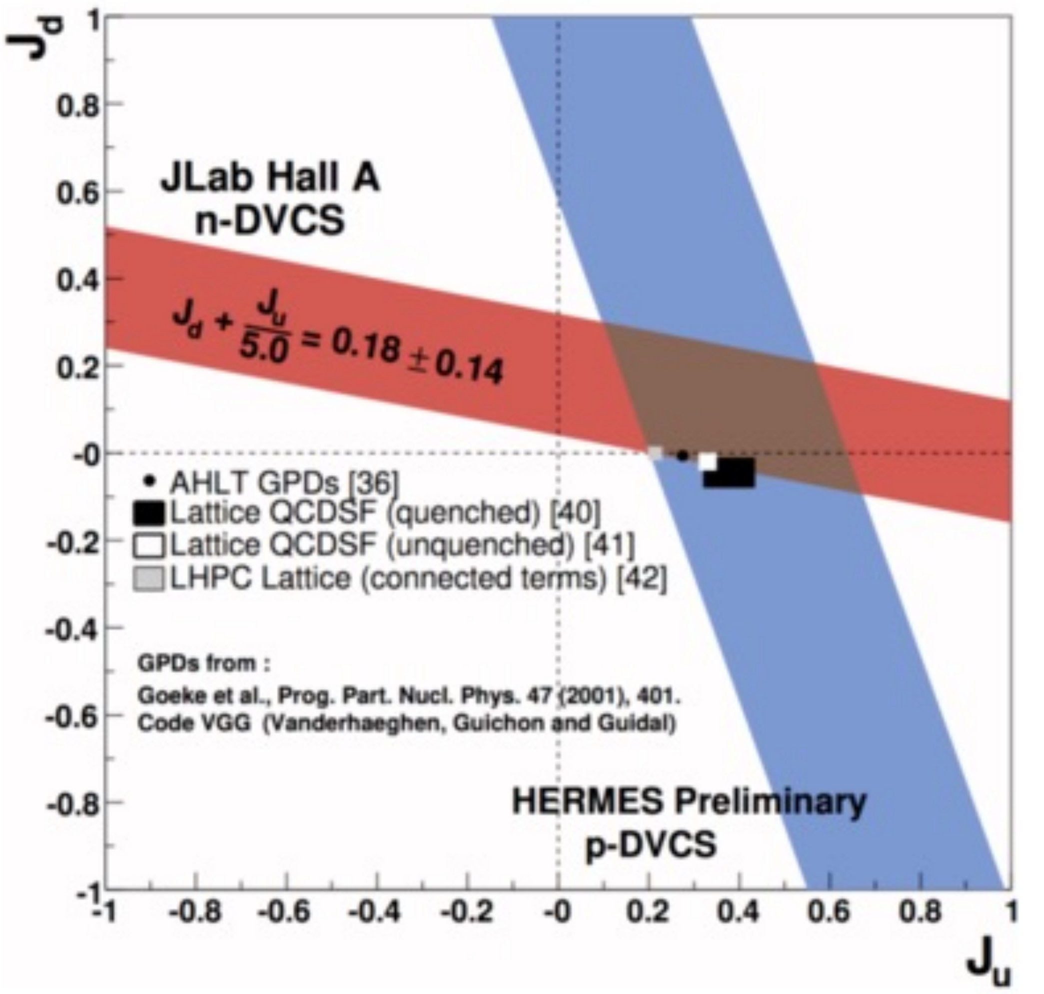

Electron Ion Collider at BNL (2031+)

EIC among the highest priority of US Nuclear Physics

- **High luminosity**: L= 10^{33}–10^{34} $cm^{-2}s^{-1}$, 10–100 fb^{-1}/year
- **Highly polarized** electron and light ion beams: ~70%
- **Large center of mass energy range**: E_{cm} = 28–140 GeV
- **Large ion species range**: proton – Uranium
- **Particle production rate**: O(5) @ ~500 kHz

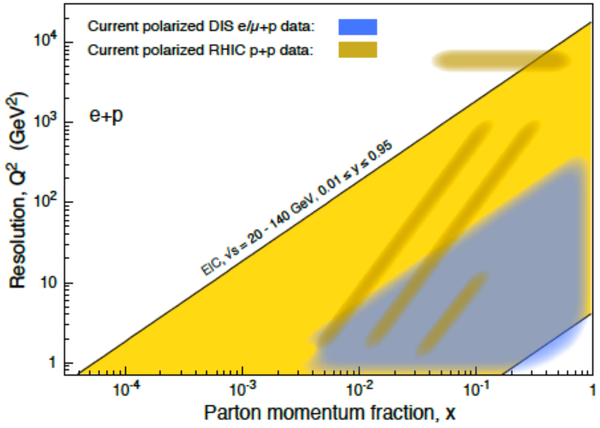

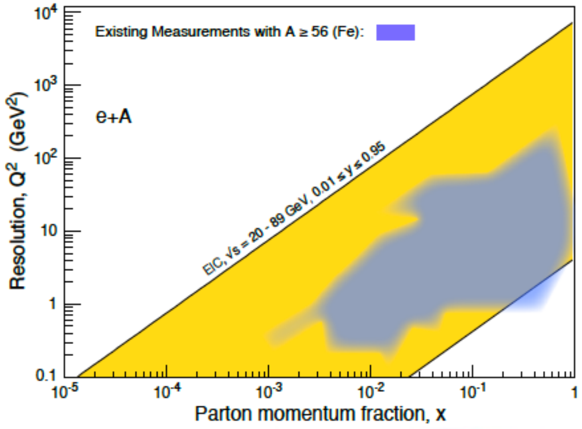

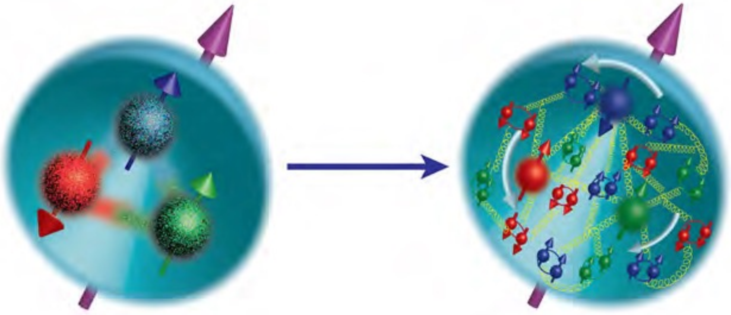

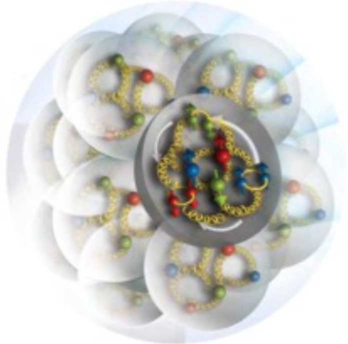

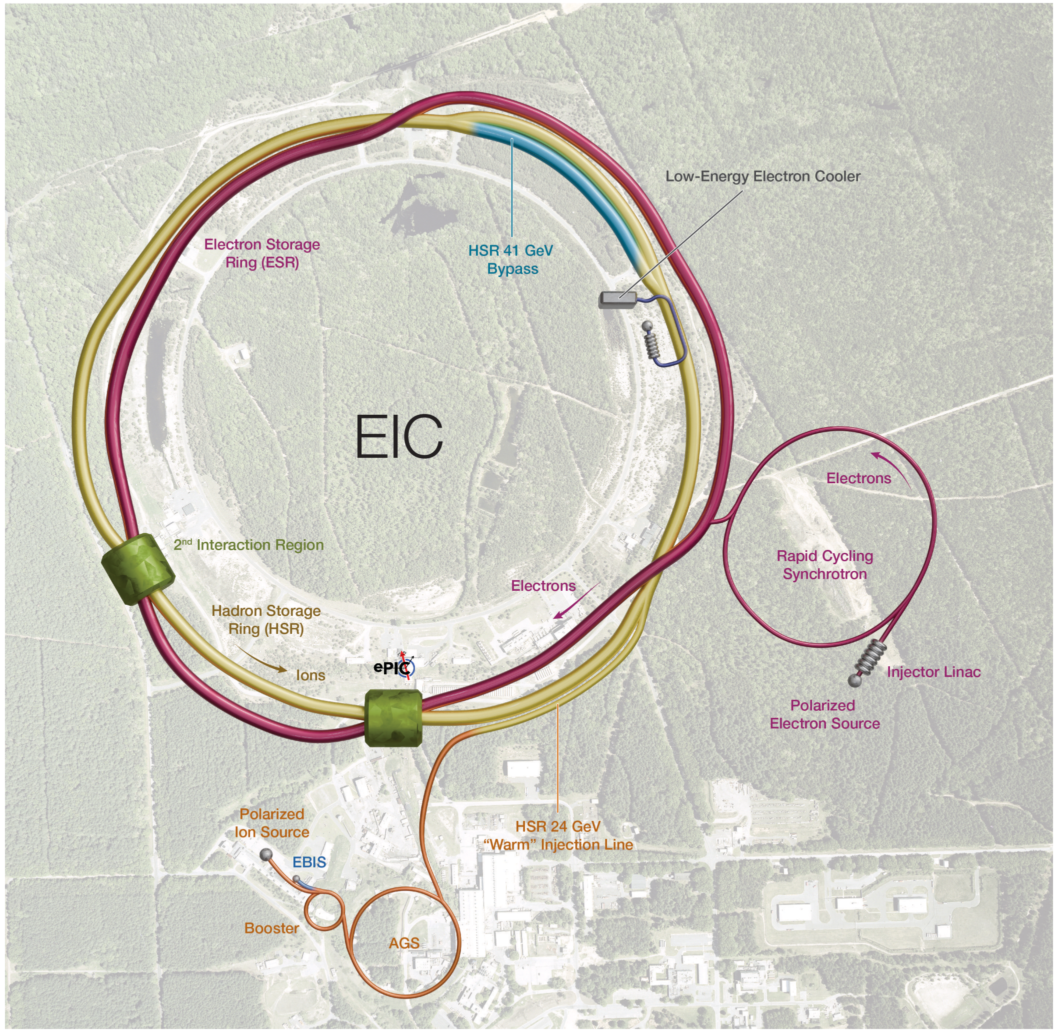

Electron Beam: 5-18 GeV
Ion: 40, 100-275 GeV

EIC Physics Program

[5] EIC Yellow Report

How are the gluons and sea quarks, and their spins, distributed in space and momentum inside the nucleon? What is the role of orbital motion in building the nucleon spin?

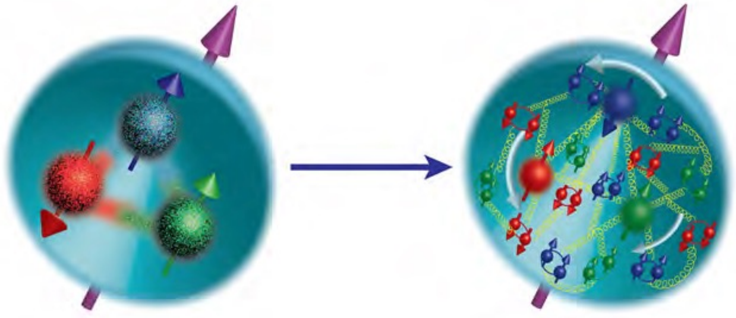

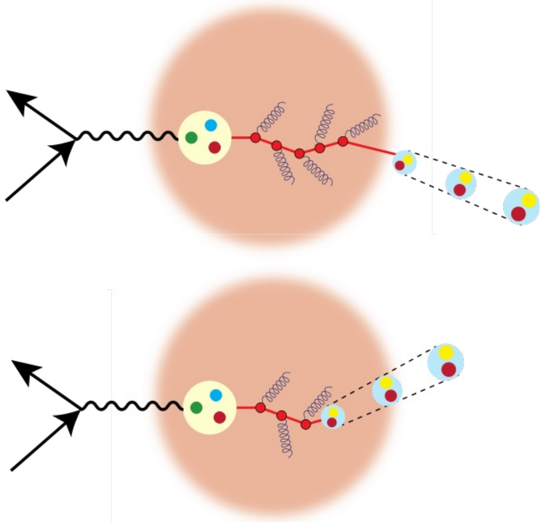

How do color-charged quarks and gluons, and colorless jets, interact with a nuclear medium? How do the confined hadronic states emerge from these quarks and gluons? How do the quark-gluon interactions create nuclear binding?

How does a dense nuclear environment affect the quarks and gluons, their correlations, and their interactions? What happens to the gluon density in nuclei? Does it saturate at high energy, giving rise to a gluonic matter with universal properties in all nuclei, even the proton?

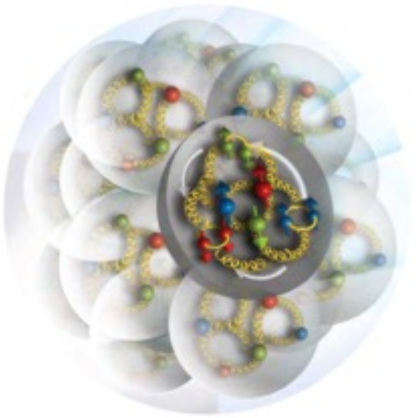

Precision EW, Beyond Standard Model, …

EIC Physics: Origin of Nucleon Spin

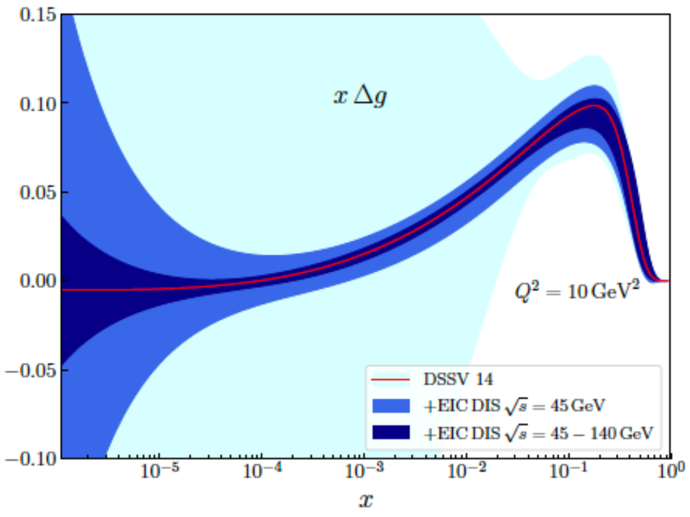

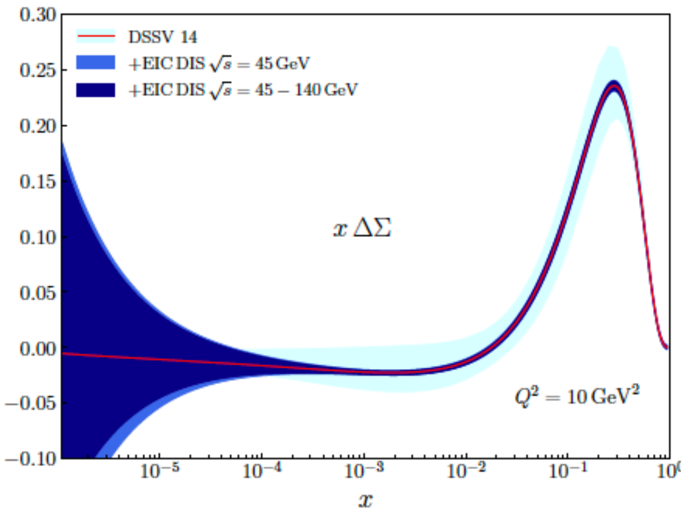

- EIC will improve polarized PDF uncertainties, in particular the polarized gluon distribution, to better understand contributions to proton spin from quark and gluon spin polarizations
- Requirements: high luminosity, highly polarized electron and light ion beams, large center of mass energy

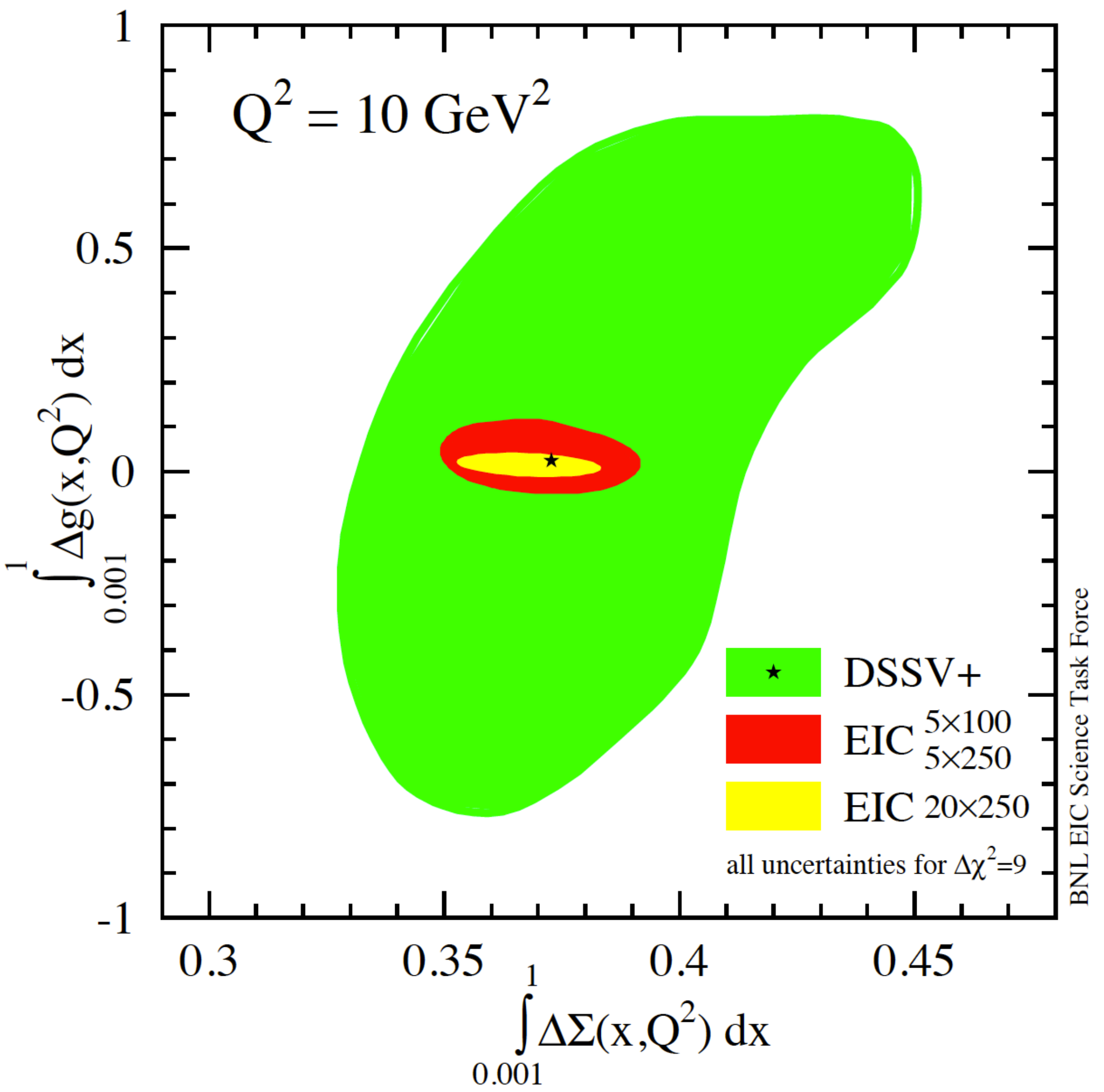

EIC Physics: 3D Structures of Nucleon

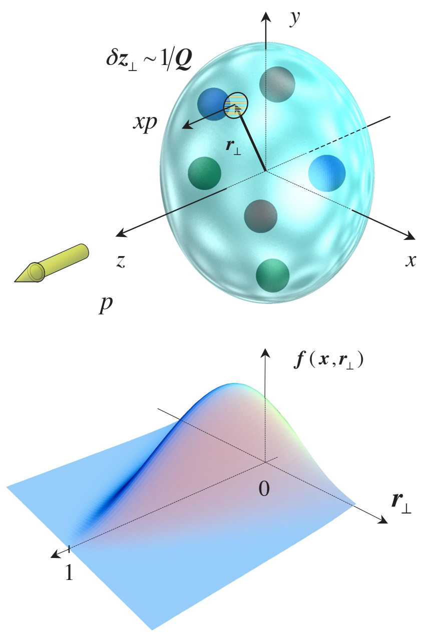

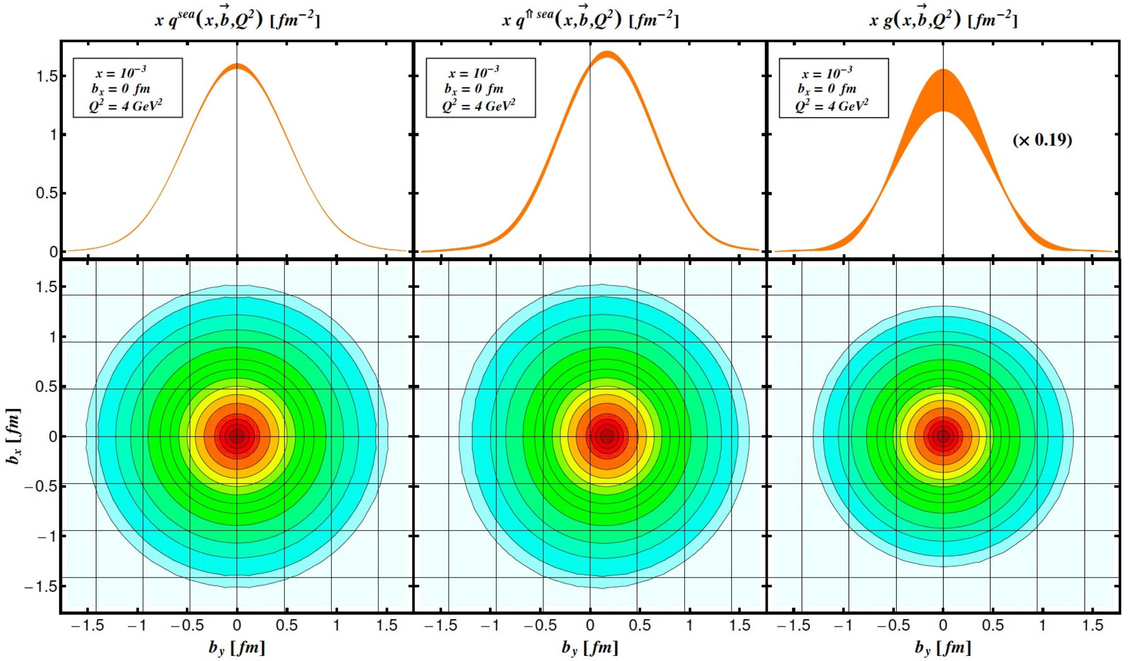

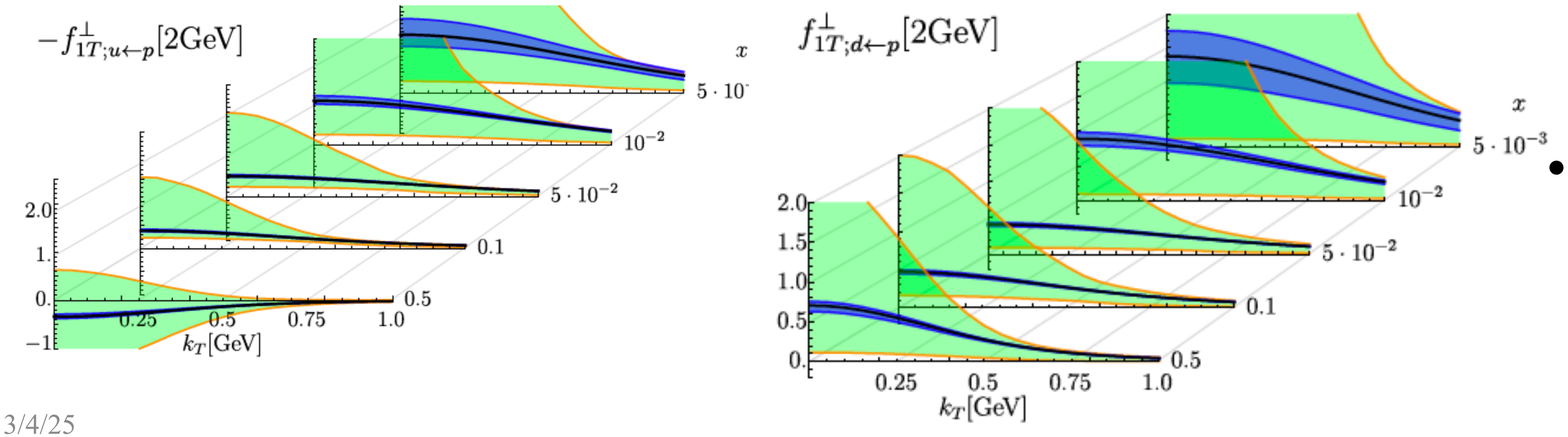

- EIC will provide 3D maps of partonic structures of nucleons and nuclei
- GPDs from exclusive processes: longitudinal momentum (x) and transverse spatial (b_T) distributions
- TMDs from semi-inclusive DIS: longitudinal (x) and transverse (k_T) momentum distributions
- Requirements: high luminosity, highly polarized beams, large detector acceptance and PID

EIC Physics: Origin of Nucleon Mass

Proposed a rest frame hadron mass decomposition based on T^{00} [PRL **74** (1995); PRD **52** (1995)]

$$M = \frac{\langle p | \int d^3x\, T^{00}(0, \boldsymbol{x}) | p \rangle}{\langle p | p \rangle}\Bigg|_{\text{at rest}} = \underbrace{M_q + M_g}_{\text{quark \& gluon energies}} + \underbrace{M_m}_{\text{quark mass}} + \underbrace{M_a}_{\text{trace anomaly}}$$

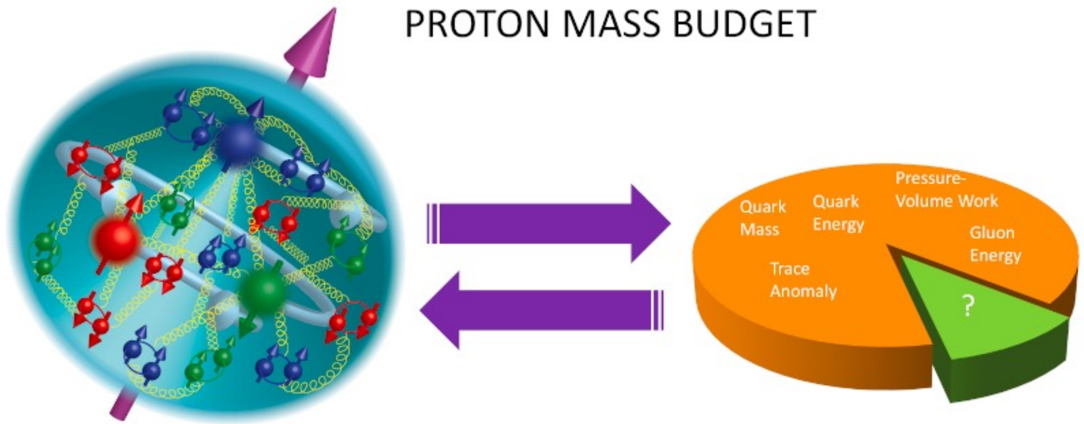

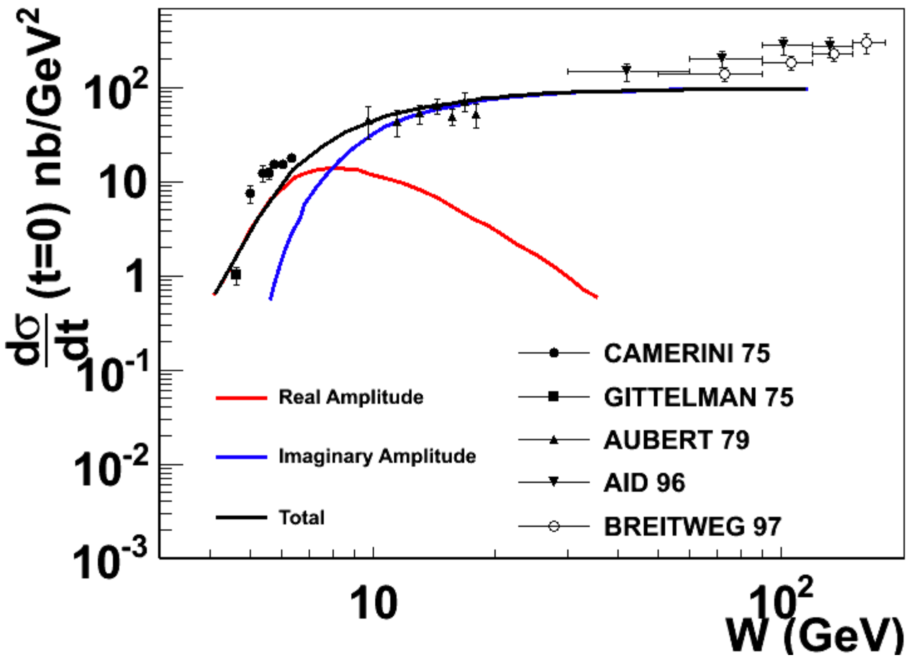

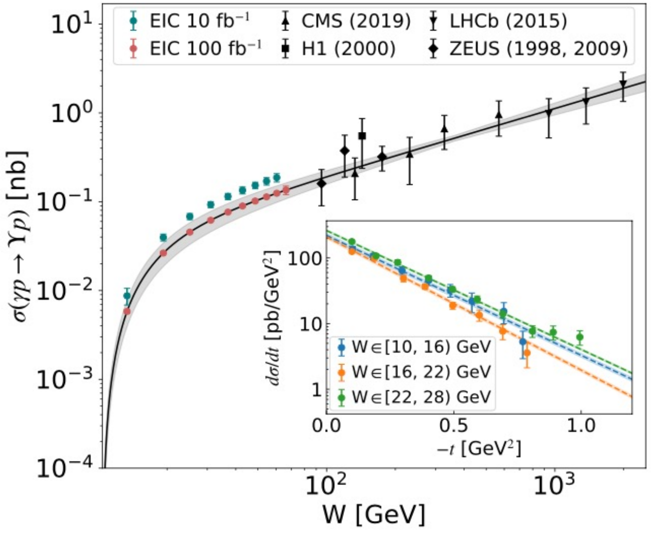

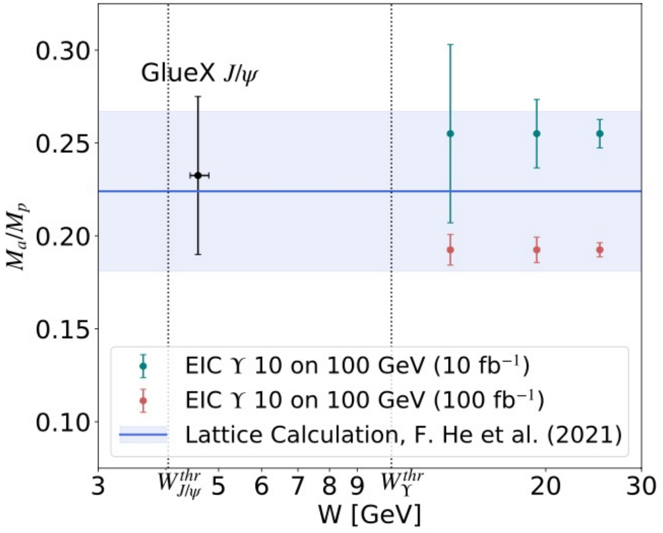

- Measurements of near-threshold quarkonium production allow access to the trace anomaly
- Q^2 dependence study in electroproduction of Upsilon near threshold is possible at EIC allowing an easier interpretation with suppressed NLO corrections

EIC Physics: Imaging Nuclei

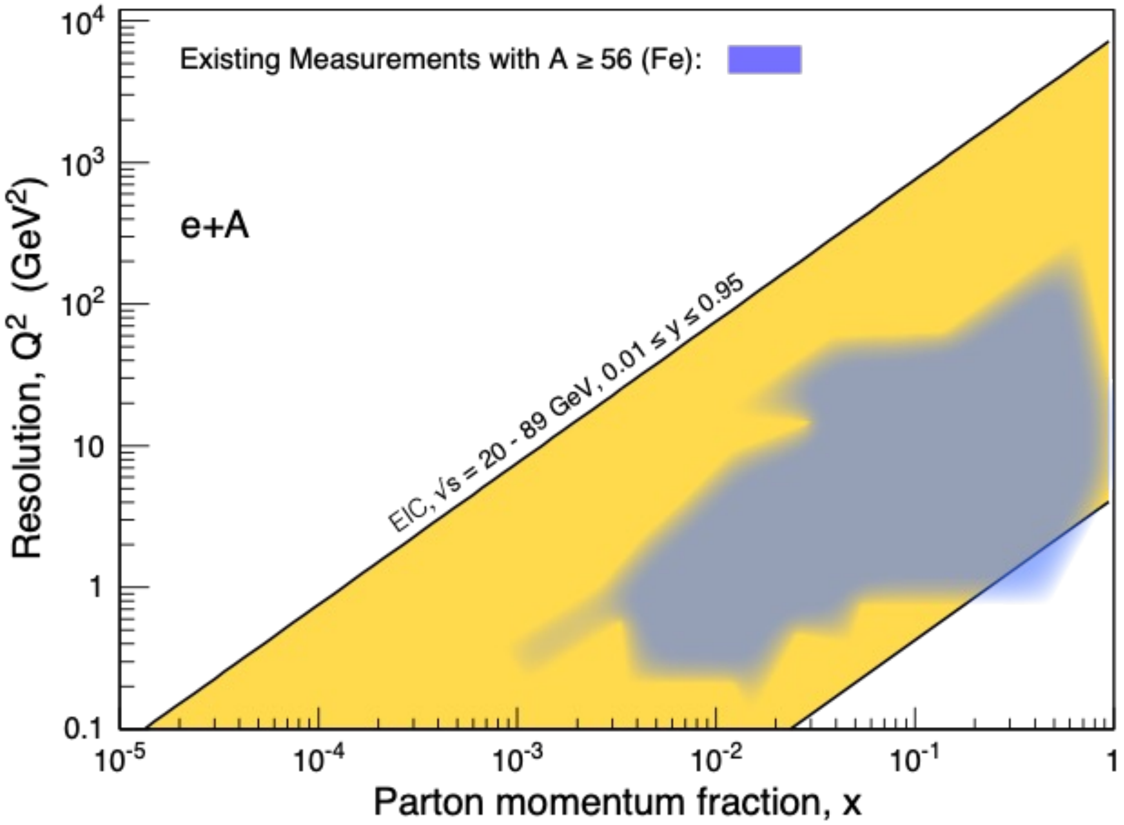

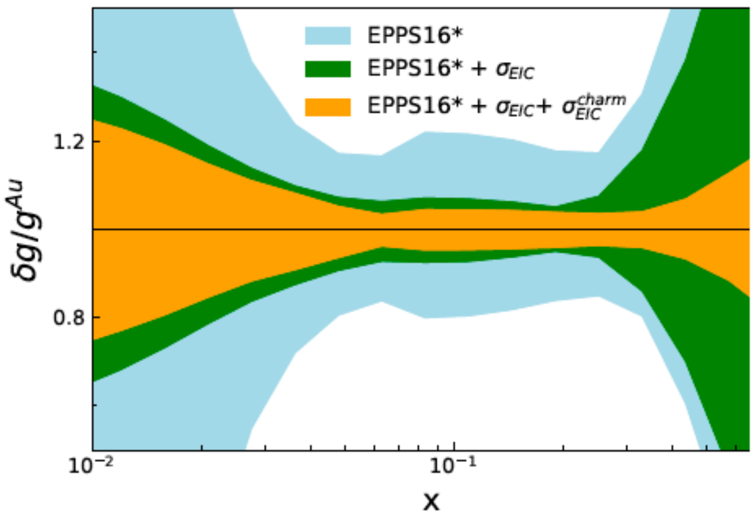

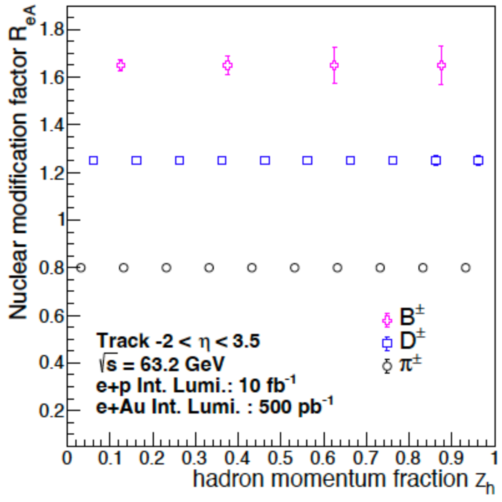

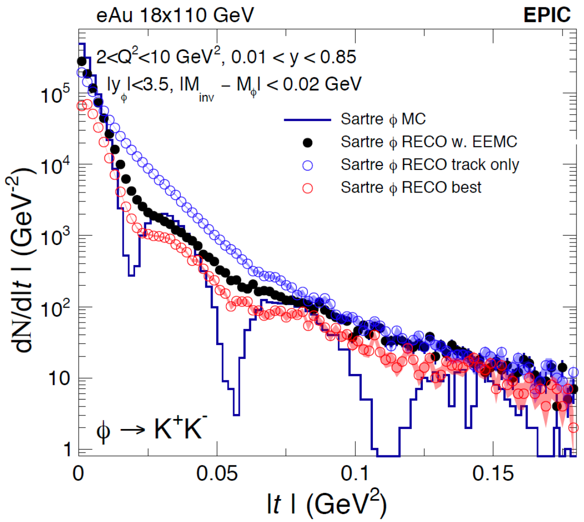

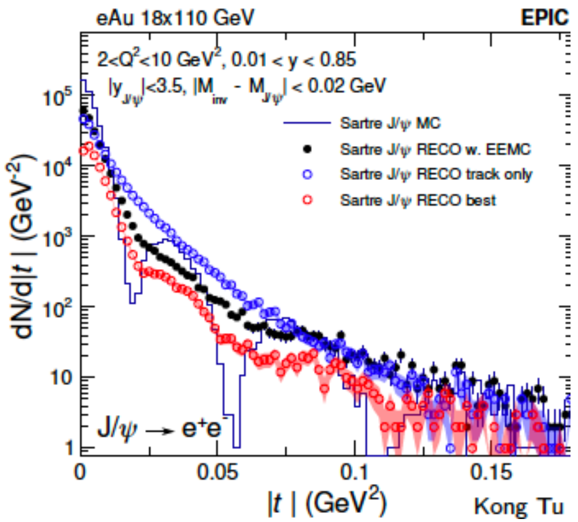

- A unique QCD laboratory to study how the dense nuclear environment affect the quarks and gluons inside nuclei

Physics Processes and Particle Detection at EIC

[6] EIC DPAP

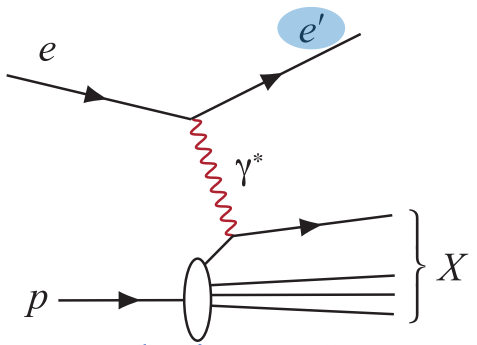

Inclusive DIS

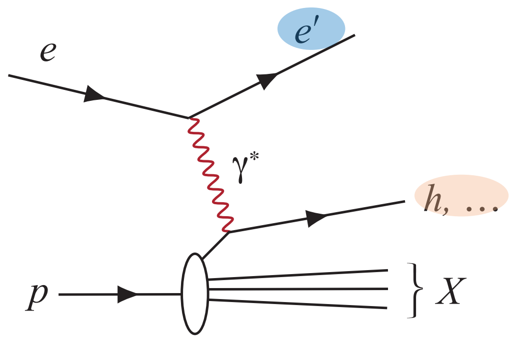

Semi-inclusive DIS

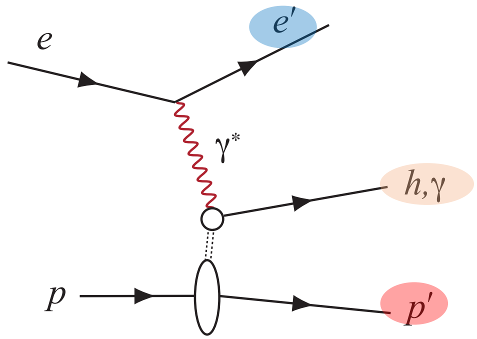

Exclusive

- Inclusive DIS : scattered electron only
- Semi-inclusive DIS: scattered electron, at least one final state hadron
- Exclusive: all the final state particles including the recoiling nucleon

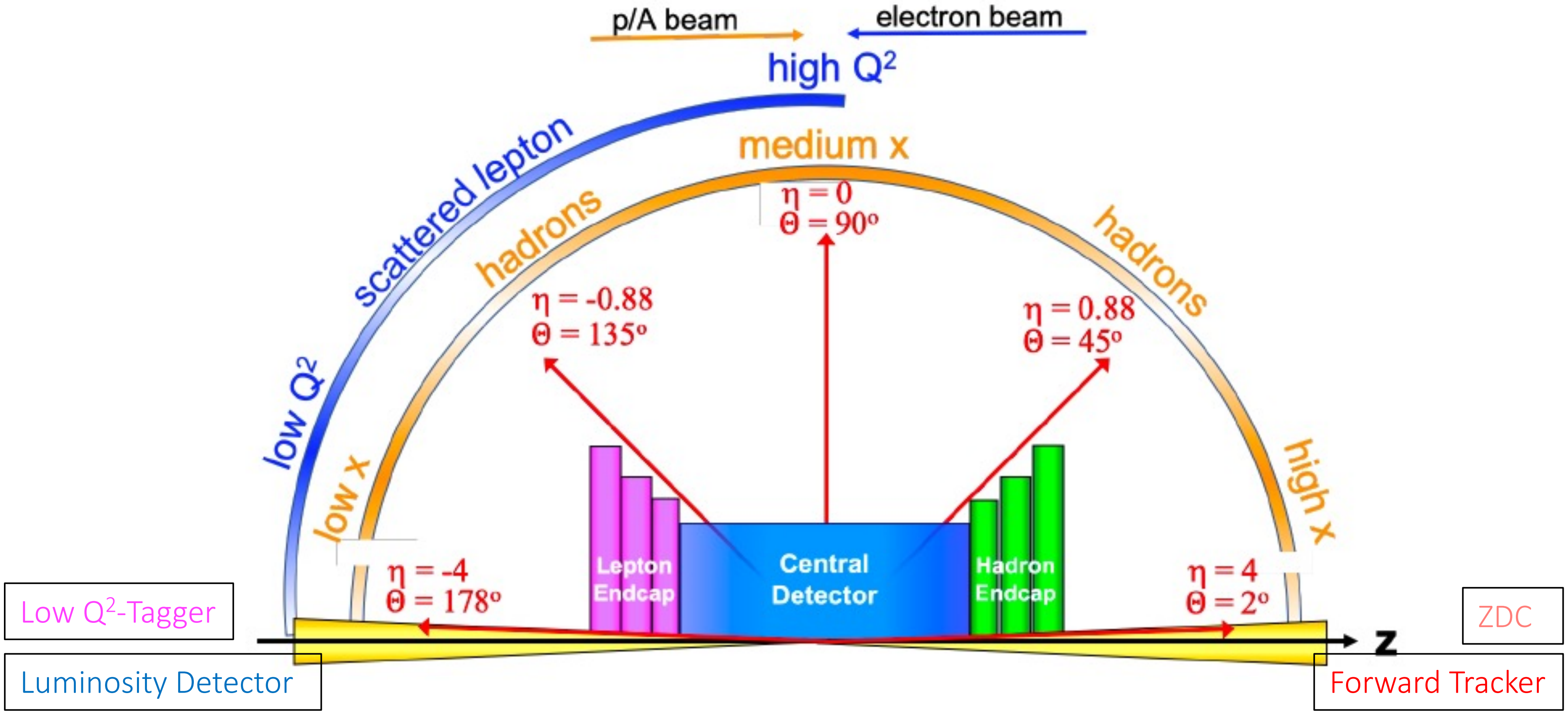

Electron-Proton and -Ion Collider detector (ePIC)

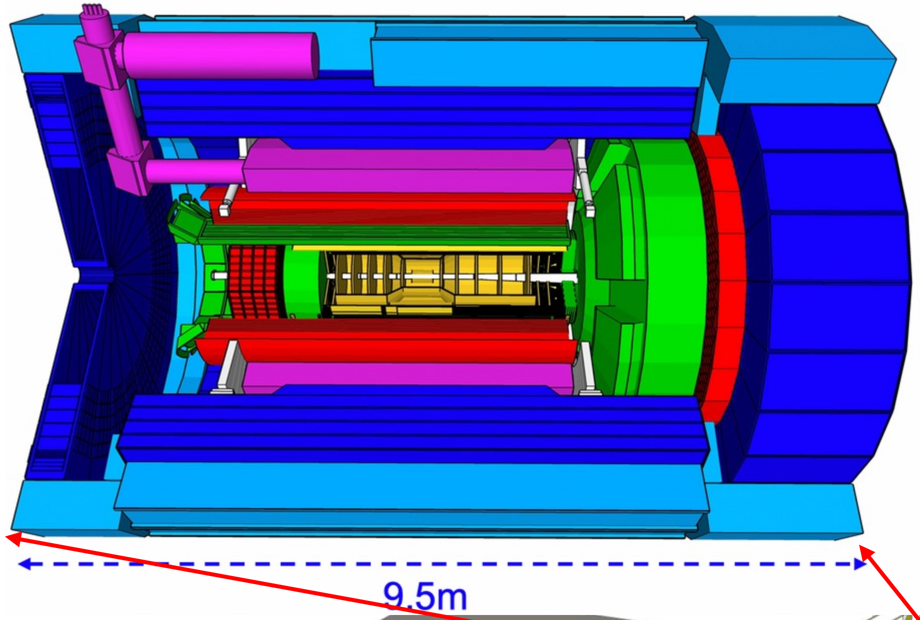

Vertexing and Tracking:
- Silicon Vertex Tracker (MAPS)
- MPGD (µRWELL/µMegas)

Particle Identification:
- TOF (AC-LGAD also for tracking)
- pfRICH (Aerogel/HRPPD)
- hpDIRC (Quartz/MCP-PMT)
- dRICH (Aerogel+C_2F_6/MCP-PMT)

EM Calorimeters:
- Barrel EMCal (Pb+SciFi/SiPM) with imaging layers (Pb+SciFi/AstroPix)
- EEMCal ($PbWO_4$/SiPM)
- FEMC (W+SciFi)

Hadronic Calorimeters:
- Backward HCAL (Fe+Sc/SiPM)
- Barrel HCal (sPHENIX re-use)
- LFHCAL (Fe+Sc&W+Sc/SiPM)

Far-Backward:
- Luminosity monitor (AC-LGAD, W+SciFi)
- Low-Q^2 tagger (Si/Timepix4)

Far-Forward:
- Roman Pots (AC-LGAD)
- B0 Magnet Spectrometer (AC-LGAD, $PbWO_4$)
- Off-Momentum Detector (AC-LGAD)
- Zero Degree Calorimeter ($PbWO_4$, Fe/SiPM)

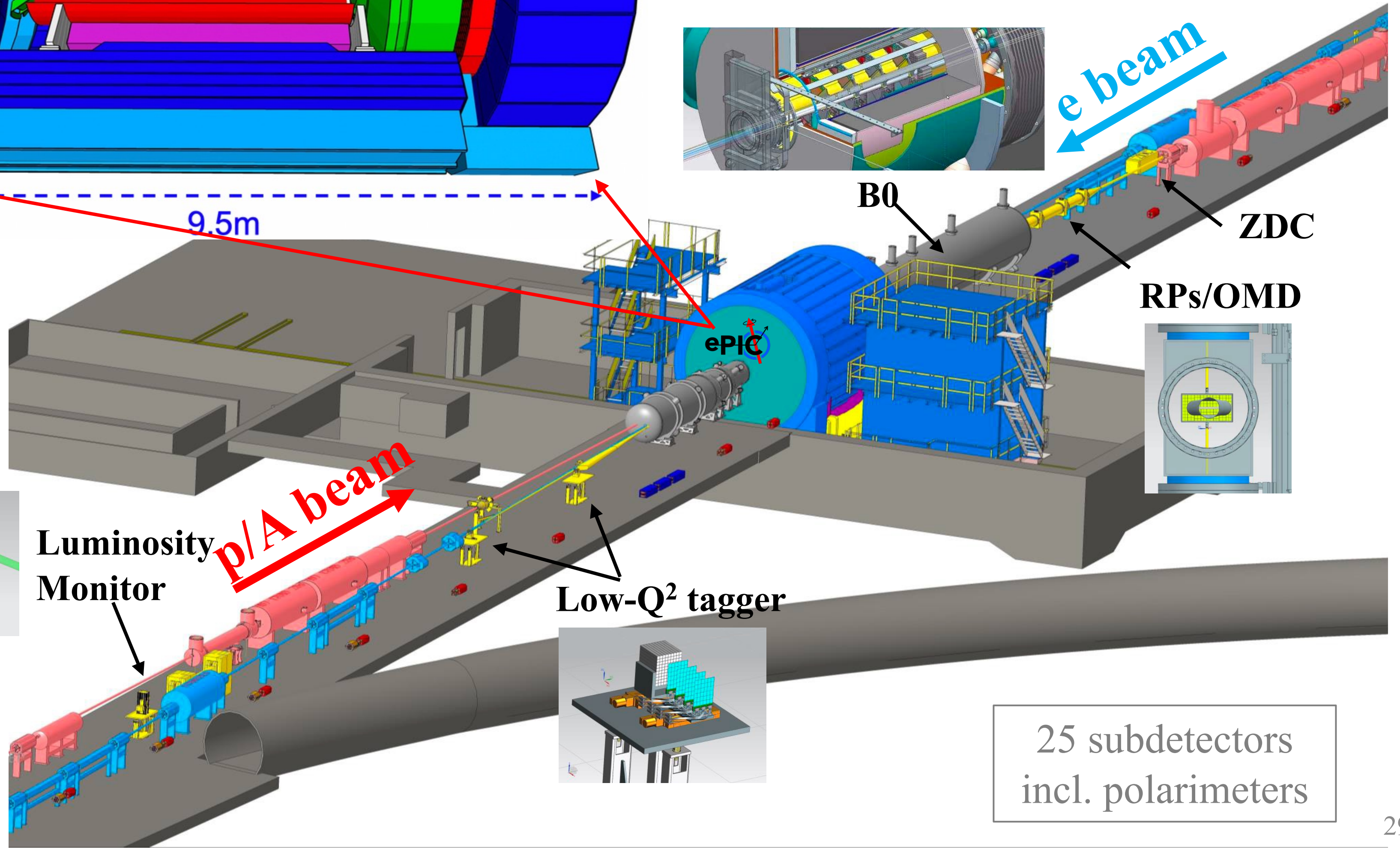

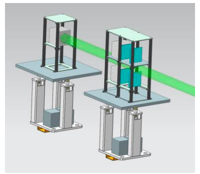

25 subdetectors
incl. polarimeters

Electron-Proton and -Ion Collider detector (ePIC)

Vertexing and Tracking:

- Silicon Vertex Tracker (MAPS)
- MPGD (µRWELL/µMegas)

Particle Identification:

- TOF (AC-LGAD also for tracking)
- pfRICH (Aerogel/HRPPD)
- hpDIRC (Quartz/MCP-PMT)
- dRICH (Aerogel+C_2F_6/MCP-PMT)

EM Calorimeters:

- Barrel EMCal (Pb+SciFi/SiPM) with imaging layers (Pb+SciFi/AstroPix)
- EEMCal ($PbWO_4$/SiPM)
- FEMC (W+SciFi)

Hadronic Calorimeters:

- Backward HCAL (Fe+Sc/SiPM)
- Barrel HCal (sPHENIX re-use)
- LFHCAL (Fe+Sc&W+Sc/SiPM)

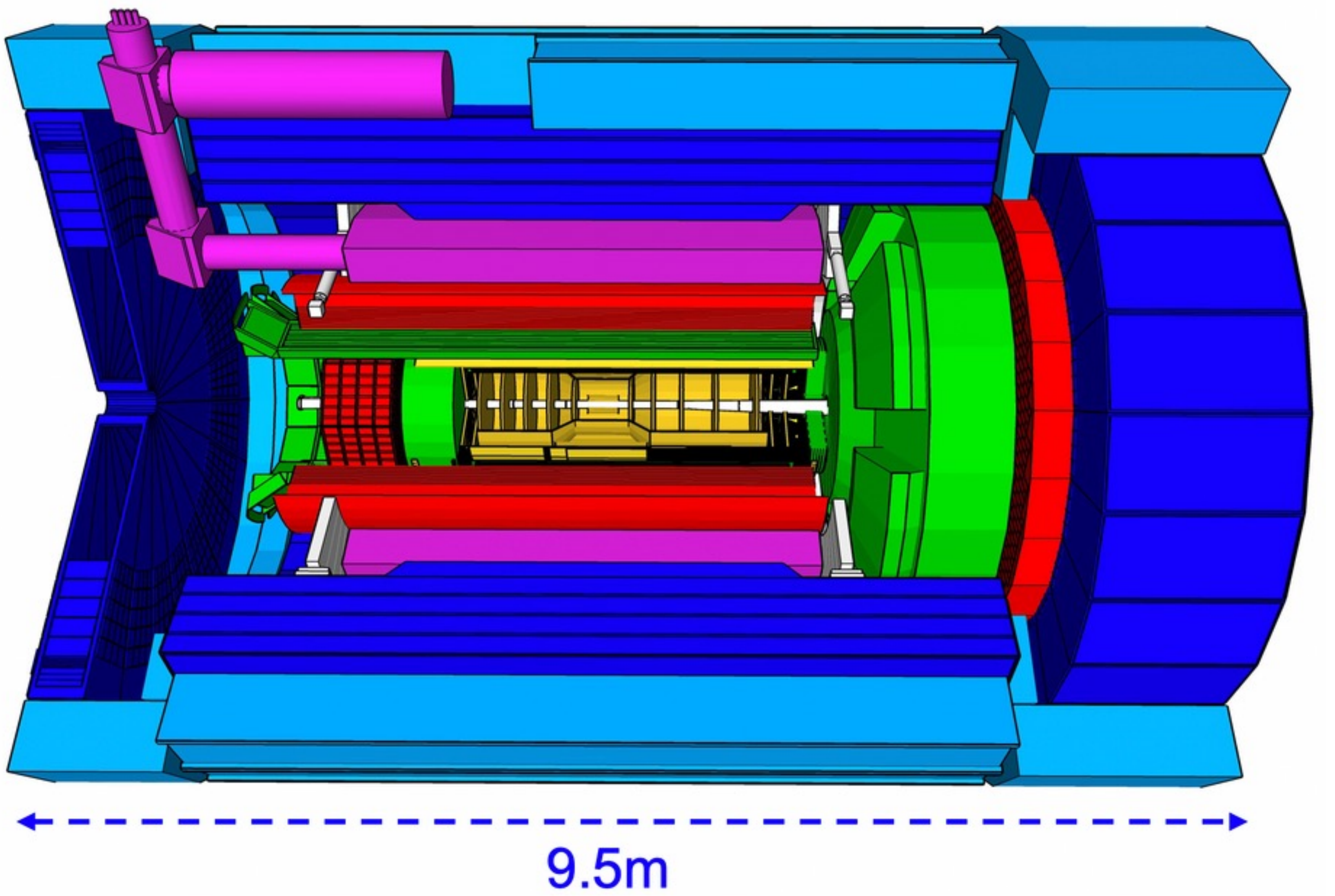

Tracking and Vertexing

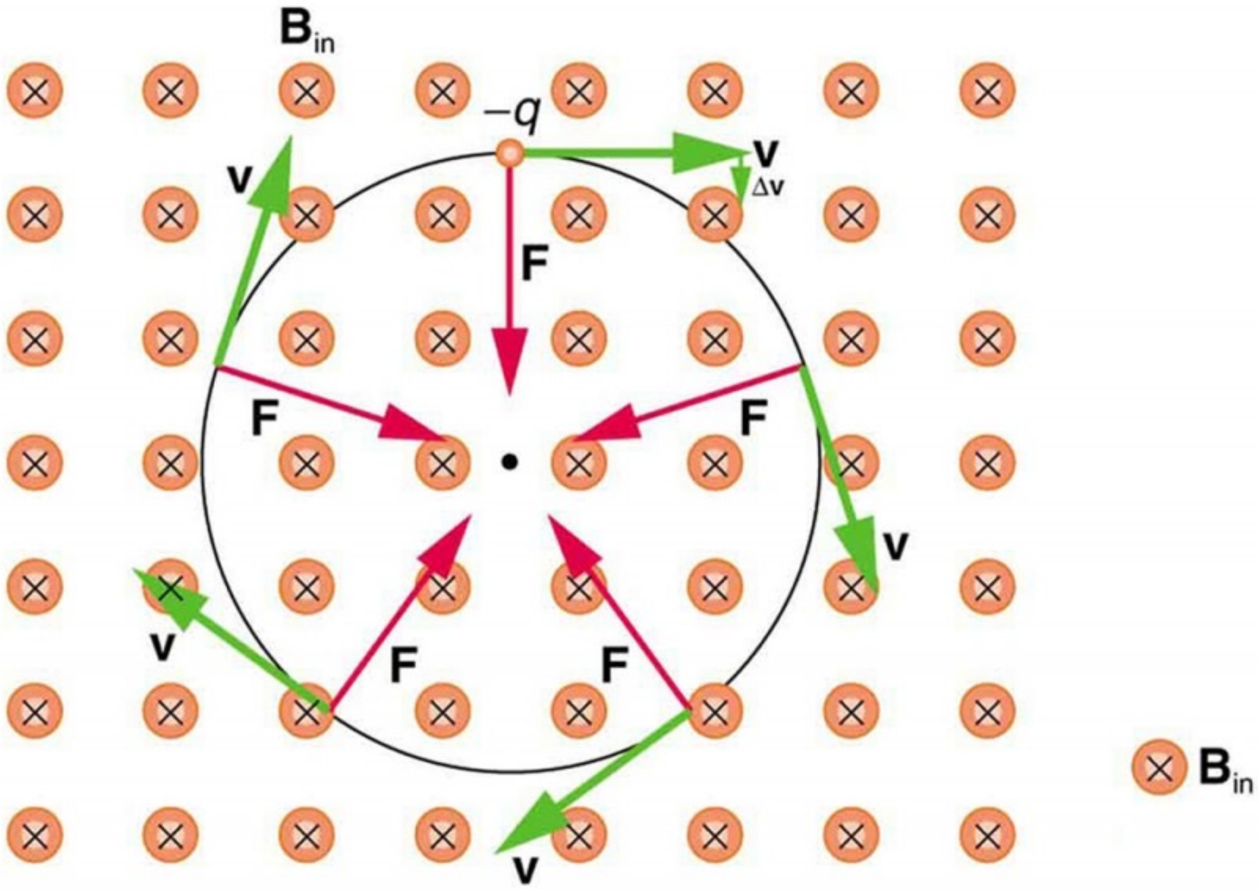

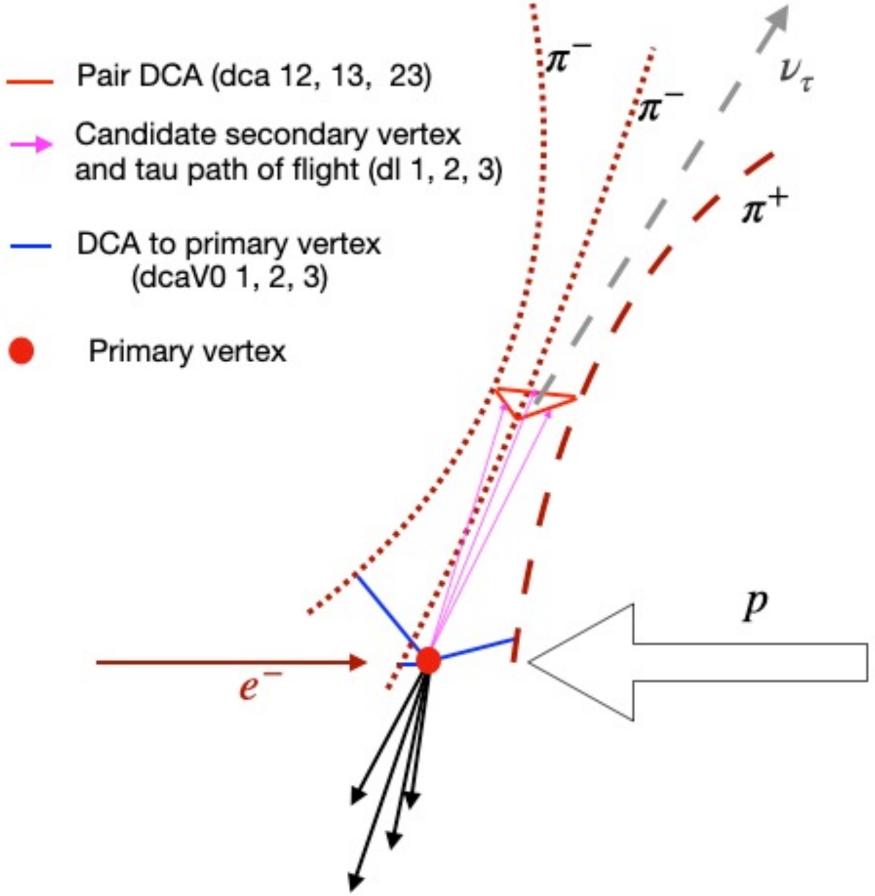

Figure of merit for the VXD: Impact Parameter Resolution

$$\sigma_{ip} = \boldsymbol{a} \oplus \frac{\boldsymbol{b}}{\boldsymbol{p}(GeV)\sin^{3/2}\theta}\ (\mu\text{m})$$

- **a** depends on the single point resolution of the sensor and the lever arm, which is equal to $R_{ext} - R_{int}$
- **b** depends on the distance of the innermost layer to IP and the material budget
- **P** and θ are the particle momentum and polar angle

Multiple Scattering Effects

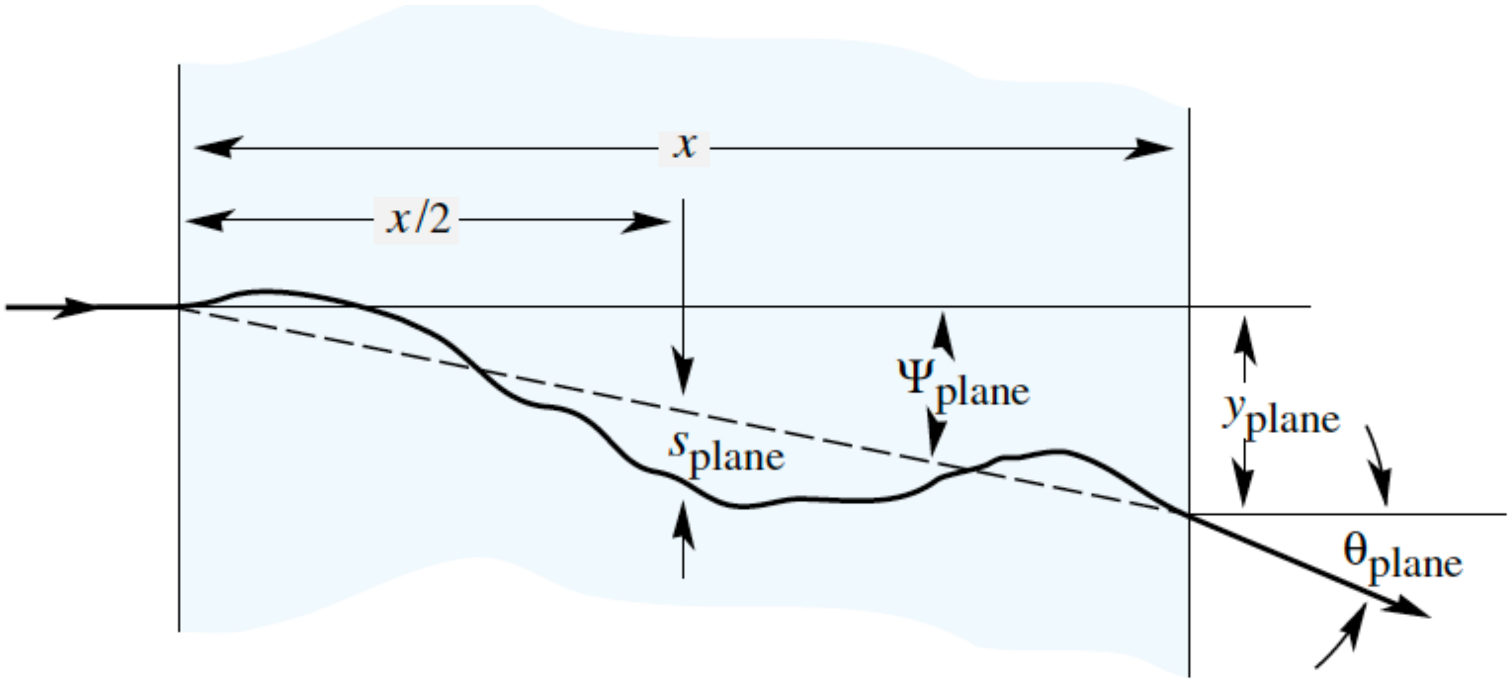

$$\theta_0 = \theta^{\rm rms}_{\rm plane} = \frac{1}{\sqrt{2}}\theta^{\rm rms}_{\rm space}$$

$$\theta_0 = \frac{13.6\ \mathrm{MeV}}{\beta c p}\, z\, \sqrt{\frac{x}{X_0}}\left[1 + 0.088\log_{10}\left(\frac{x\, z^2}{X_0 \beta^2}\right)\right]$$

PDG Review Article, “Passage of particle through matter”

Hybrid vs Monolithic Silicon Detector

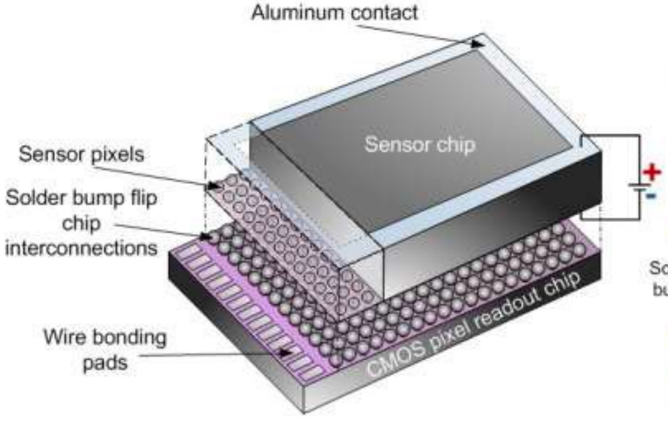

Generic pixel detector

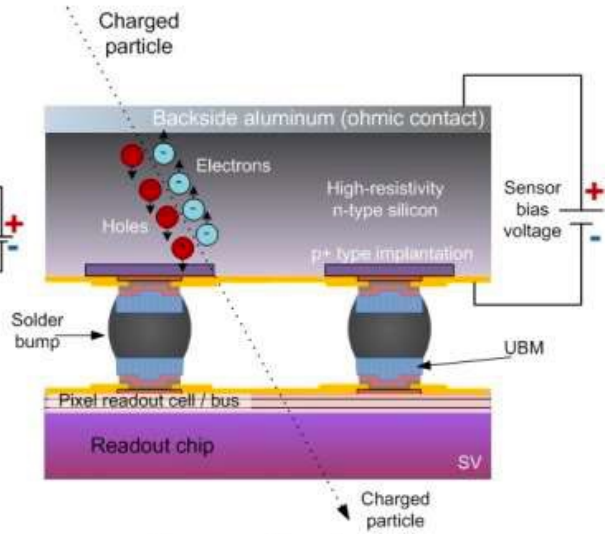

Cross-sectional cut

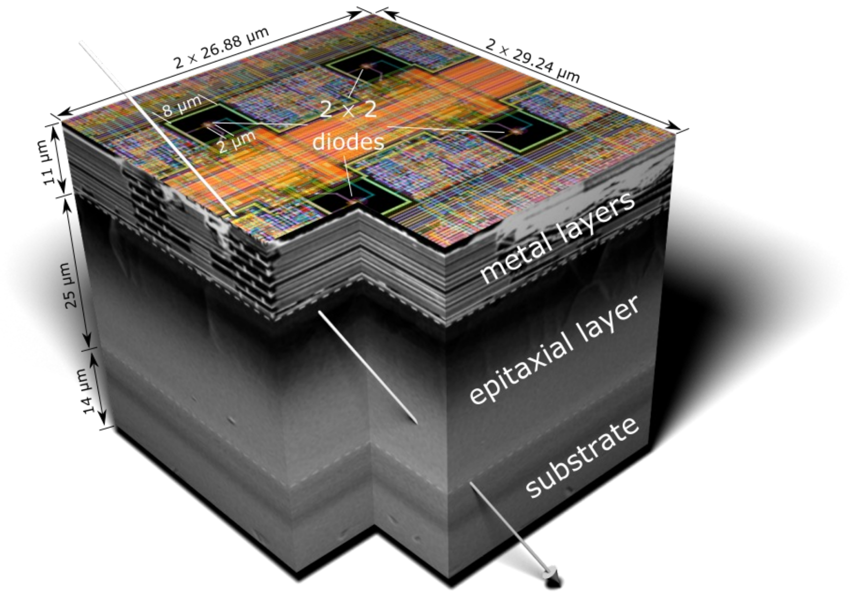

Hybrid

- Used in large majority of installed systems
- 100% fill factor easily obtained
- Sensor and readout circuit can be optimized separately
  - Other materials for the sensor
  - Standard ASIC CMOS (often denser than imaging processes)

Material budget 1-2% X_0

Monolithic

- Easier integration, lower cost
- Promising not only for pixels but also for trackers
- Potentially a significant impact on the material budget
- MAPS are installed in STAR and adopted for the upgrade of the ALICE ITS

Material budget 0.05-0.3% X_0

STAR and ALICE MAPS Detectors

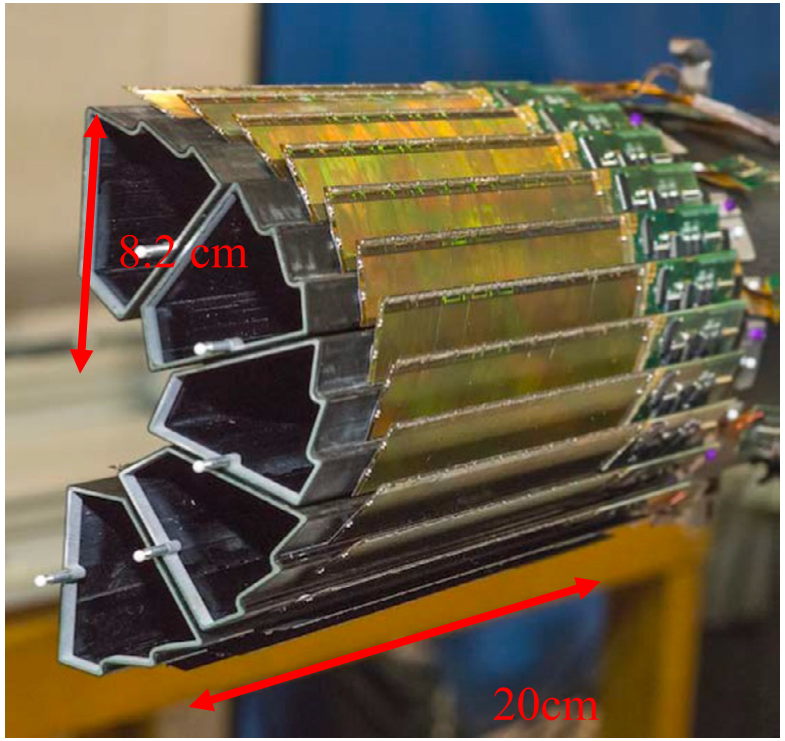

STAR HFT (2014-2016)

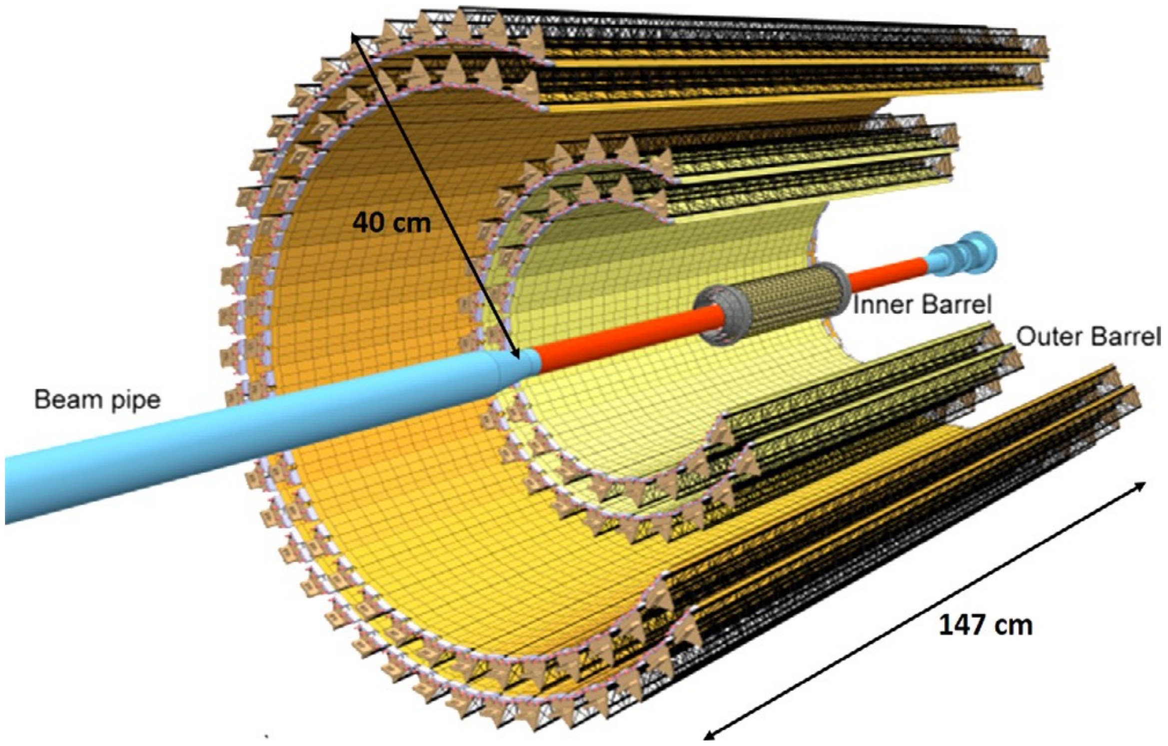

ALICE ITS2 (2021-present)

	STAR PXL	ALICE ITS UPGRADE
Silicon Area	0.16 m^2	10 m^2
# Pixels	356 M	12.5 G
# Layers	2	7
Integration Time	186 µs	10–20 µs
Trigger Rate	~1 kHz	~50 kHz (Pb–Pb), ~100 kHz (p–p)
X/X_0 Inner Layer	~0.4%	~0.3%
Readout Speed	160 MHz	1.2 GHz

Recent Development in MAPS

Thinned ITS2 ALPIDE chips bent to different radii

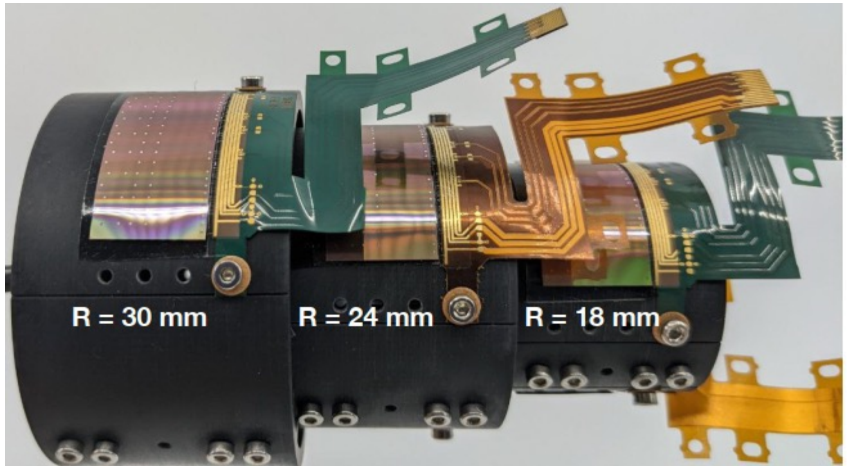

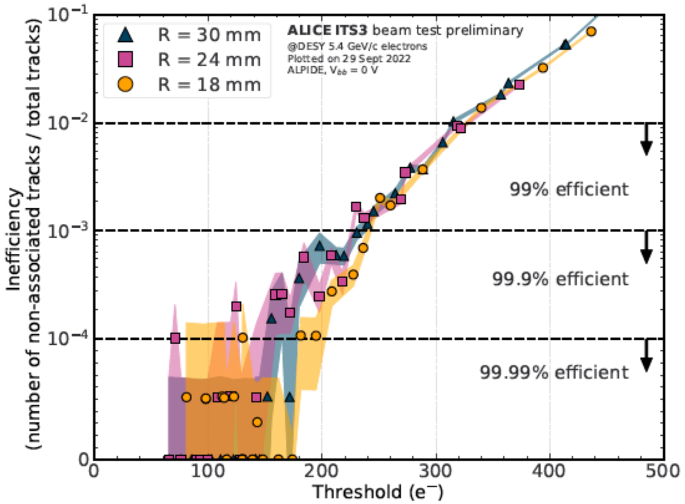

ALICE ITS3 ER1 Wafer (12')

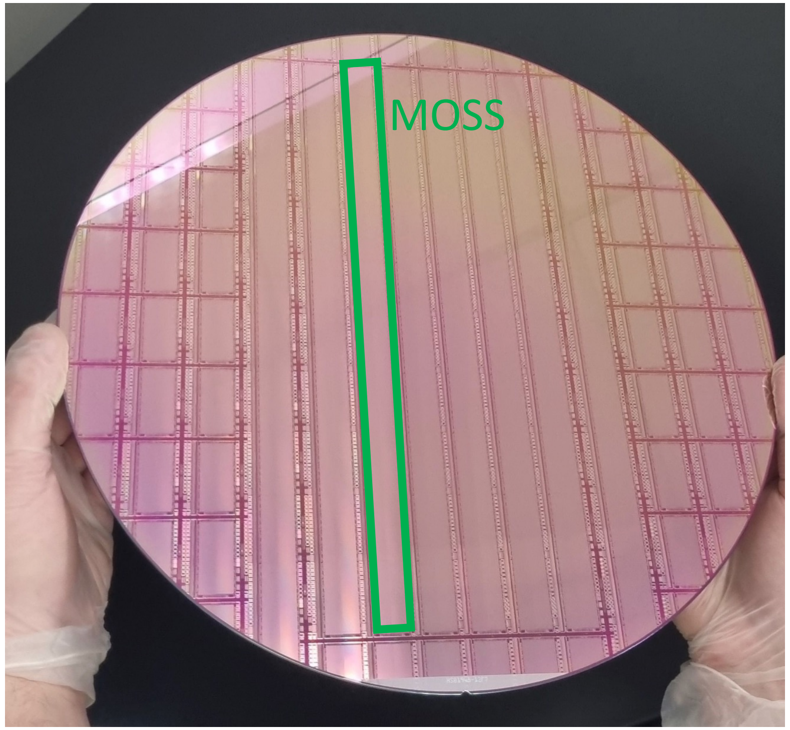

Stitching Technology

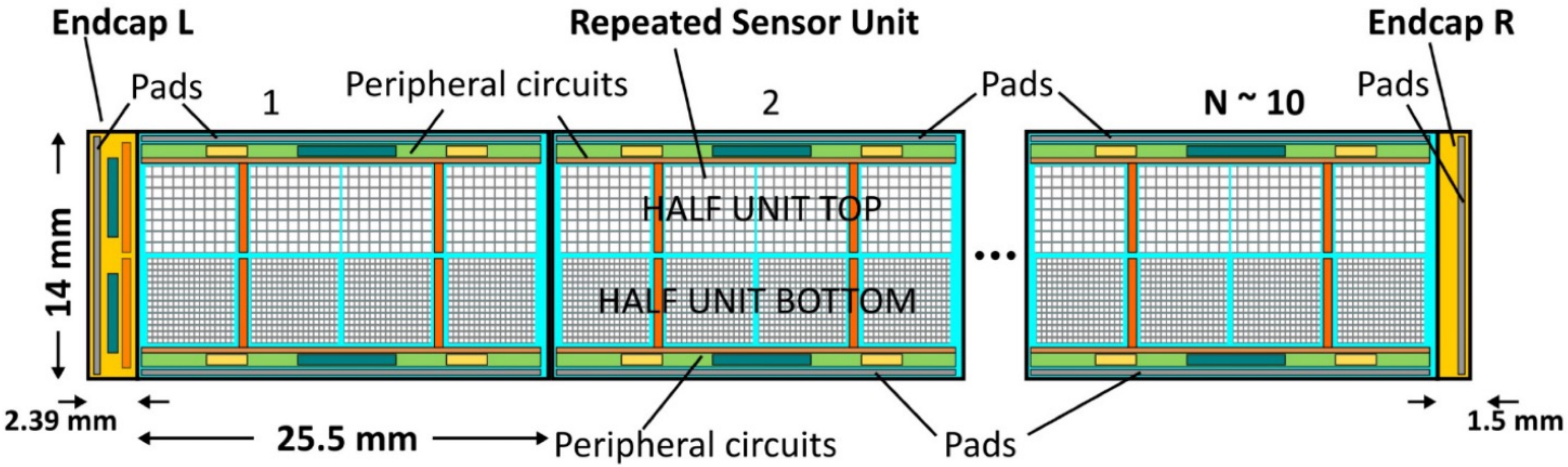

Recent Development in MAPS

ALICE ITS2

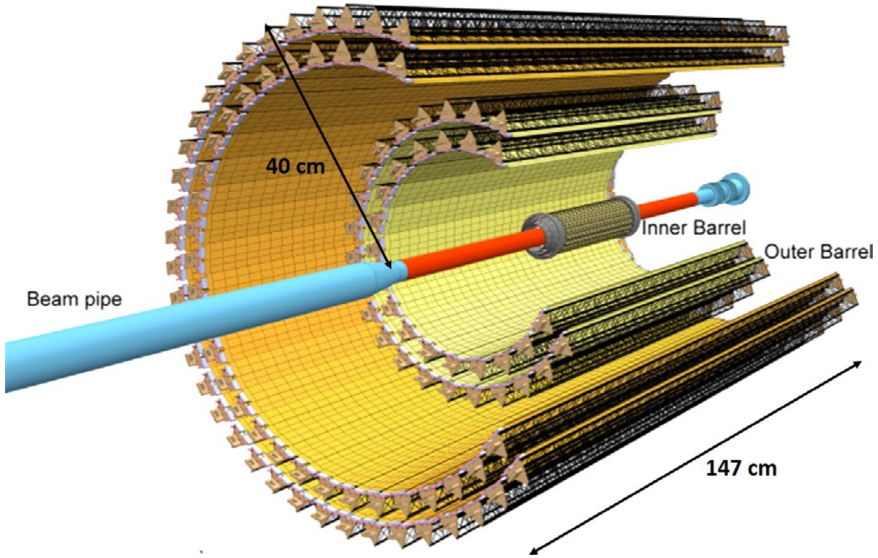

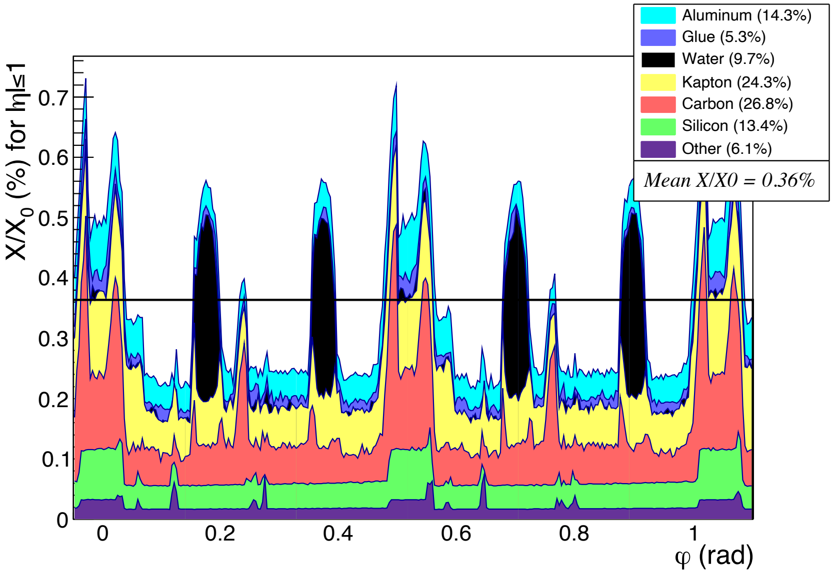

ALICE ITS3

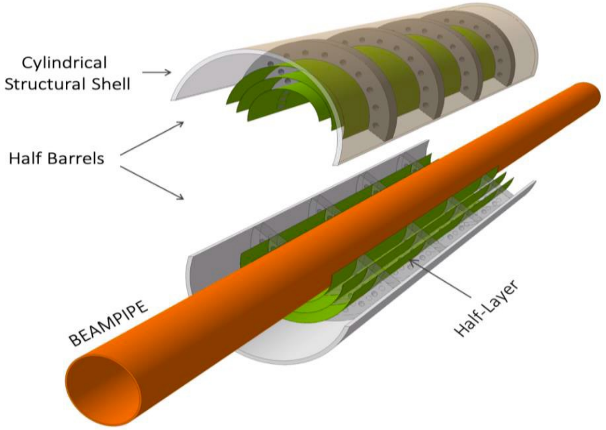

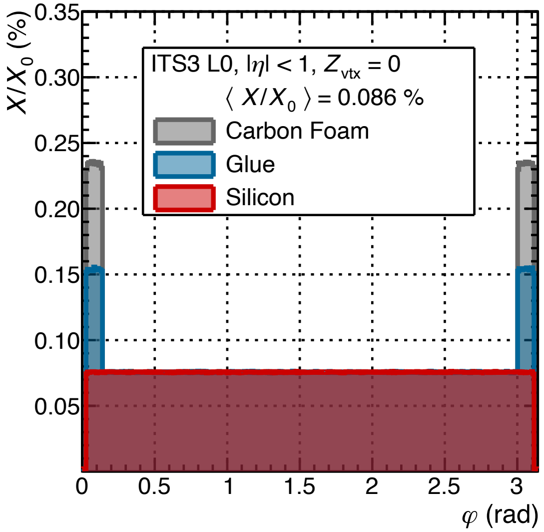

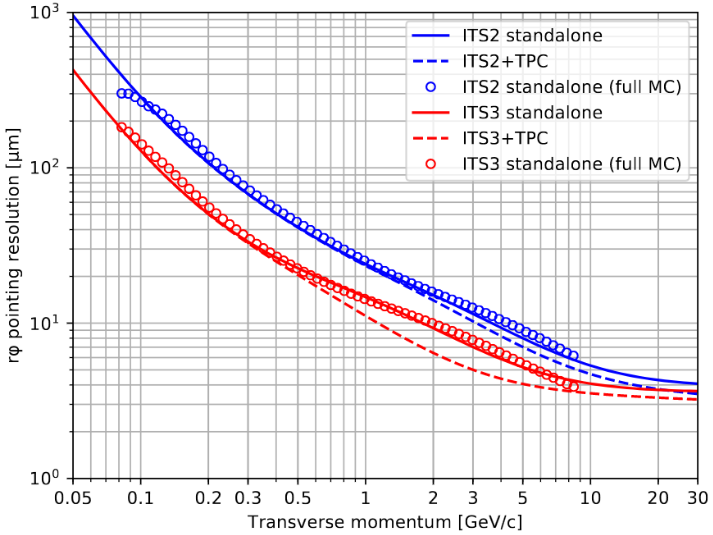

BabyMOSS Beam Tests at FTBF – May/July 2024

babyMOSS Telescope at Fermilab Test Beam Facility

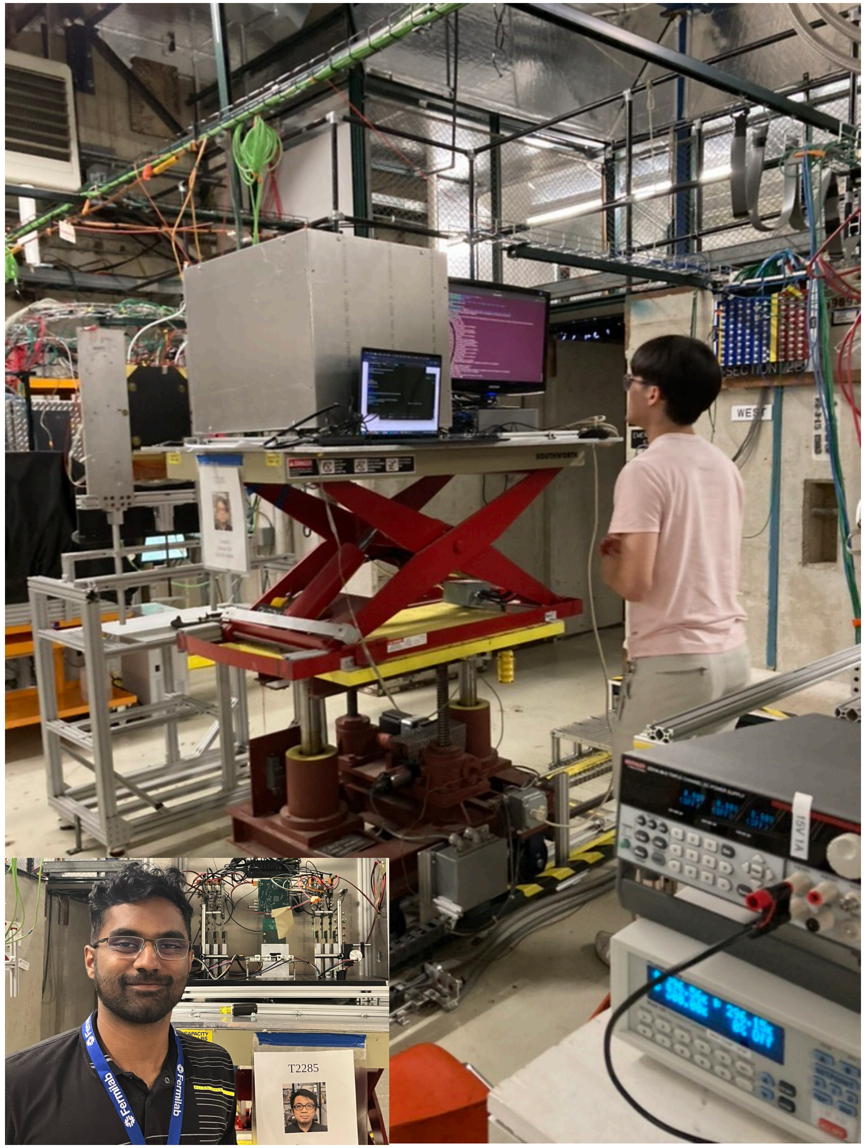

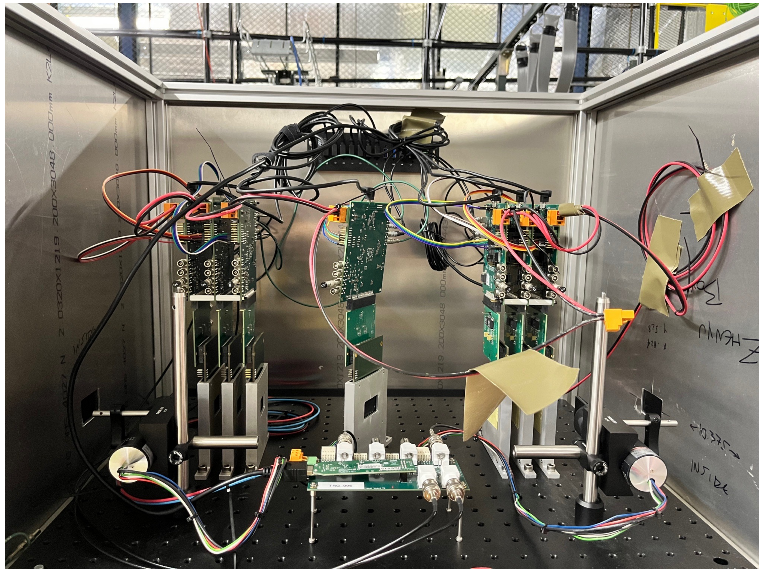

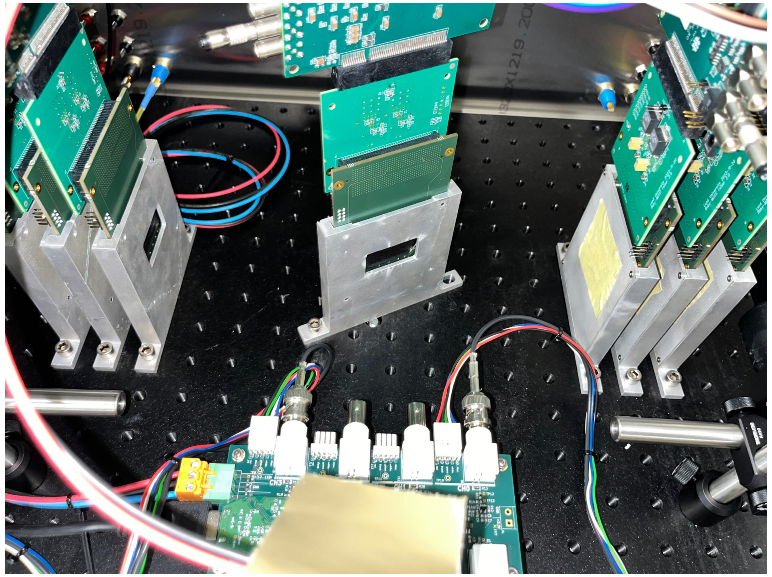

A 120 GeV proton beam event

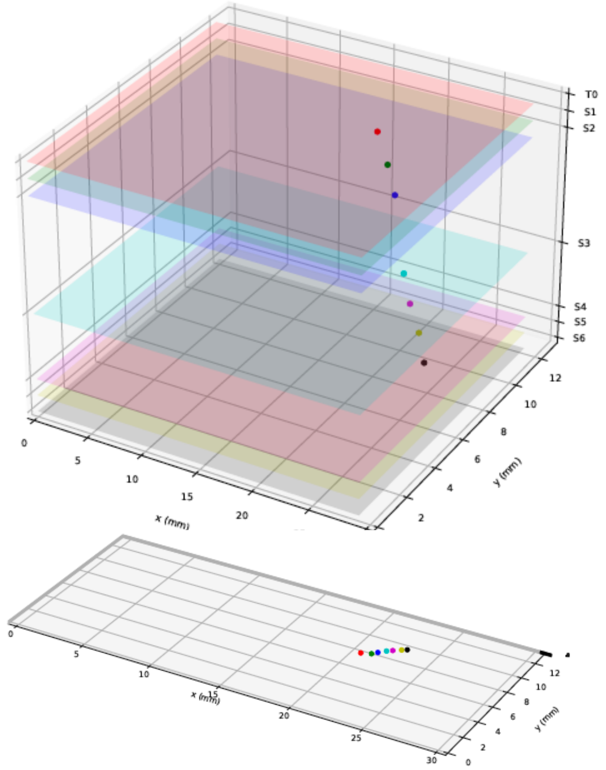

Residual of the DUT (~6 um)

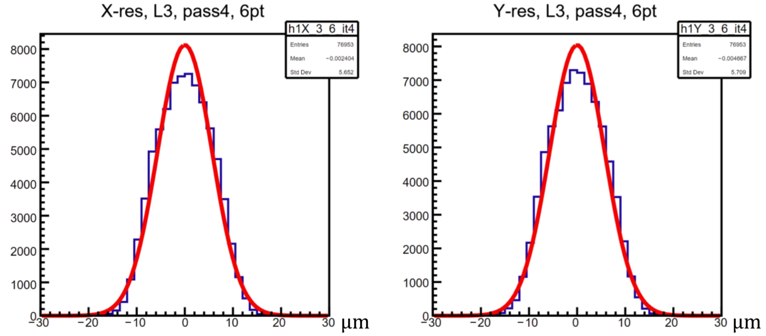

UCB: Tucker Hwang, **UIC:** Danush Shekar; **LBL:** Zhenyu Ye

BabyMOSS SEL Tests at BASE – May/July 2024

babyMOSS SEL Setup at Berkeley Accelerator Space Effects Facility

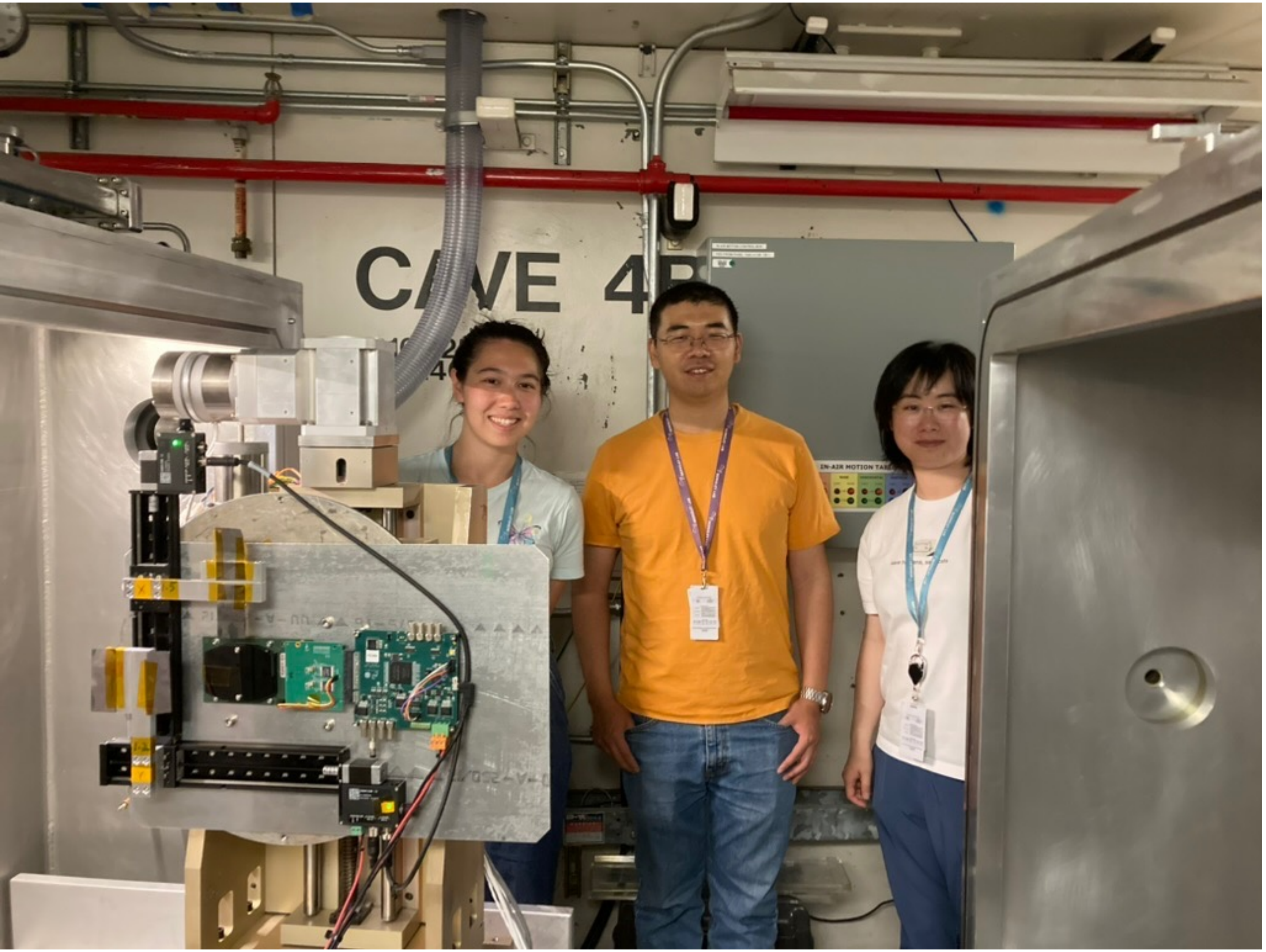

ALPIDE Single Event Upset

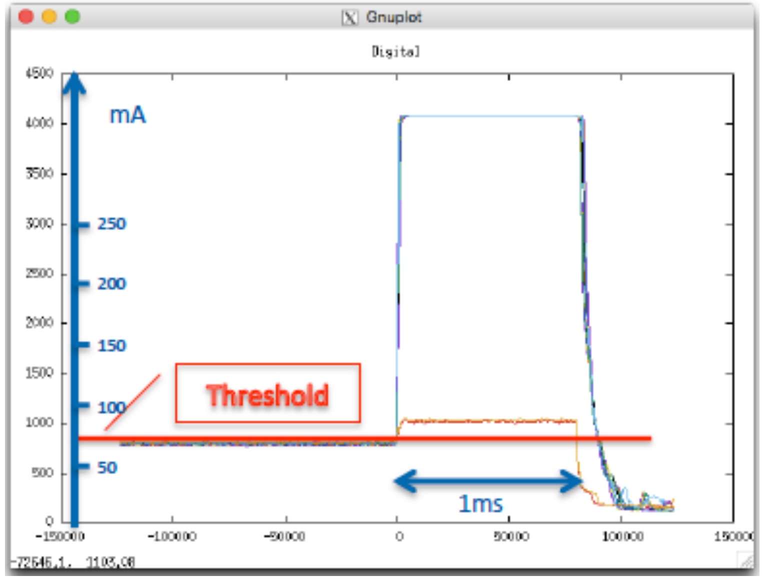

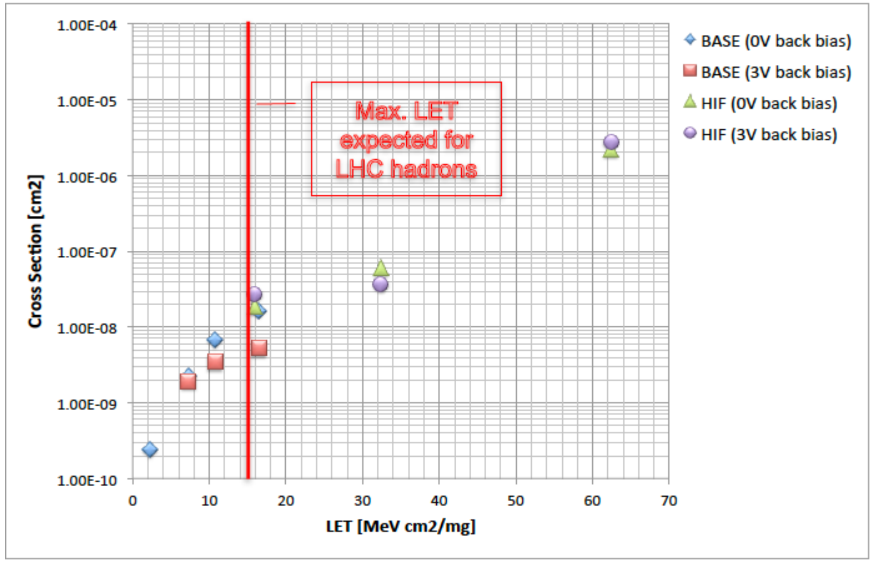

UCB: Barbara Jacak, Beatrice Liang-Gilman, Anjali Nambrath, Emma Yeats; **LBL:** Yu Hu, Shujie Li, Zhenyu Ye; **CERN:** Hartmut Hillemanns; **KU:** Nicola Minafra; **UC Riverside:** Barak Schmookler

ePIC Tracking and Vertexing Detectors

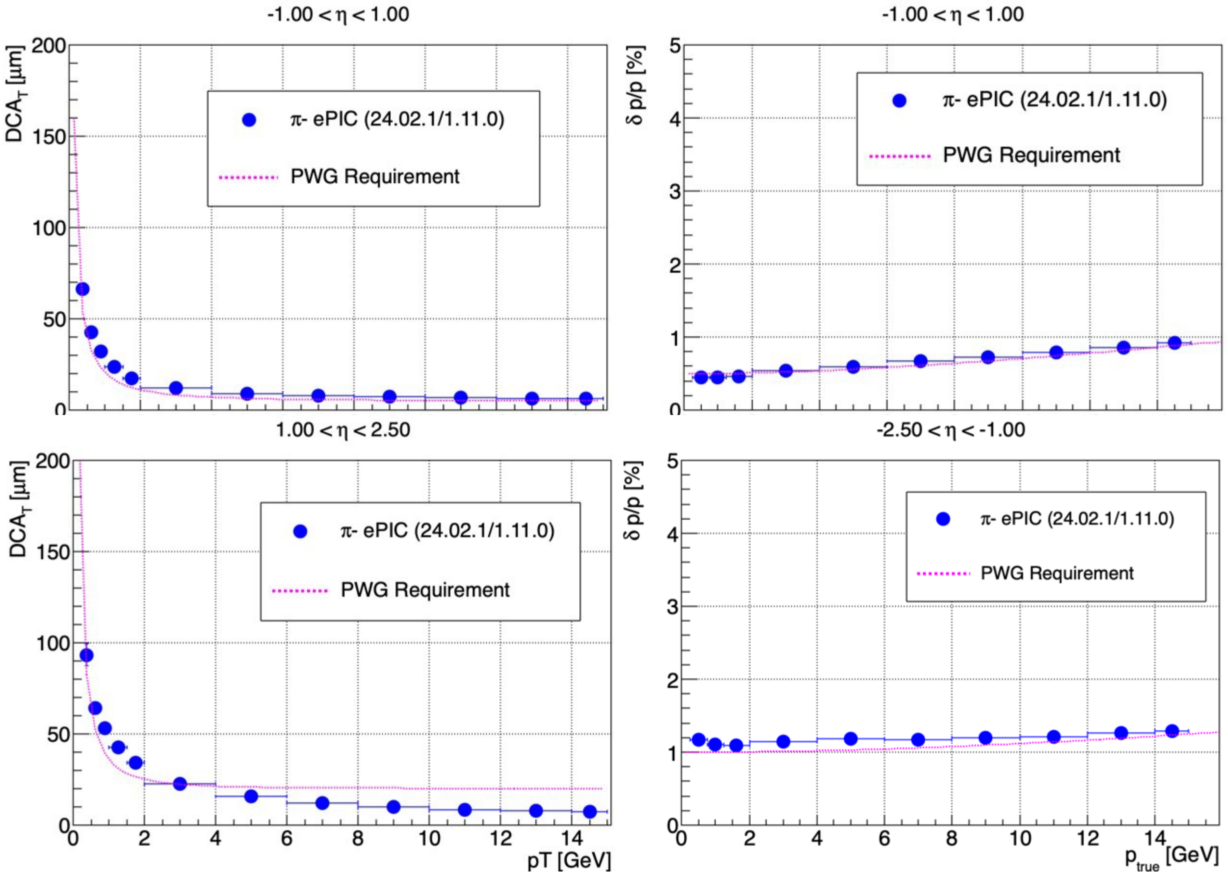

Rapidity Range	Momentum Resolution	Spatial Resolution
Backward (-3.5 to -2.5)	~0.10%×p ⊕ 2.0%	~30/pT μm ⊕ 40μm
Backward (-2.5 to -1.0)	~0.05%×p ⊕ 1.0%	~30/pT μm ⊕ 20μm
Barrel (-1.0 to 1.0)	~0.05%×p ⊕ 0.5%	~20/pT μm ⊕ 5μm
Forward (1.0 to 2.5)	~0.05%×p ⊕ 1.0%	~30/pT μm ⊕ 20μm
Forward (2.5 to 3.5)	~0.10%×p ⊕ 2.0%	~30/pT μm ⊕ 40μm

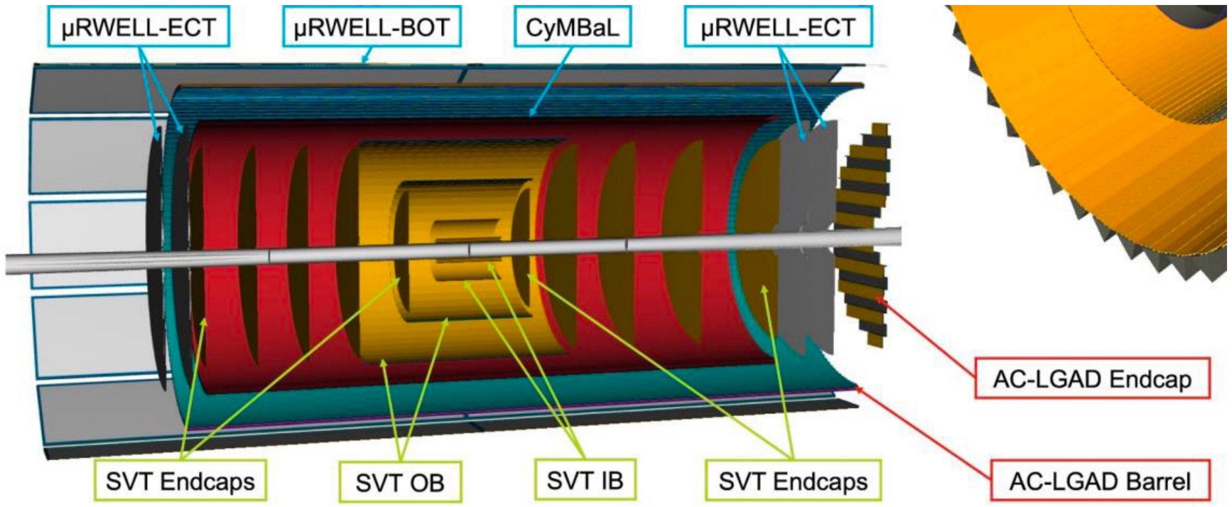

Silicon Vertex Tracker (SVT): ~6 μm point resolution

- **3 inner barrels**: ITS3-curved wafer-scale sensor, 0.05% X/X_0
- **2 outer barrels**: ITS3-based sensors (EIC-LAS), 0.25/0.55% X/X_0
- **5 disks** (forward/backward), EIC-LAS, 0.25% X/X_0

AC-coupled LGAD TOF: 30 μm + 30 ps resolutions

- Barrel TOF: 0.05 x 1 cm strip, 1% X/X_0
- Forward TOF: 0.05 x 0.05 cm pixel, 5% X/X_0

Multi Pattern Gas Detectors (MPGD):10 ns+150 μm resolutions

- **2 GEM-μRwell endcaps**: 1-2% X/X0
- **1 inner Micromegas barrel**: 0.5% X/X0
- **1 outer GEM-μRwell planar layer + Barrel ECAL AstroPix**: improve angular and space point resolution on hpDIRC

ePIC Silicon Vertex Tracker – Barrel Layers

Inner barrels (L0-L2) inspired by ITS3

- Same sensor as ALICE ITS3 with thinned, curved, self-supporting wafer-scale MAPS sensors
- Pixel pitch O(20×22.5) μm^2; power consumption 40 mW/cm^2; integration time 2 μs;
- Radii of 36, 48, and 120 mm; length of 27 cm
- X/X_0 ~0.05%

Outer barrels (L3, L4)

- **EIC large area sensors (EIC-LAS)** with design modified based on ITS3, mounted on more conventional staved structure with CF support and integrated air/water cooling
- **AncASIC** for sensor bias, serial power and slow control
- Radii of 27 and 42 cm; lengths of 42 and 84 cm
- X/X_0 ~0.25% and 0.55%

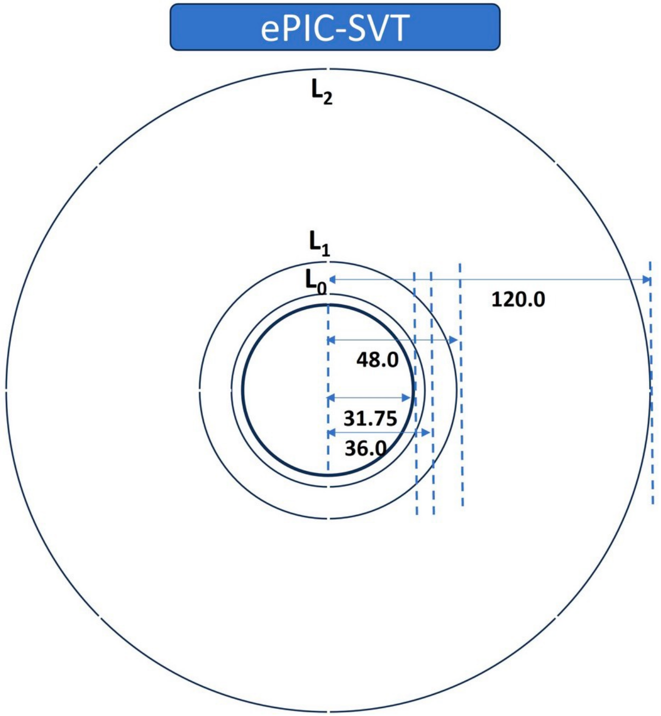

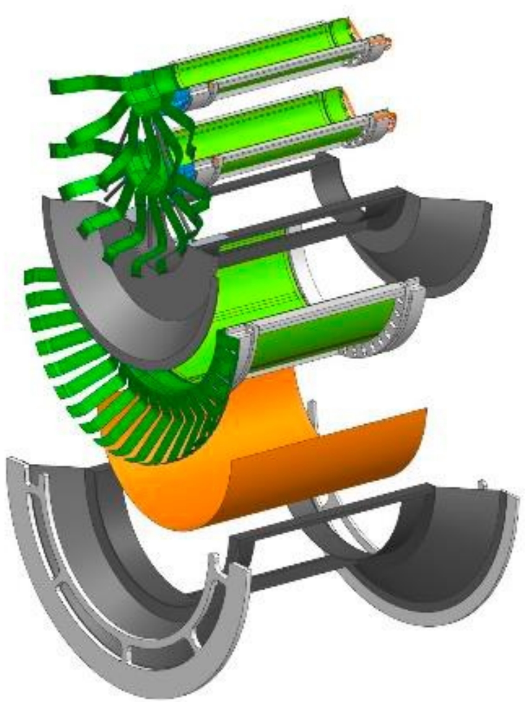

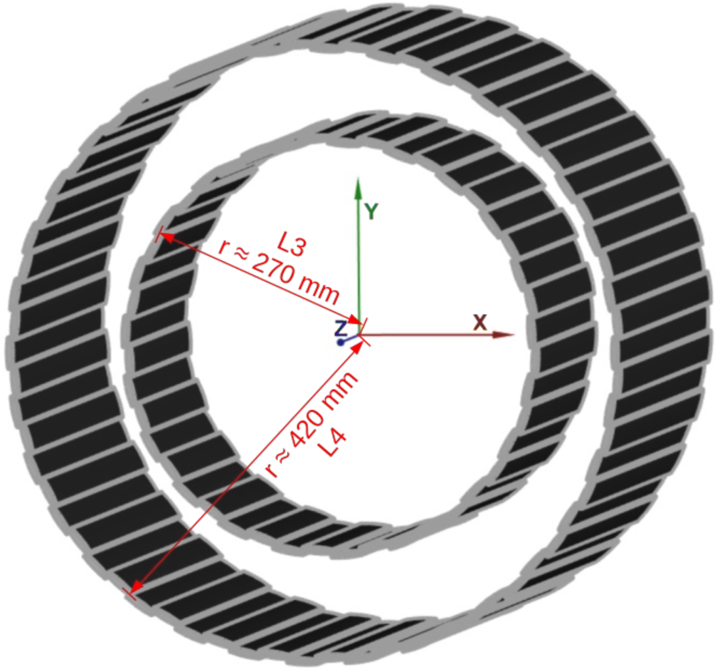

ePIC Silicon Vertex Tracker – Disks

Disks (5 electron + 5 hadron going direction):

- **EIC large area sensors (EIC-LAS)** with design modified based on ITS3, mounted on conventional structure with CF support and integrated air cooling
- **AncASIC** for sensor bias, serial power and slow control
- Outer radii of 25 and 40 cm
- X/X_0 ~0.25%

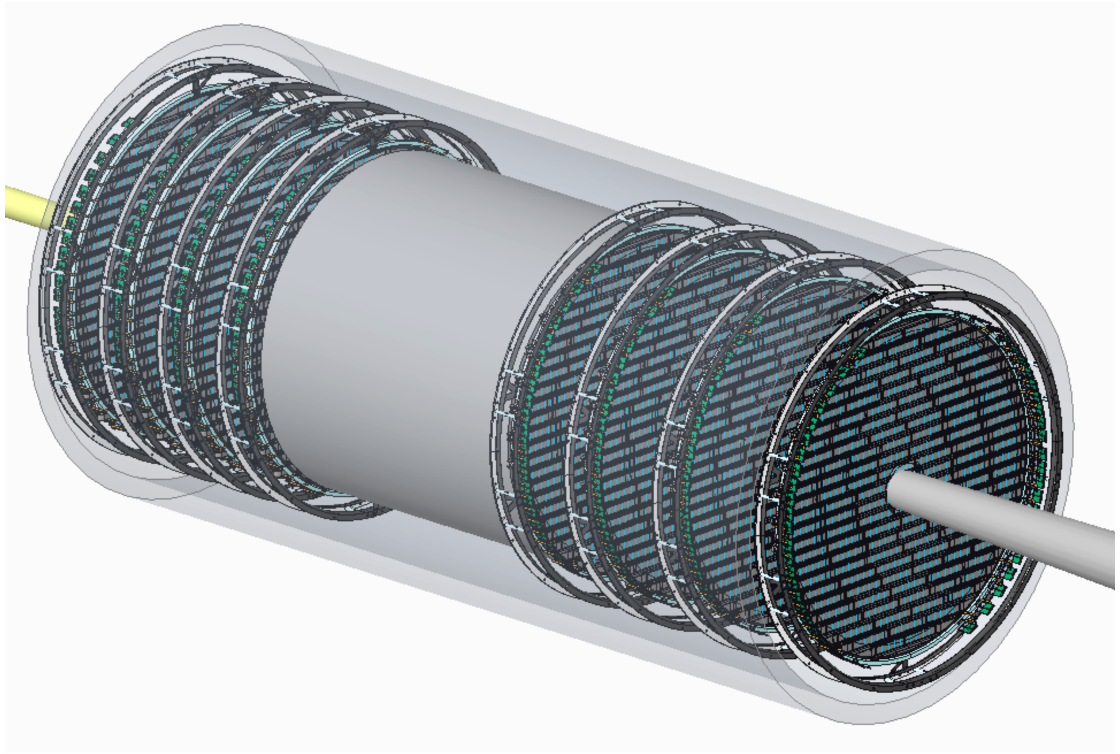

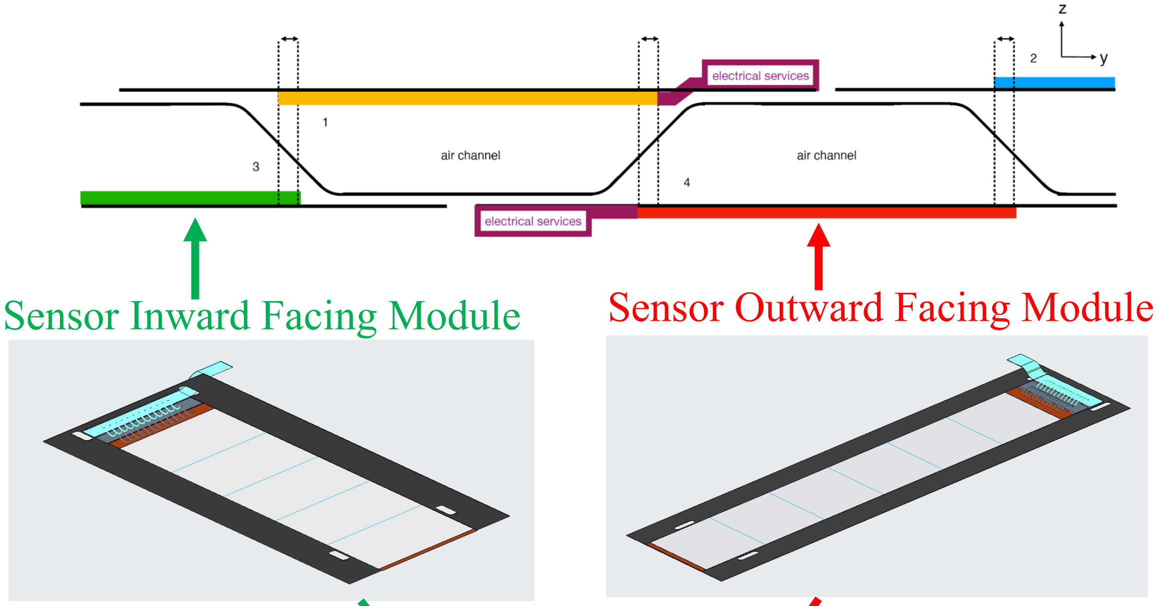

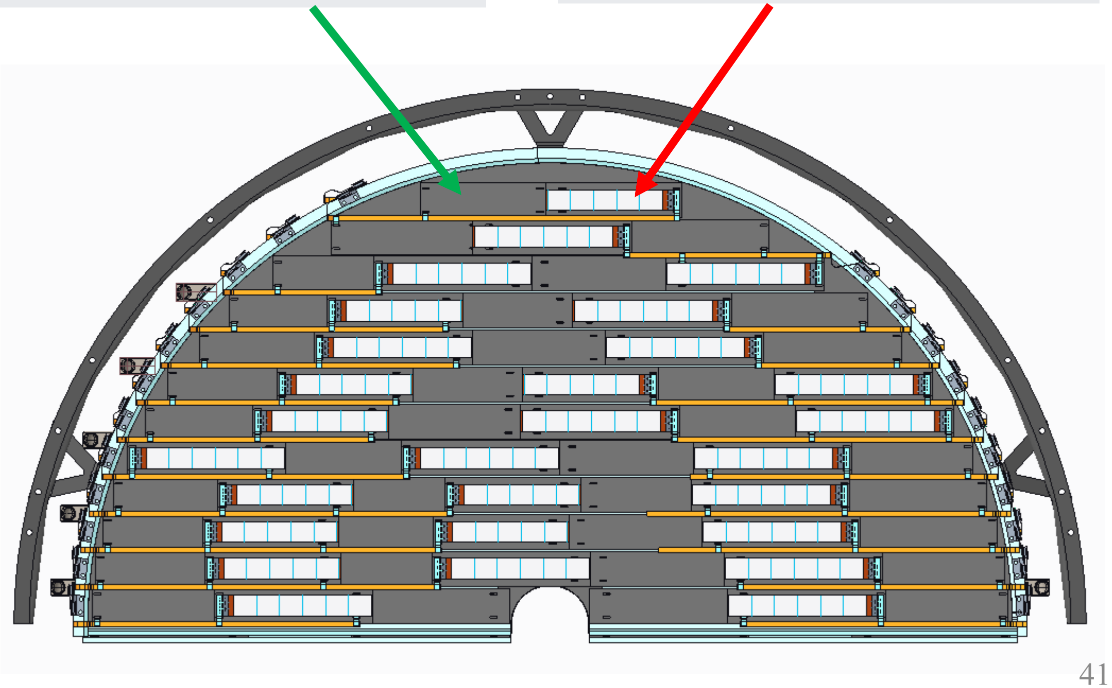

Particle Identification

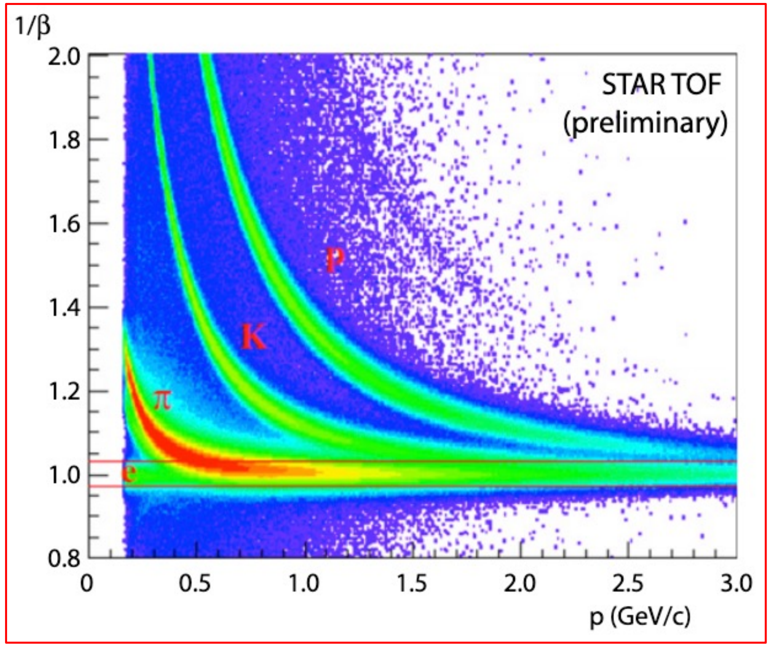

Time of Flight

$$1/\beta = t/L = \sqrt{1 + \left(\frac{mc}{p}\right)^{-2}}$$

Particle Identification

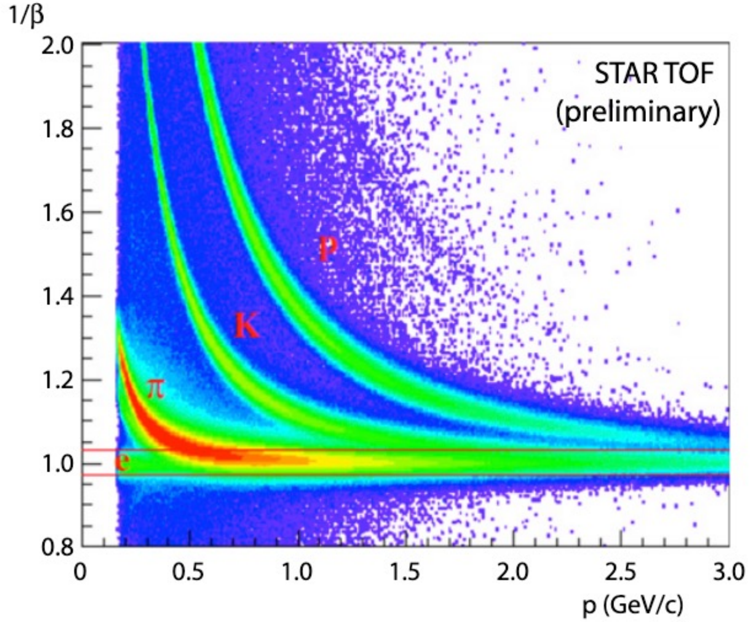

Time of Flight

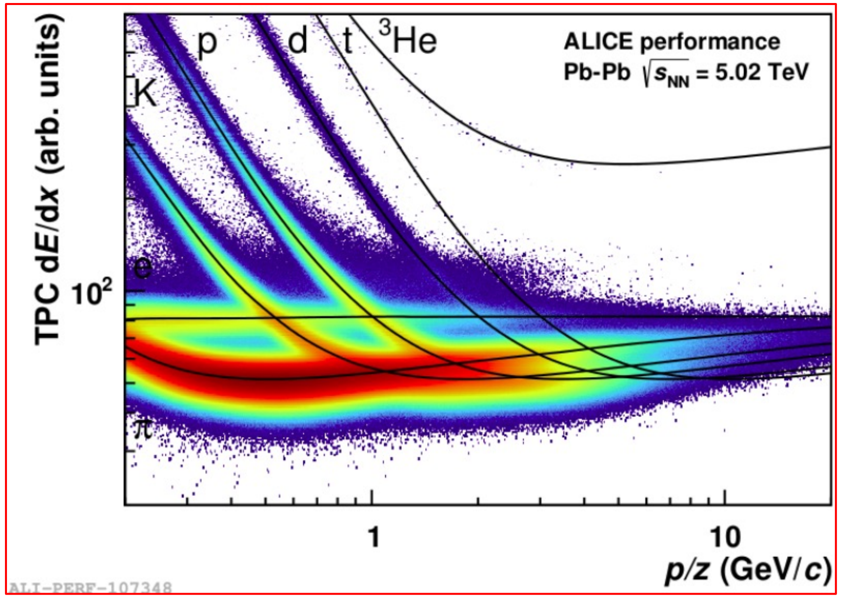

dE/dx

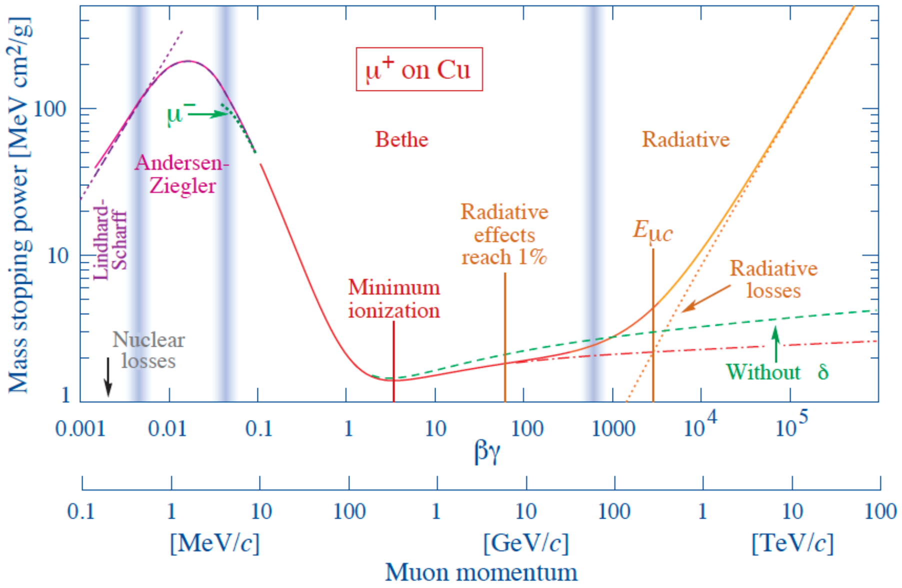

$$\left\langle -\frac{dE}{dx} \right\rangle = K z^2 \frac{Z}{A} \frac{1}{\beta^2} \left[\frac{1}{2} \ln \frac{2 m_e c^2 \beta^2 \gamma^2 W_{\max}}{I^2} - \beta^2 - \frac{\delta(\beta\gamma)}{2} \right]$$

Particle Identification

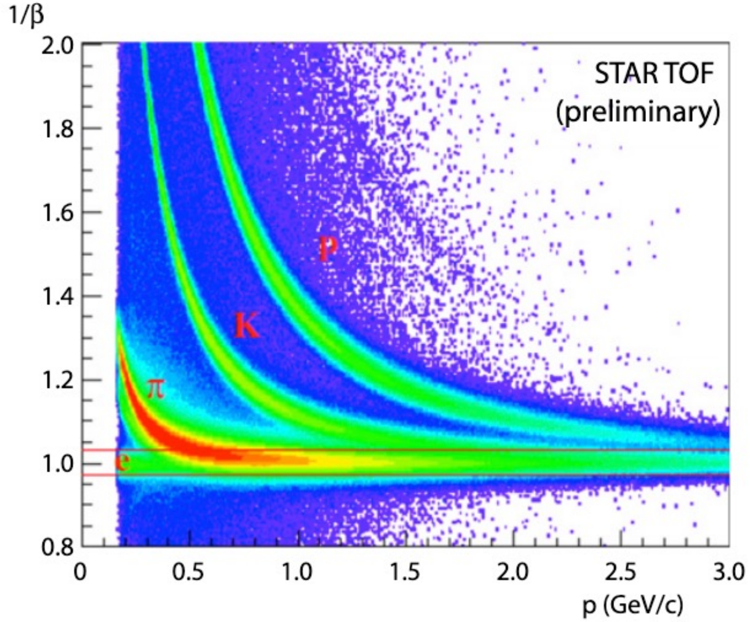

Time of Flight

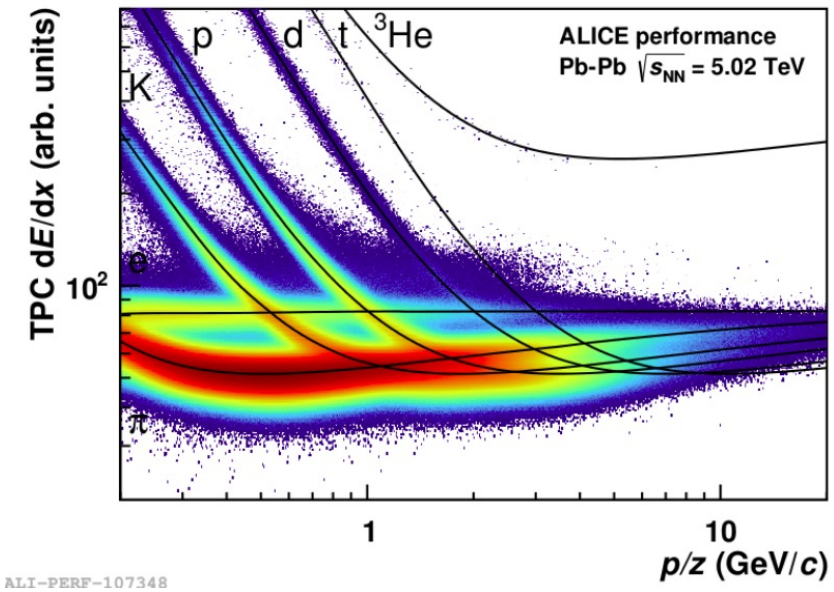

dE/dx

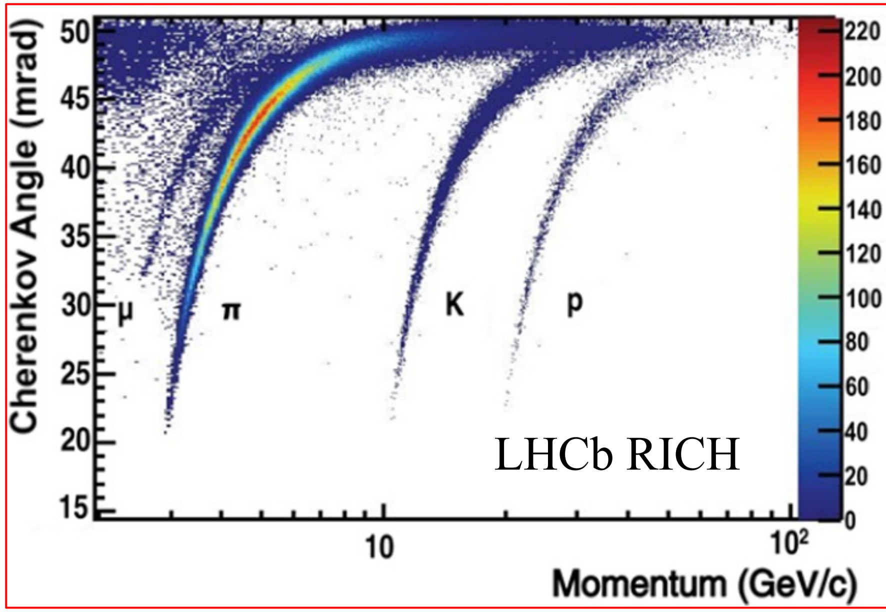

Cherenkov Radiation

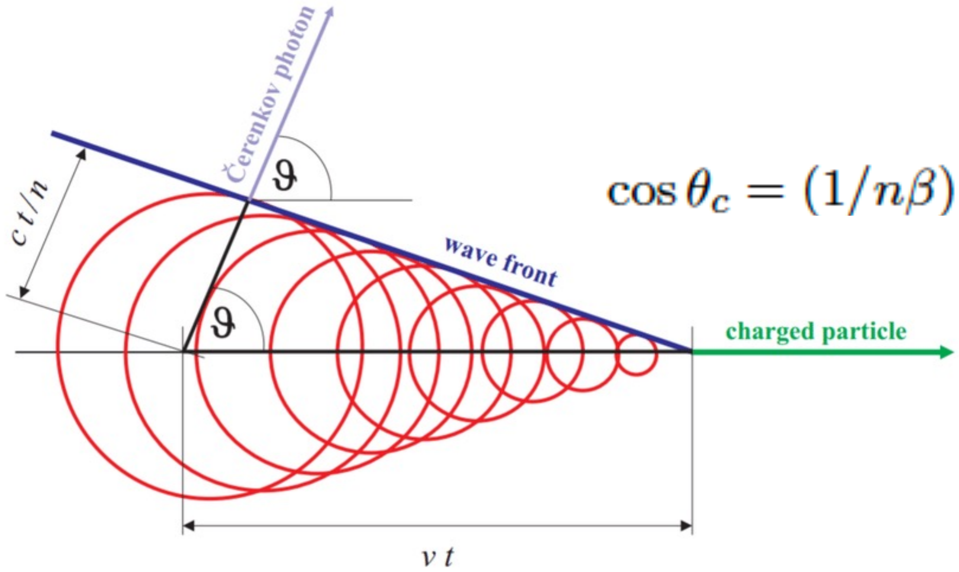

$$\cos\theta_c = (1/n\beta)$$

ePIC PID Detectors

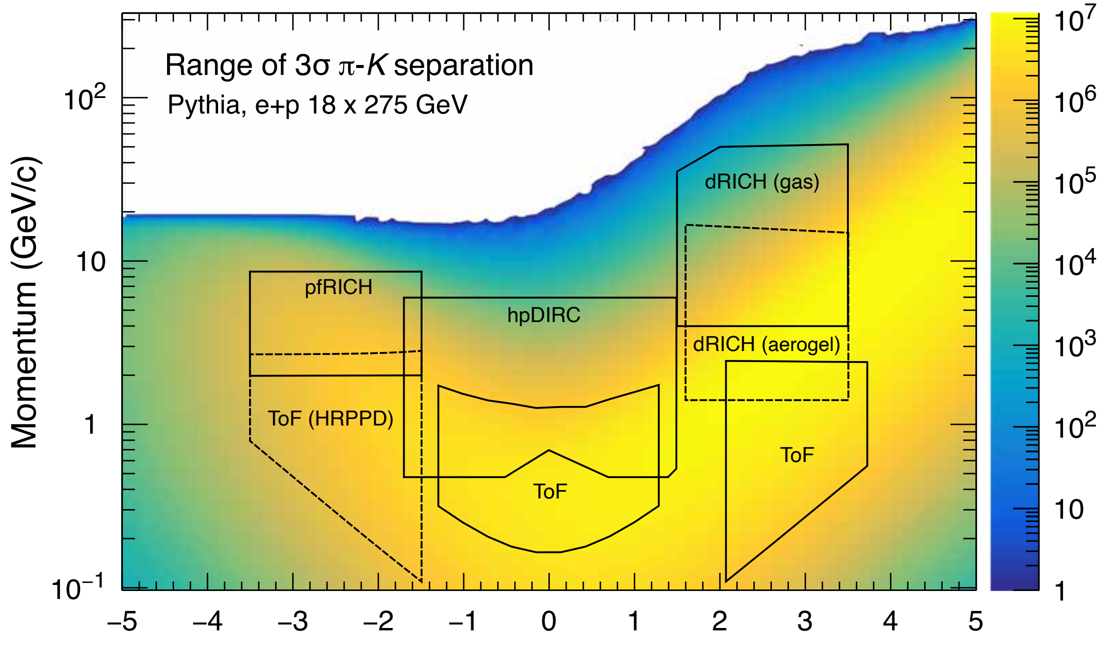

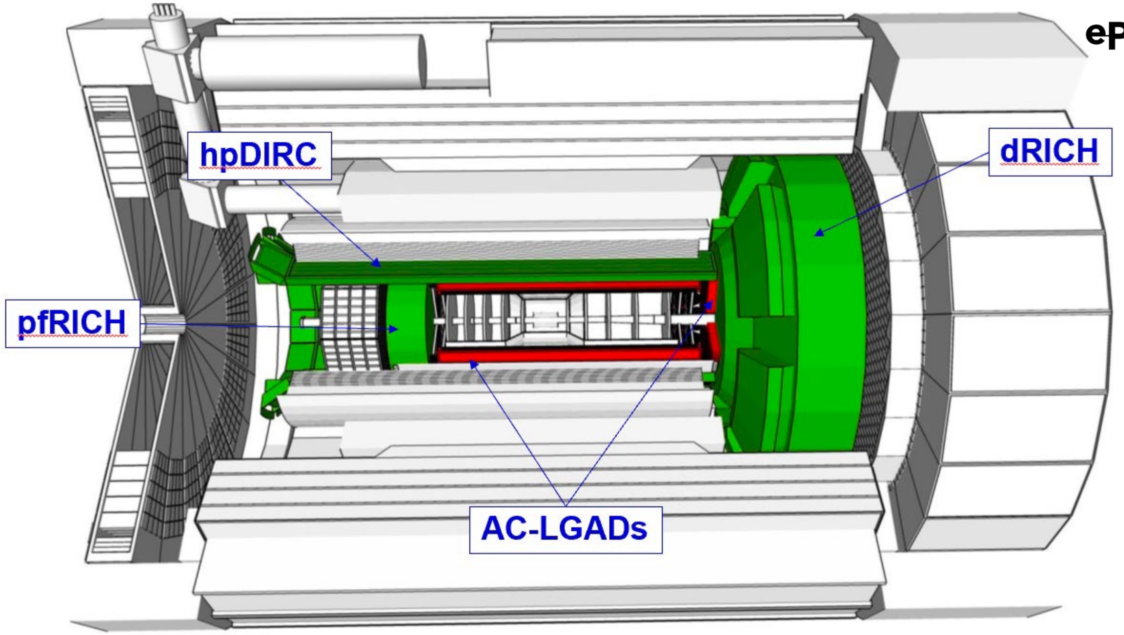

Time-of-Flight: AC-LGAD

- Backward: HRPPD with 10-20 ps resolution
- Barrel: AC-LGAD strip sensors with 35 ps resolution
- Forward: AC-LGAD pixel sensors with 25 ps resolution

dRICH: dual radiator RICH

- Aerogel and C_2F_6 gas with SiPM for light detection

pfRICH: proximity focusing RICH

- Single volume with long proximity gap (~30 cm), using Aerogel as radiator and HRPPD as photon sensors

hPDIRC: high performance DIRC

- Quartz bar radiator (BABAR bars reuse) with MCP-PMT

dRICH

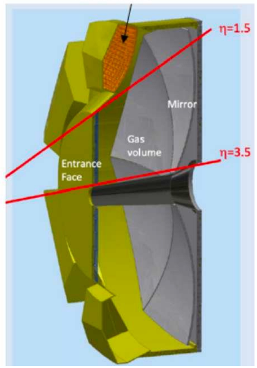

hpDIRC

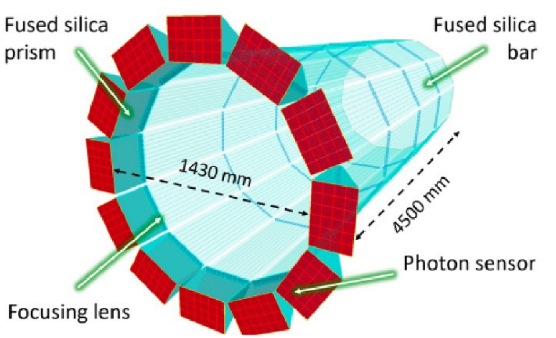

pfRICH

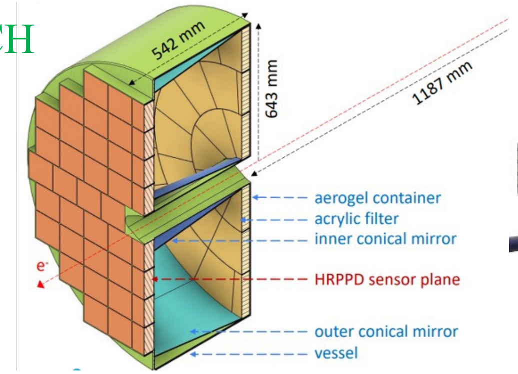

AC-LGAD TOF

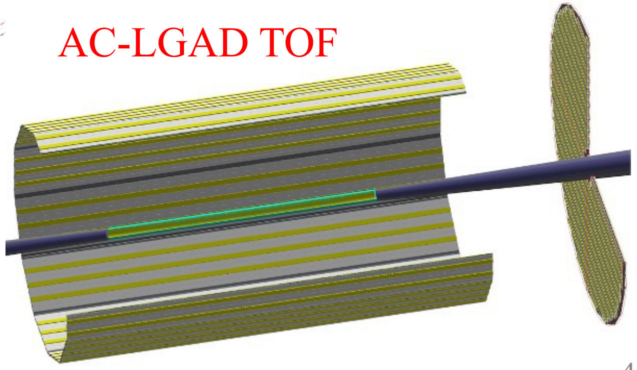

ePIC AC-LGAD TOF Detectors

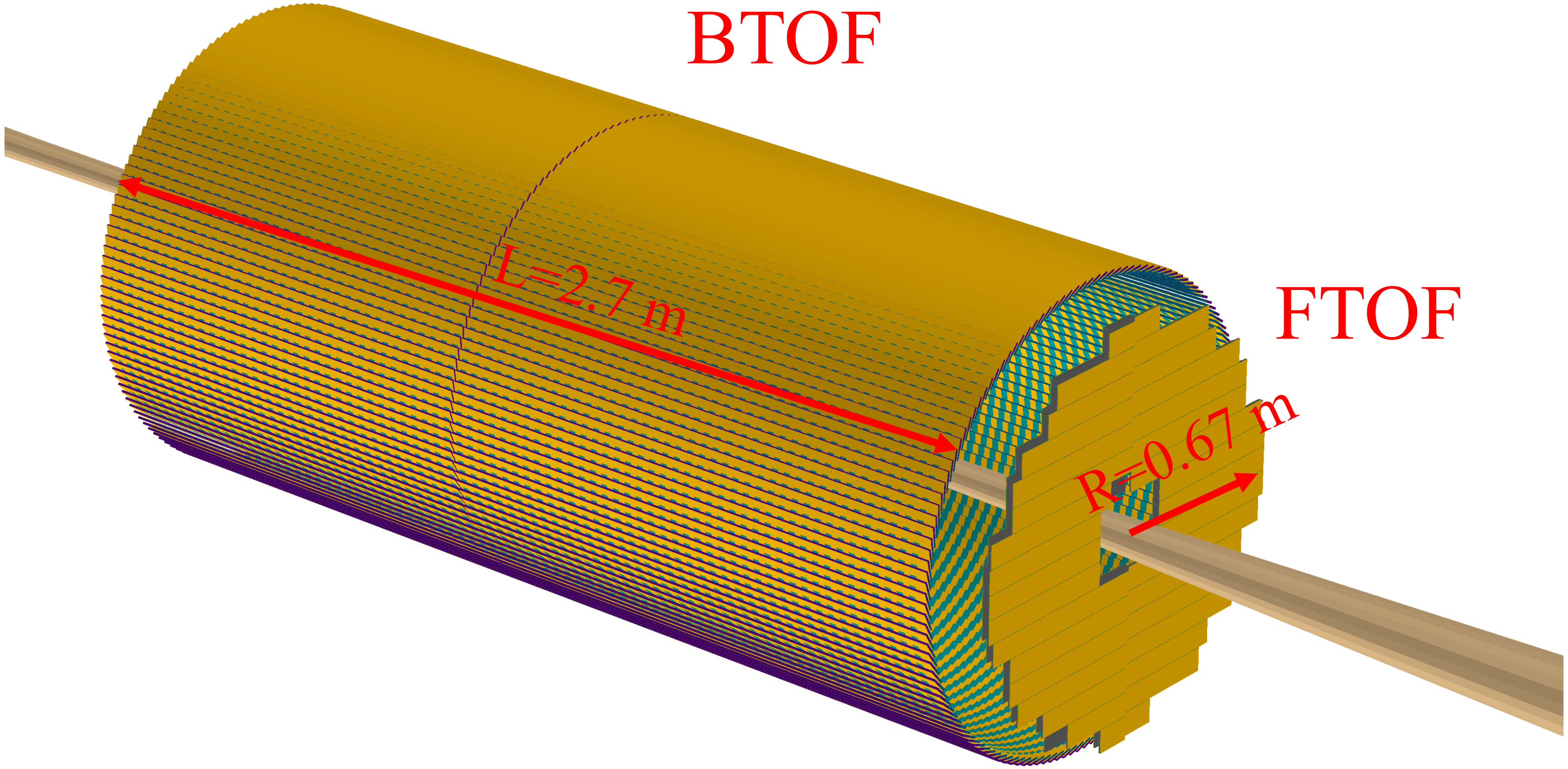

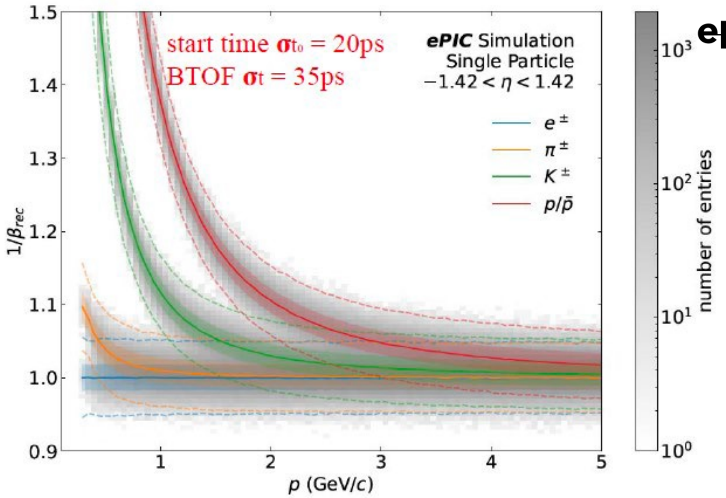

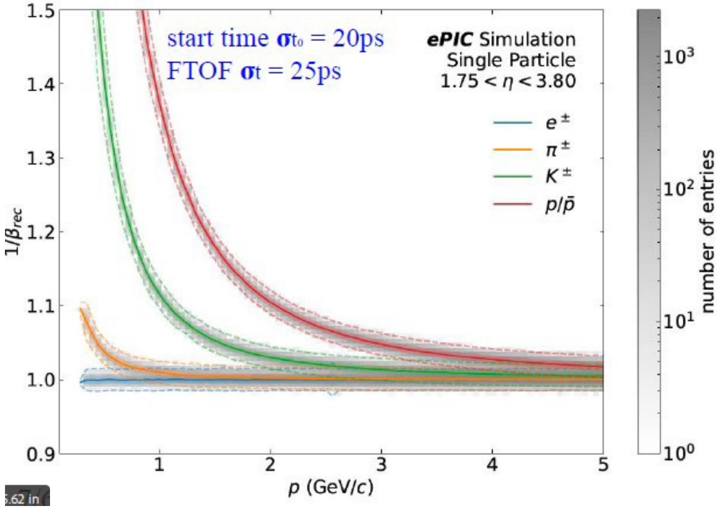

	Area (m^2)	Channel size (mm^2)	# of Channels	Timing Resolution	Spatial resolution	Material budget
Barrel TOF	10	0.5*10	2.4M	35 ps	30 μm in $r \cdot \varphi$	0.01 X_0
Forward TOF	1.4	0.5*0.5	5.6M	25 ps	30 μm in x and y	0.05 X_0
B0 tracker	0.07	0.5*0.5	0.28M	30 ps	20 μm in x and y	0.05 X_0
RPs/OMD	0.14/0.08	0.5*0.5	0.56M/0.32M	30 ps	140 μm in x and y	no strict req.

Time-of-Flight Measurements

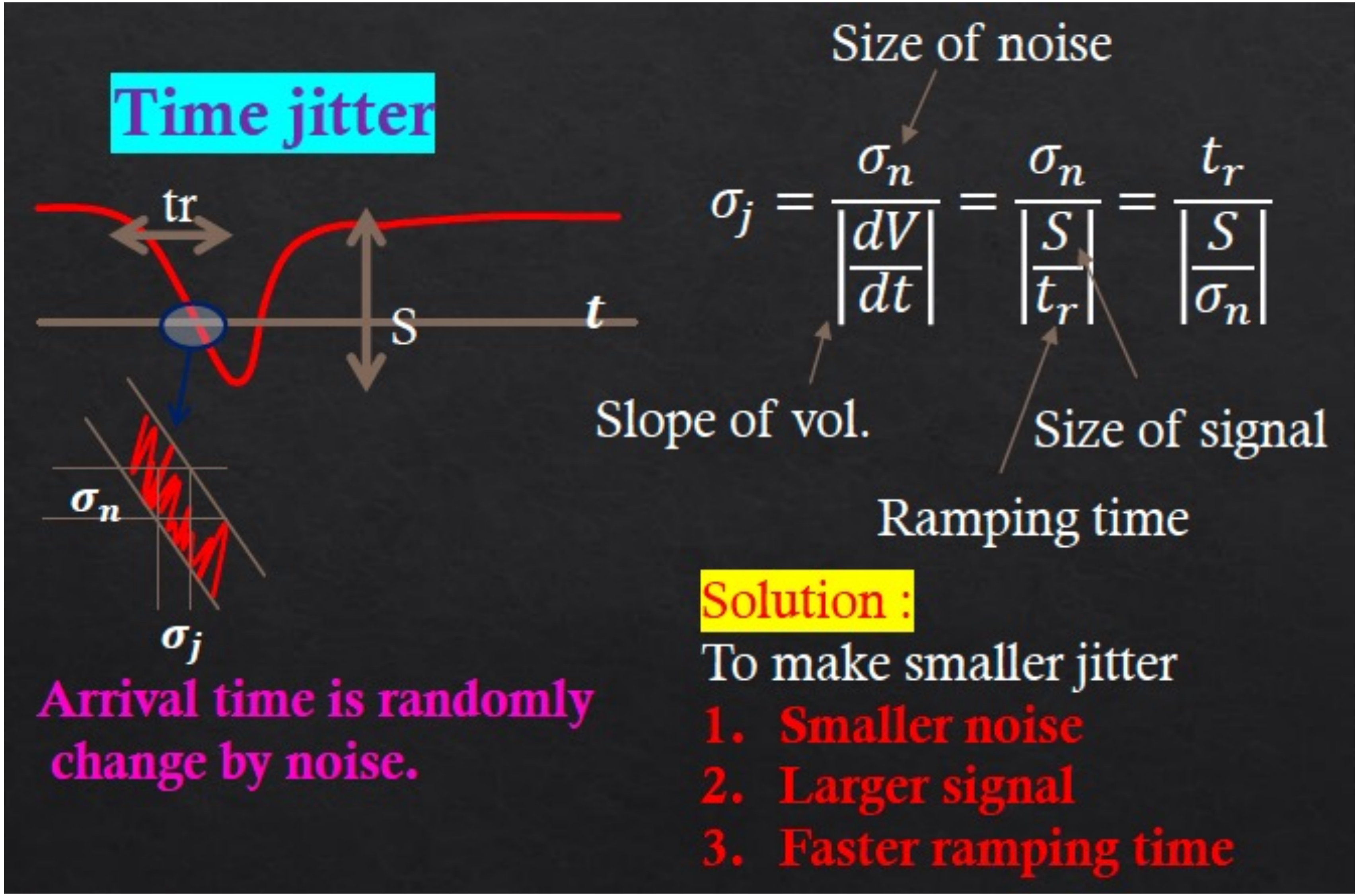

Low Gain Avalanche Diode

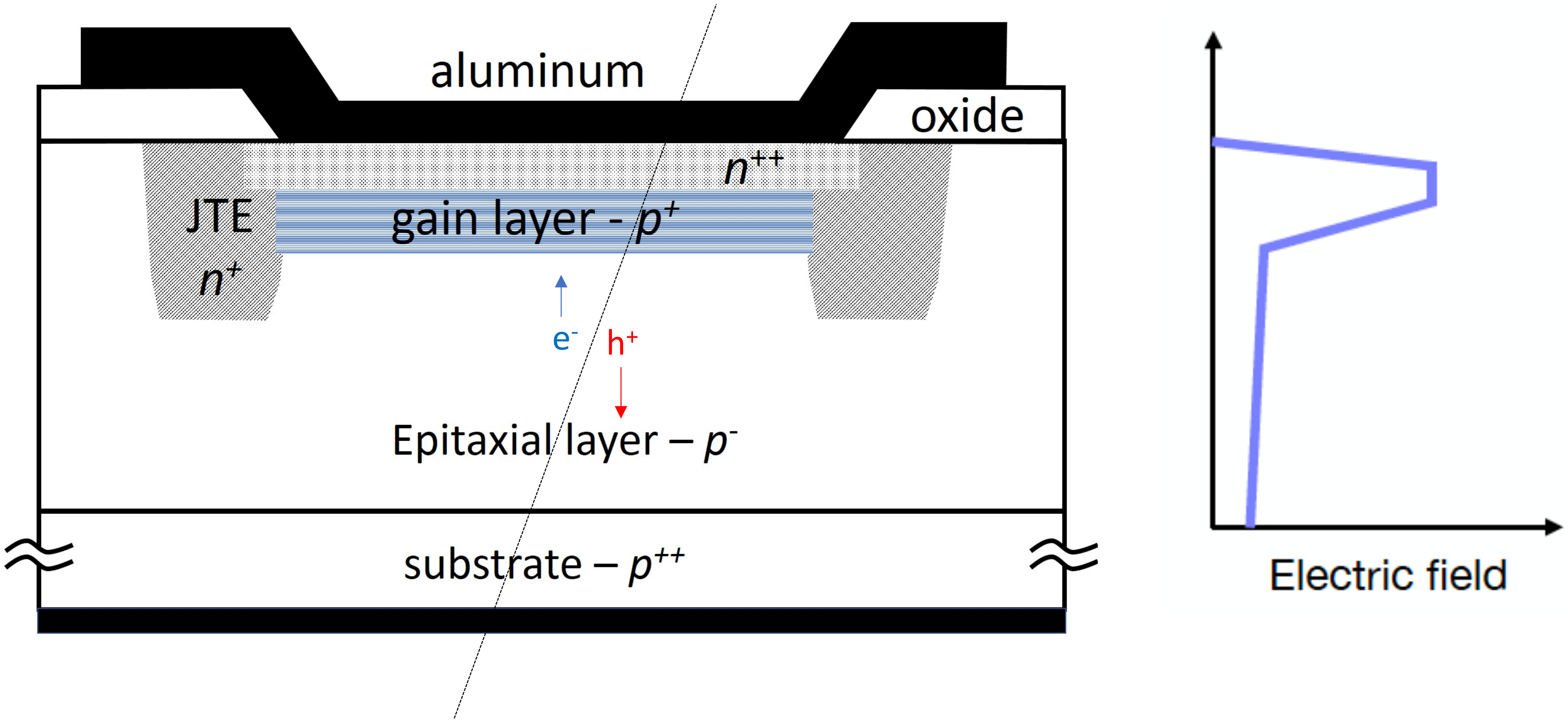

Ultra-fast silicon detectors with a highly doped p+ gain layer
Moderate internal gain : 10-30

LGAD Sensor

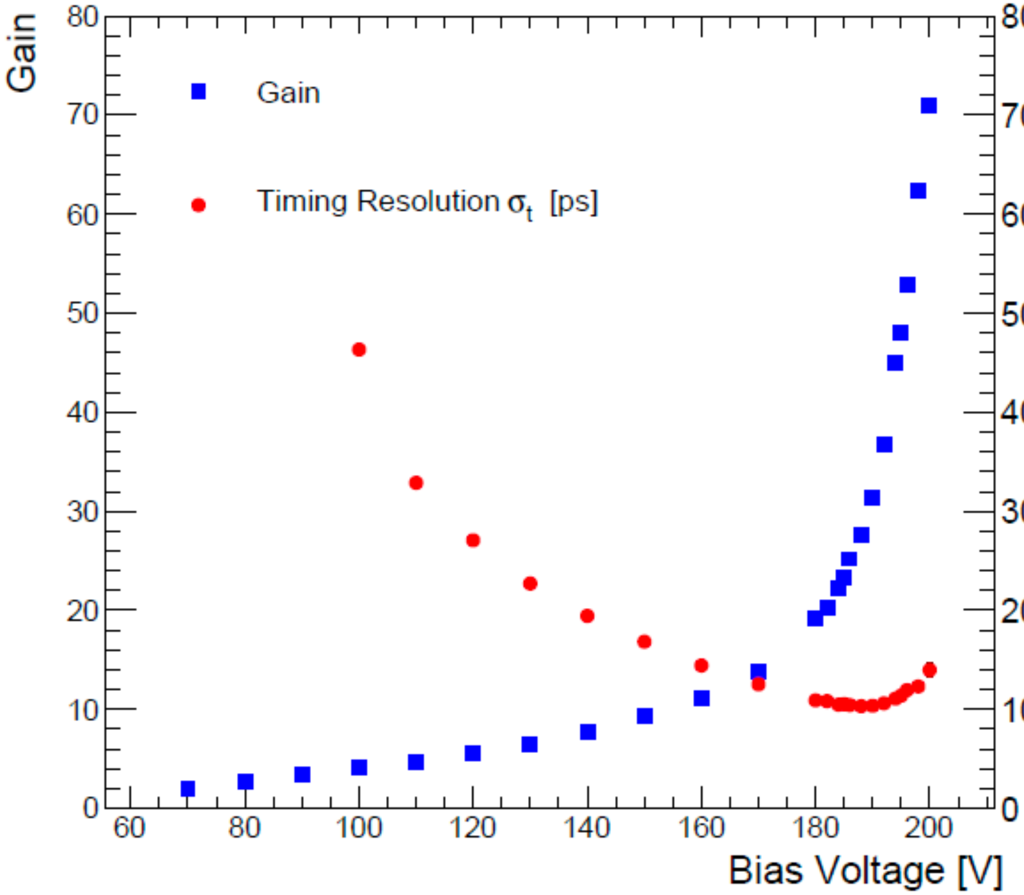

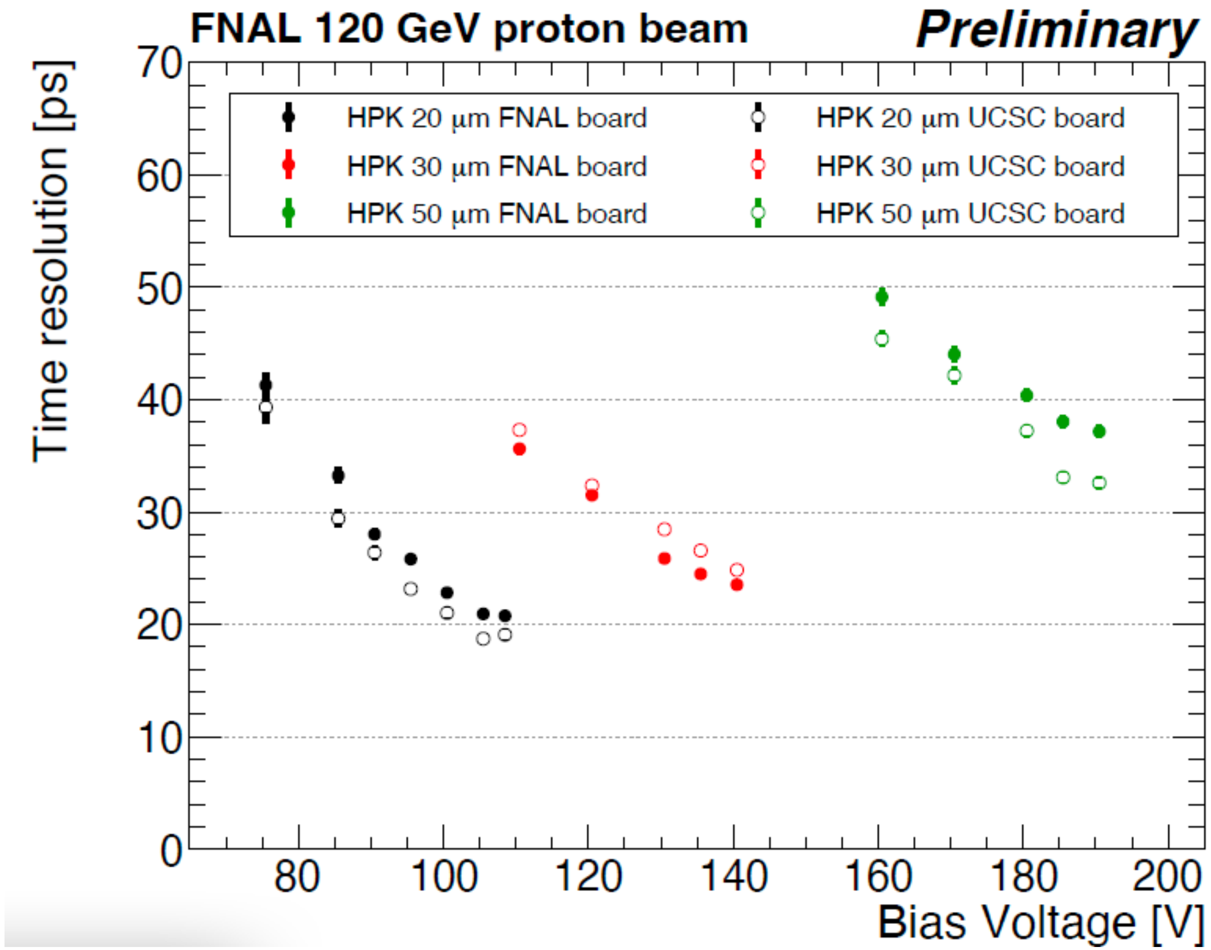

LGAD Wafer

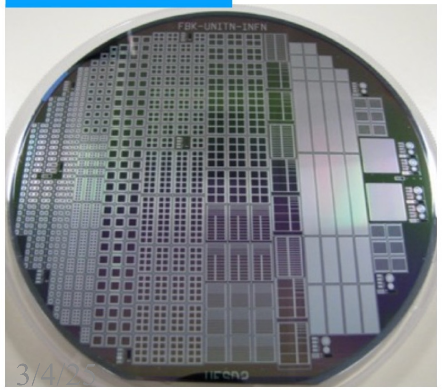

$$\sigma_t = \sigma_{avalanche} + \sigma_{charge\text{-}collection} + \sigma_{pre\text{-}amp\text{-}jitter} + \sigma_{comp\text{-}jitter} + \sigma_{timewalk} + \sigma_{tdc}$$

Sensor related noise

Readout ASIC related noise

LGAD Sensor

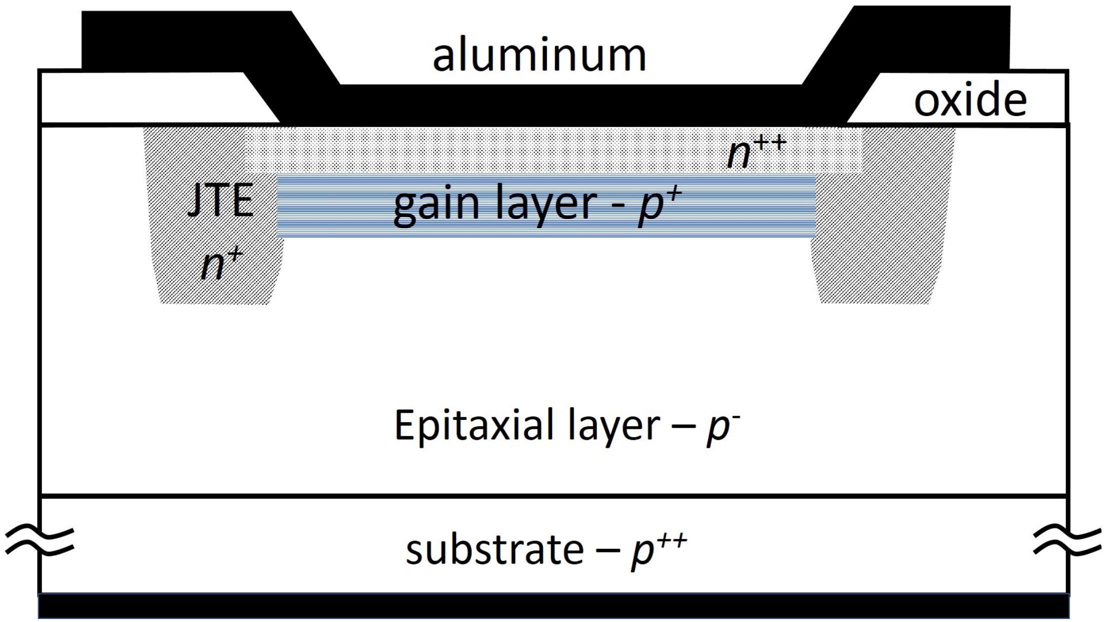
aluminum
oxide
n^{++}
JTE
gain layer - p^{+}
n^{+}
Epitaxial layer – p^{-}
substrate – p^{++}

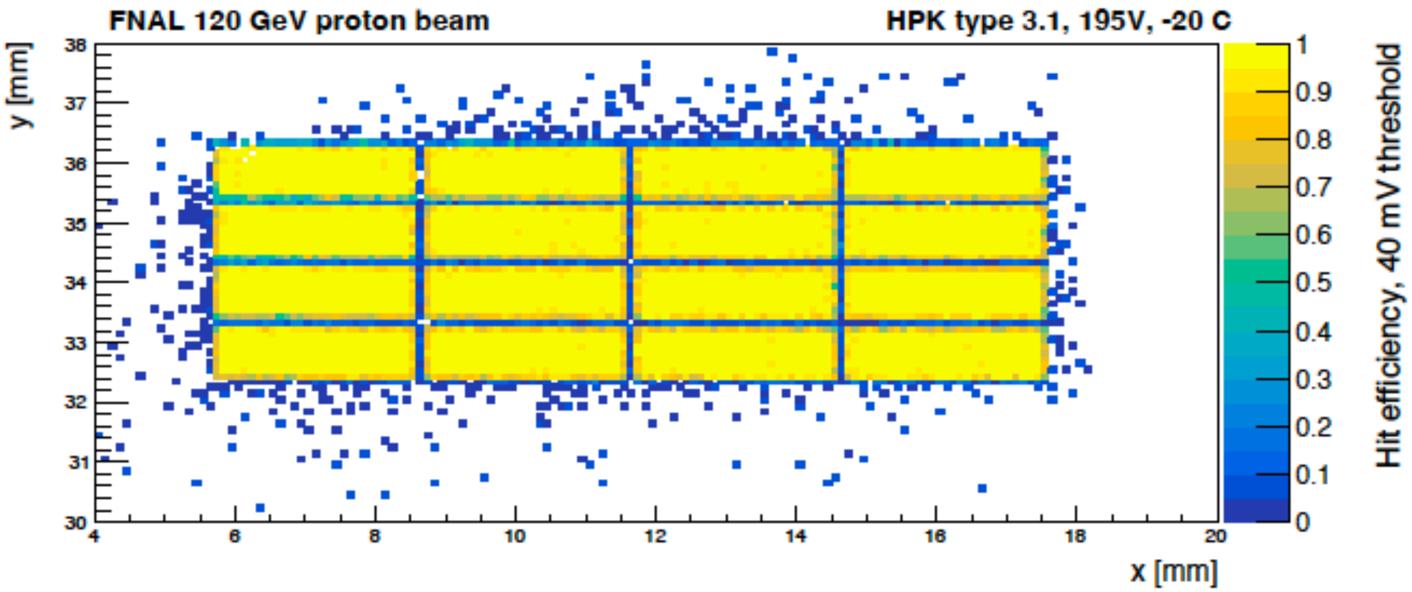
FNAL 120 GeV proton beam
HPK type 3.1, 195V, -20 C
y [mm]
x [mm]
Hit efficiency, 40 mV threshold

AC-Coupled LGAD Sensor

- Due to the presence of JTE and the gap between LGAD cells, 100% fill factor can not be achievec in LGAD. The position resolution is limited to be $\sqrt{1/12}$ of cell size.

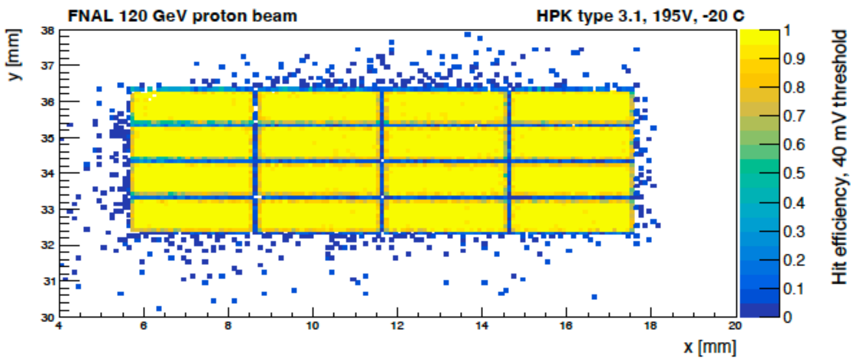

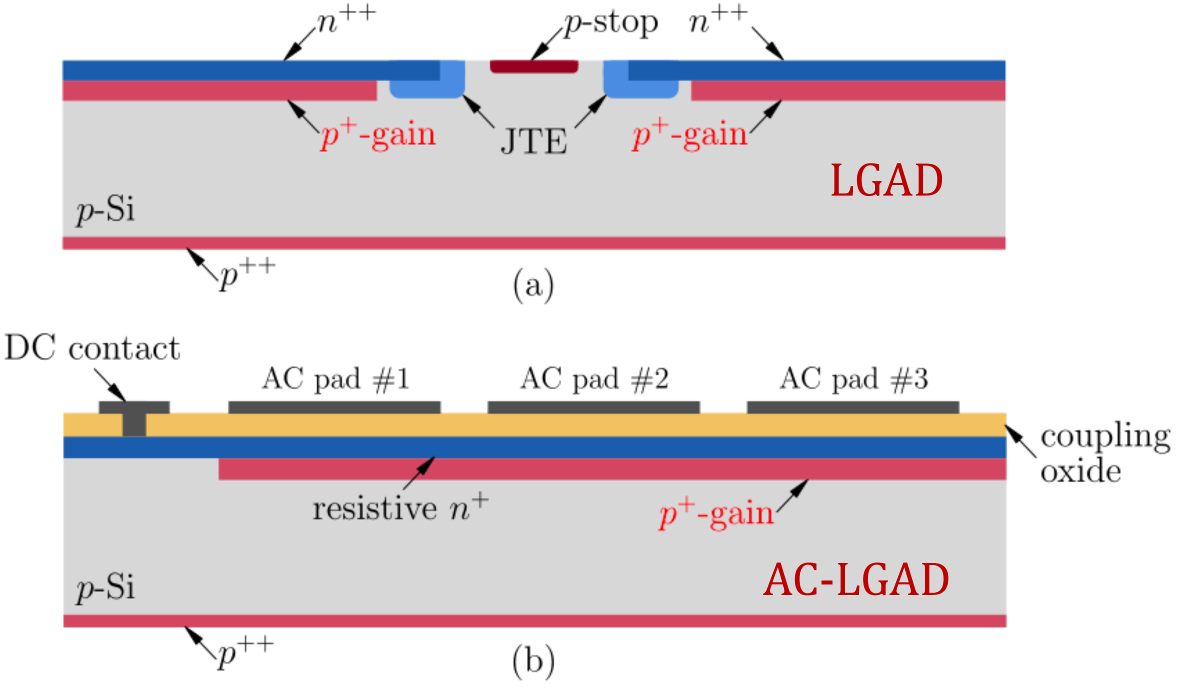

- AC-LGAD: replacement of the segmented n^{++} layer by a less doped but continuous n^+ layer. Electrical signals in the n^+ layer are AC-coupled to neighboring metal electrodes that are separated from the n^+ layer by a thin insulator layer.

- AC-LGAD not only provides a timing resolution of a few tens of picoseconds, but also 100% fill factor and a spatial resolution that are orders of magnitude smaller than the cell size. Therefore, it is a good candidate for 4D detectors at future high energy experiments.

ePIC AC-LGAD Sensor R&D

Fermilab Test Beam Setup

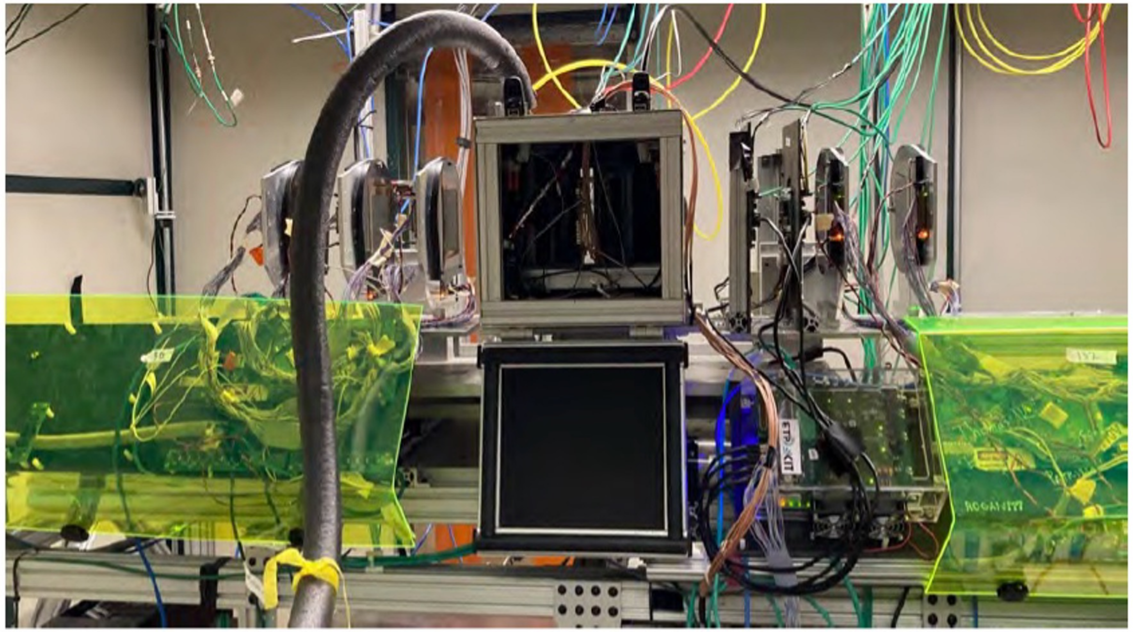

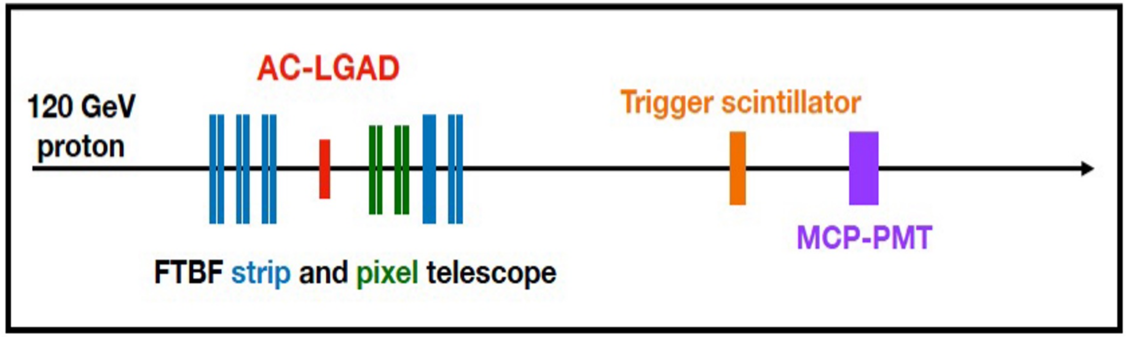

HPK Strip Sensor (4.5x10 mm²)

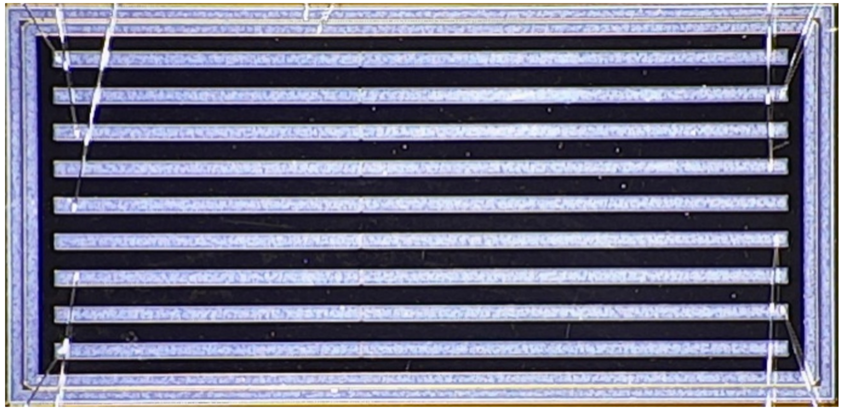

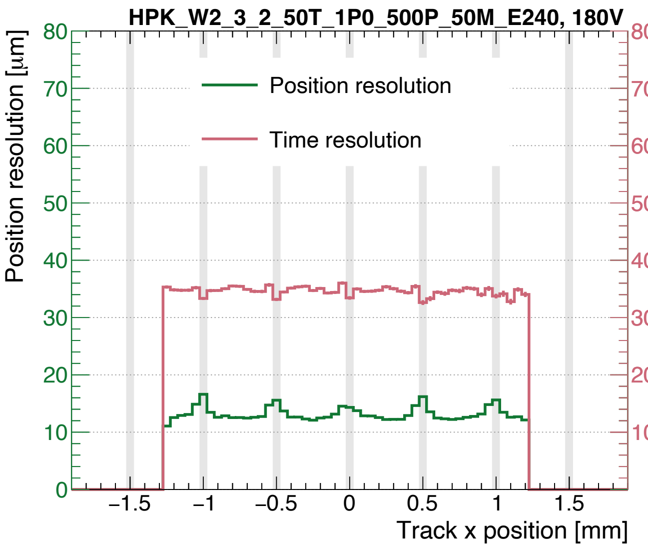

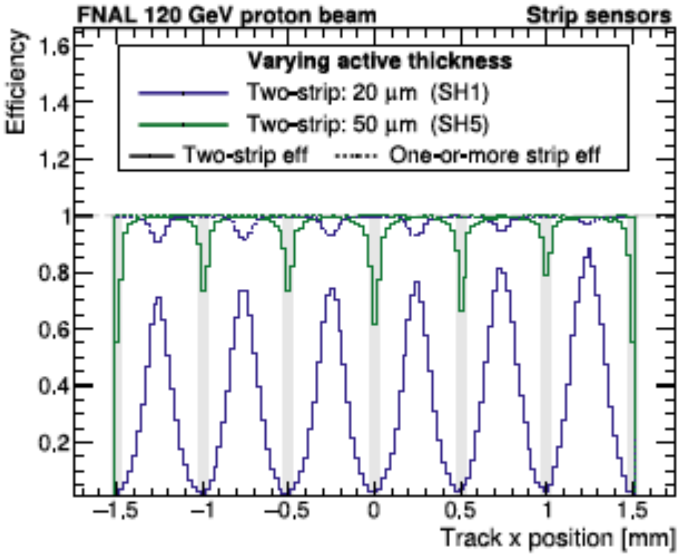

NIMA 1072 (2025) 170224

Leading Edge vs Constant Fraction Discriminator

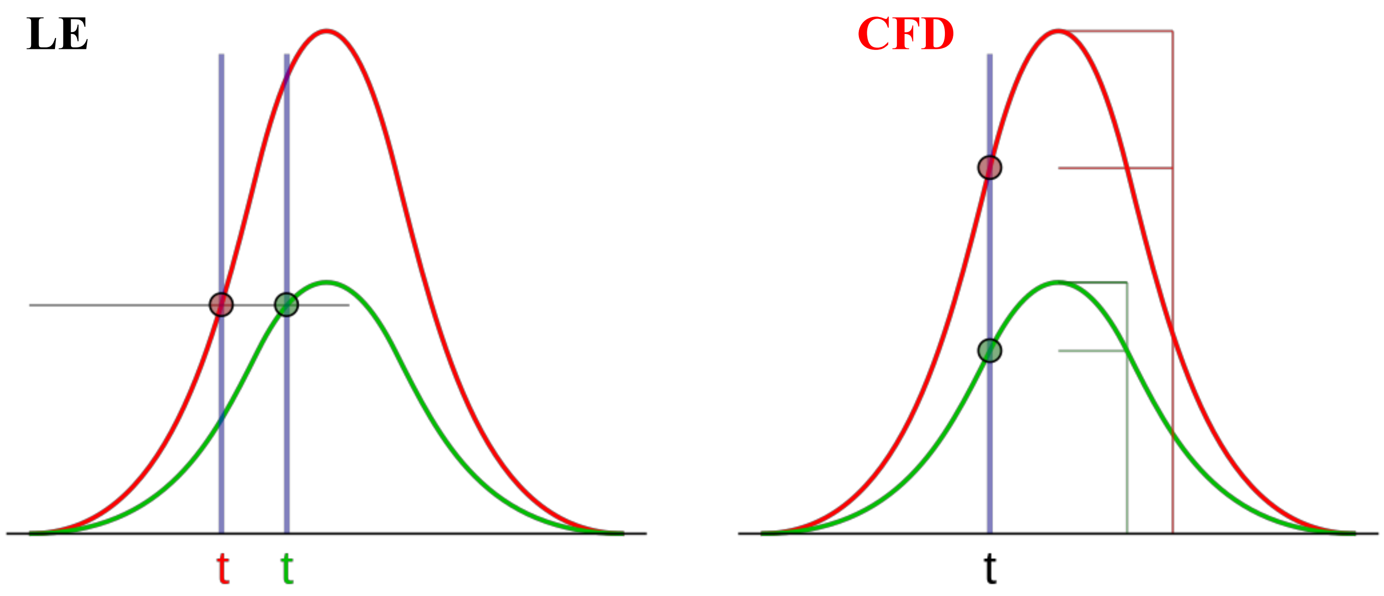

- Time cross the threshold of a LE discriminator dependent on signal amplitude
- Time cross the threshold of a CFD independent on signal amplitude with same signal shape

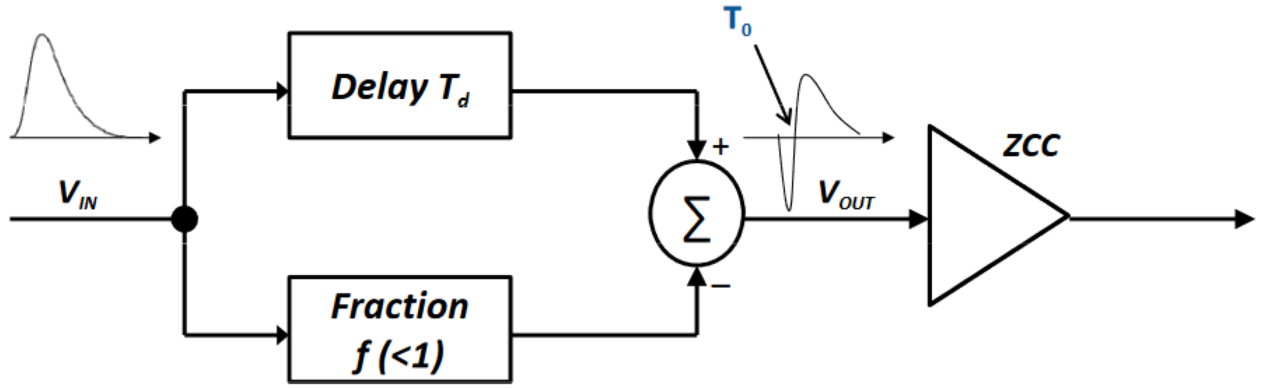

- CFD can be realized by adding the delayed signal and an inverted and scaled signal, and checking the zero-cross point

Leading Edge vs Constant Fraction Discriminator

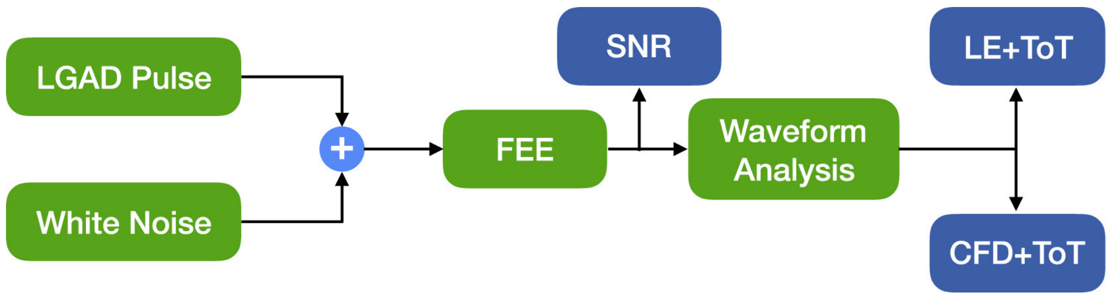

Simulation study [3] indicates that CFD outperforms LE in the timing resolution for LGAD

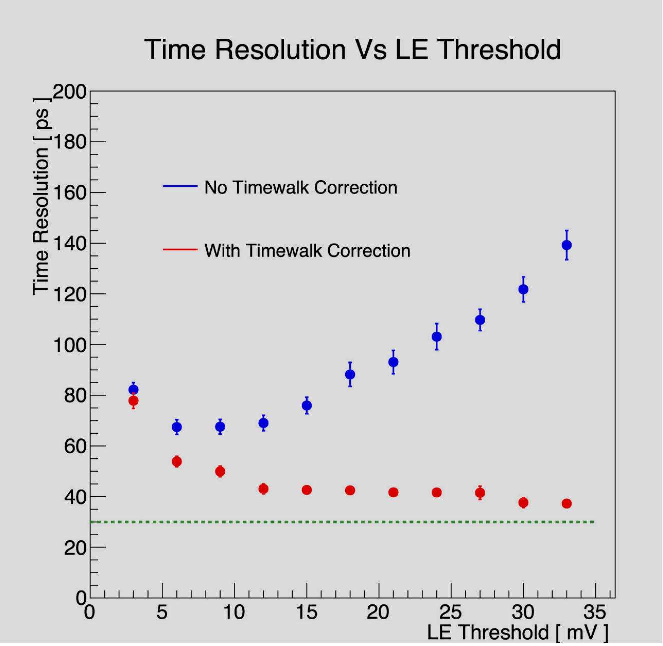

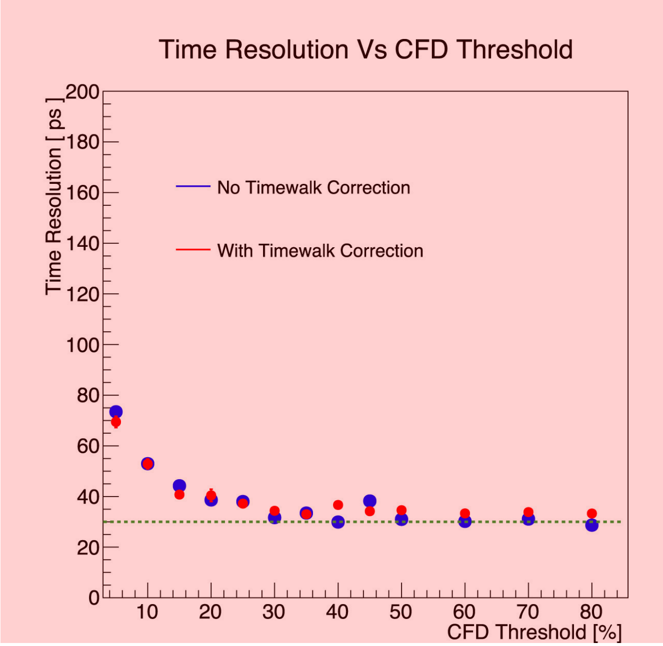

Table 2
50 µm pre-radiation LGAD sensor simulation: summary of best time resolution obtained for SNRs of 20, 30, and 100. Leading edge and constant fraction results are shown. The measured time resolutions have statistical uncertainty below 5%.

	Time resolution (ps)					
	Leading edge			Constant fraction (Ideal)		
ST (ns)	SNR = 20	SNR = 30	SNR = 100	SNR = 20	SNR = 30	SNR = 100
0.5	38	35	29	37	35	30
1.0	45	37	29	36	33	26
2.0	63	48	31	48	34	29
4.0	103	75	38	74	55	32

Fermilab CFD ASIC (FCFD)

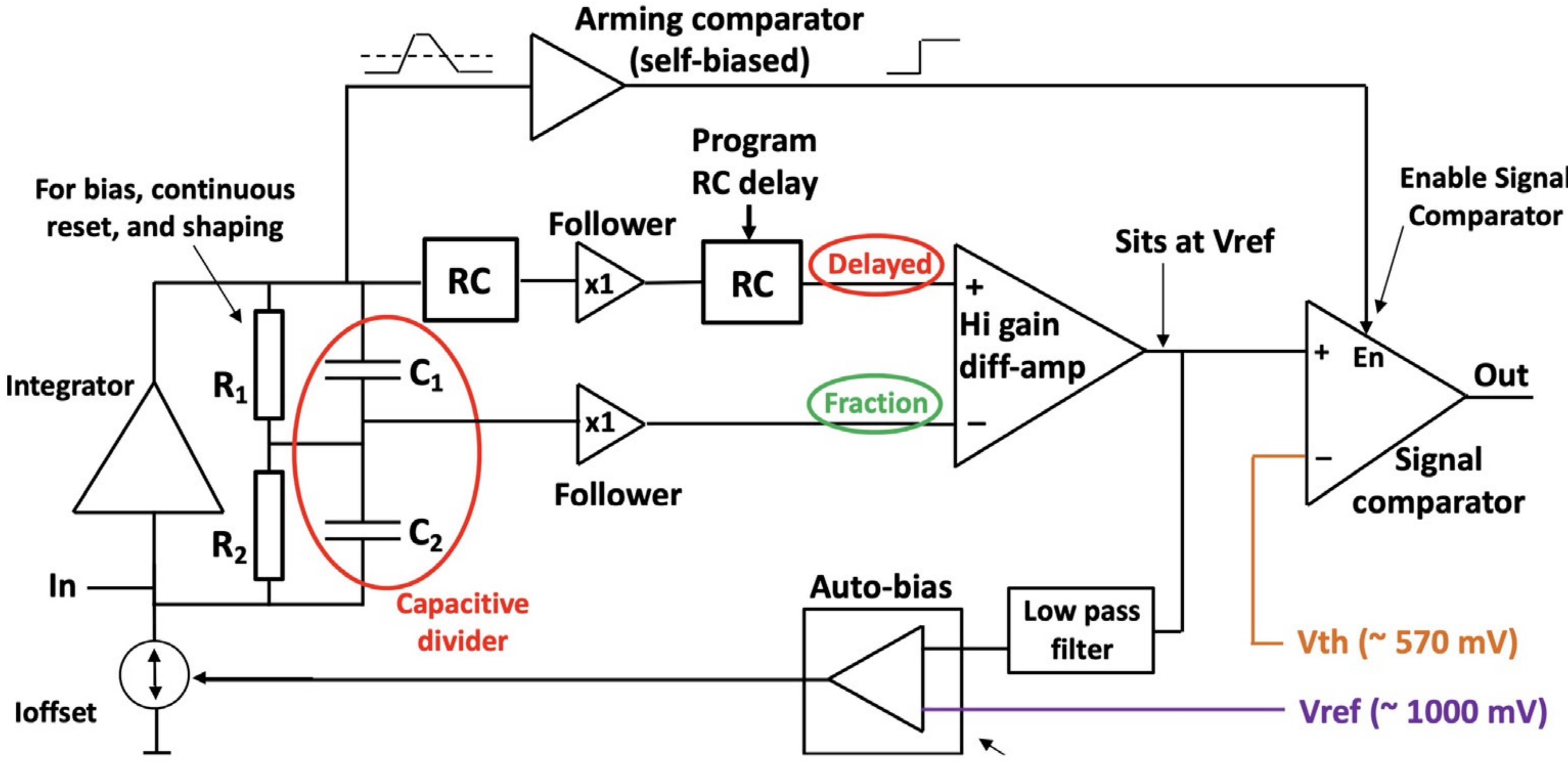

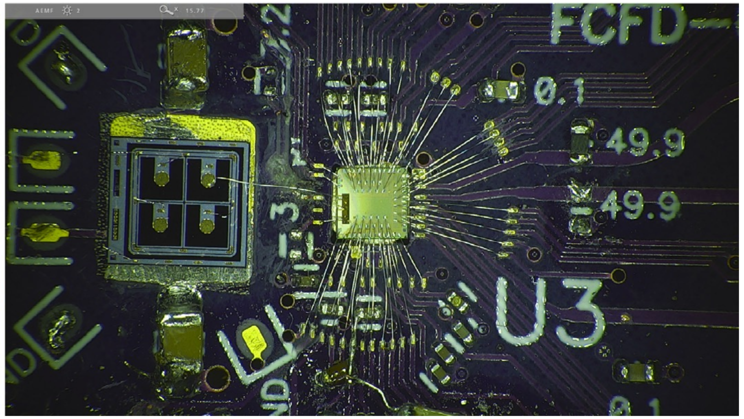

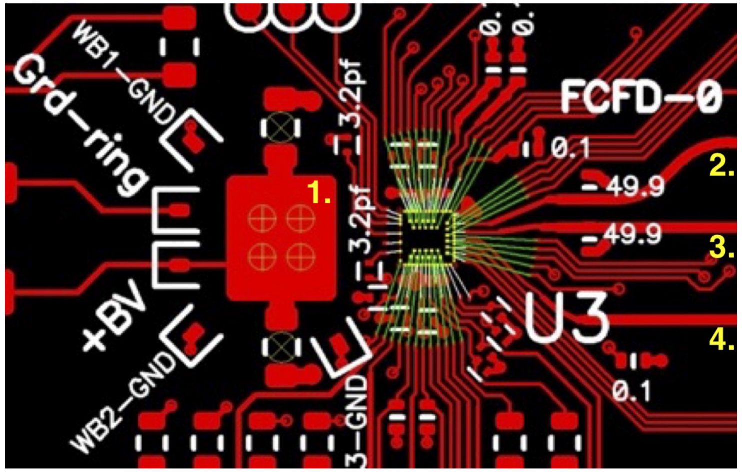

- A Constant Fraction Discriminator ASIC for LGAD detectors is being developed at Fermilab
- First version (FCFDv0) [4] with single channel analog frontend only has been extensively tested with internal charge injection, infrared laser, beta course, and 120 GeV protons.

FCFD+LGAD with 120 GeV Protons

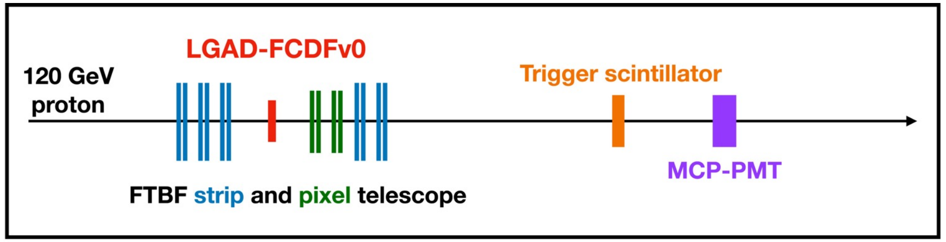

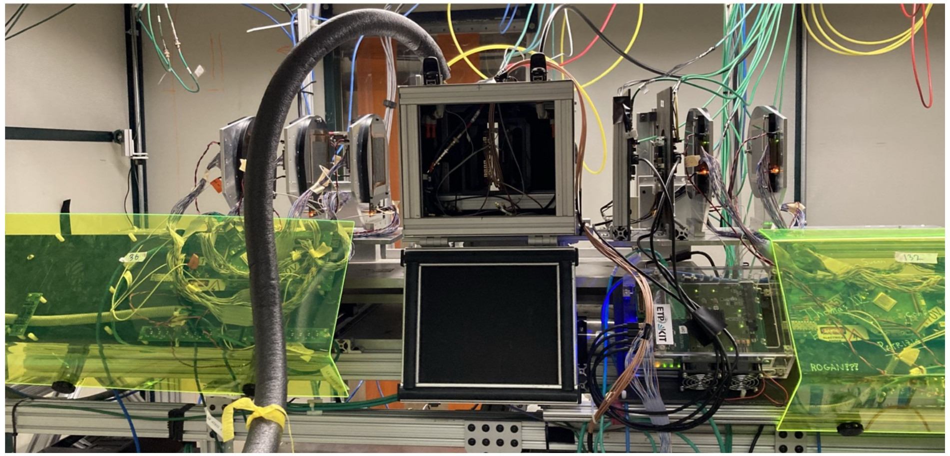

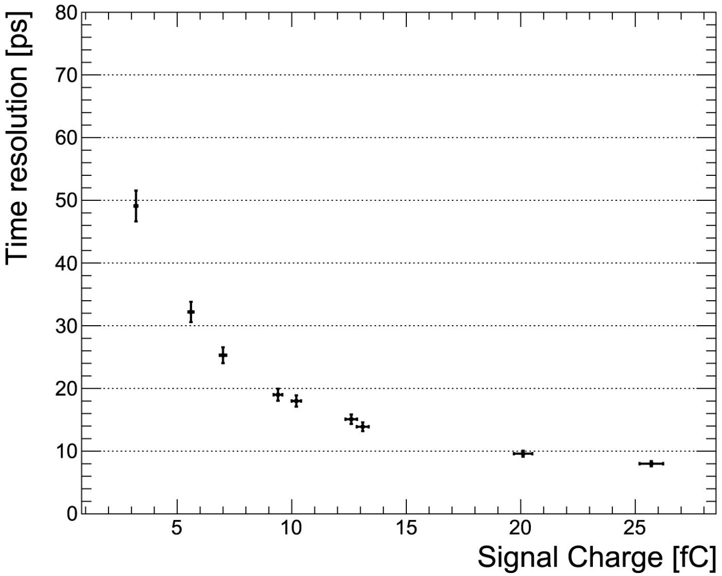

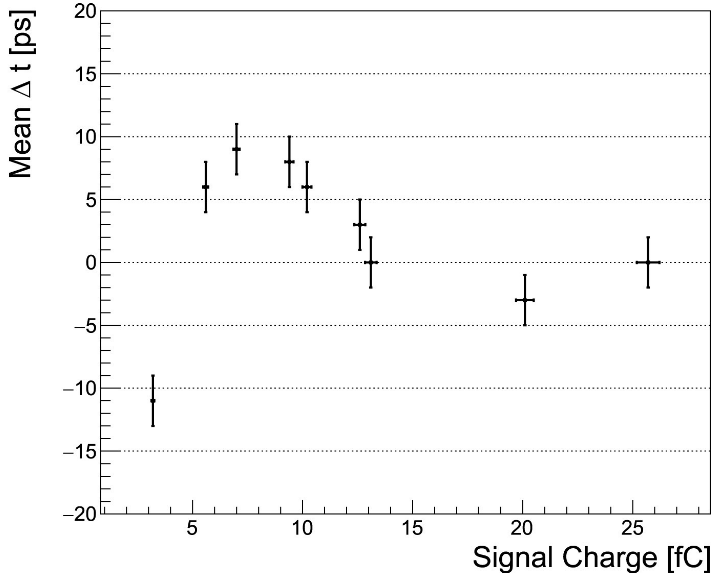

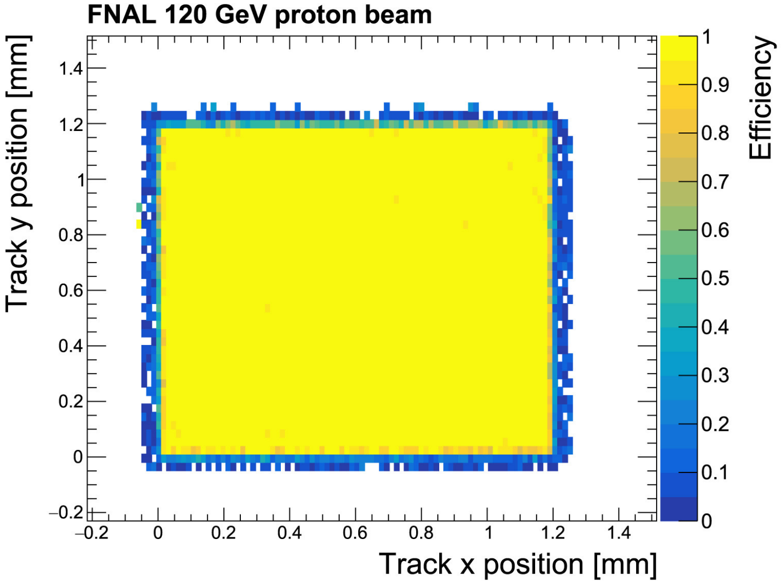

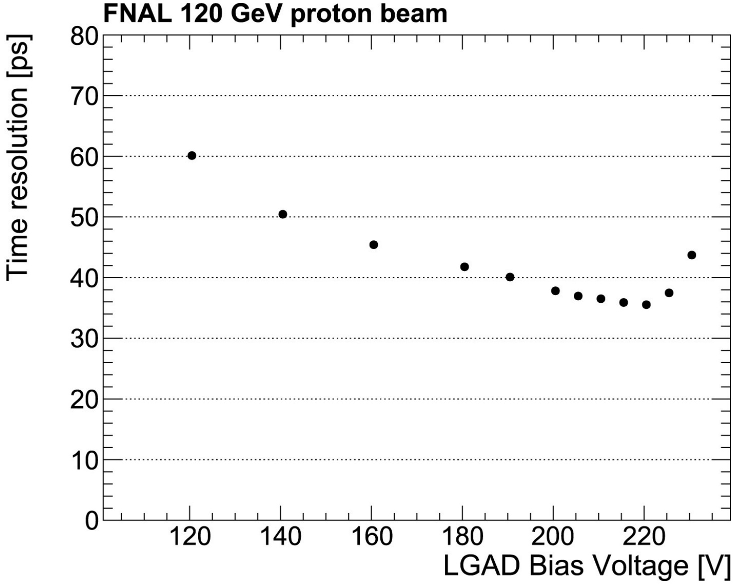

- Jitter is smaller than 20 ps for charge > 10 fC
- Mean TOA changes by less than +/-10 ps for 3-26 fC charge
- Timing resolution obtained with 120 GeV protons is around 35 ps, close to the best that the LGAD sensor provides

EIC Detector-1 Design: EM Calorimeters

EEMC

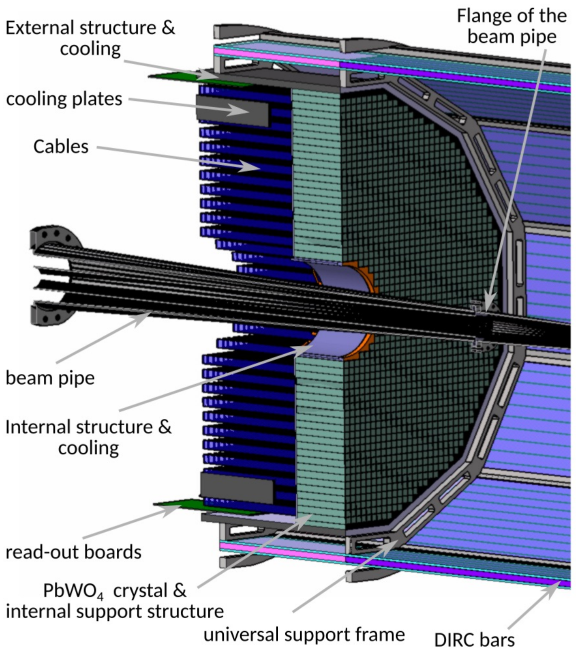

$1\%E \oplus 2.5\%/\sqrt{E} \oplus 1\%$

BEMC

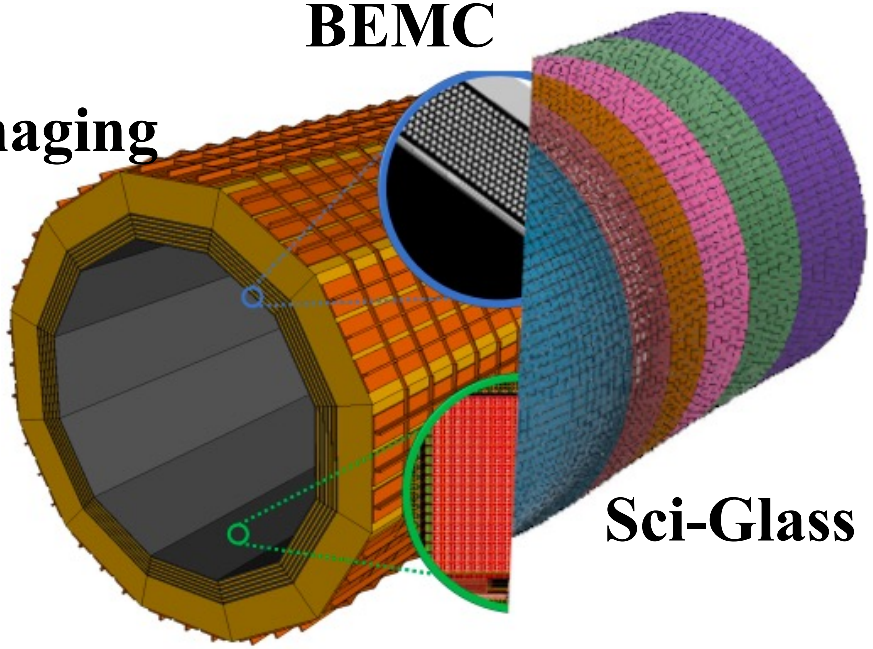

$2\%E \oplus 4-8\%/\sqrt{E} \oplus 2\%$

FEMC

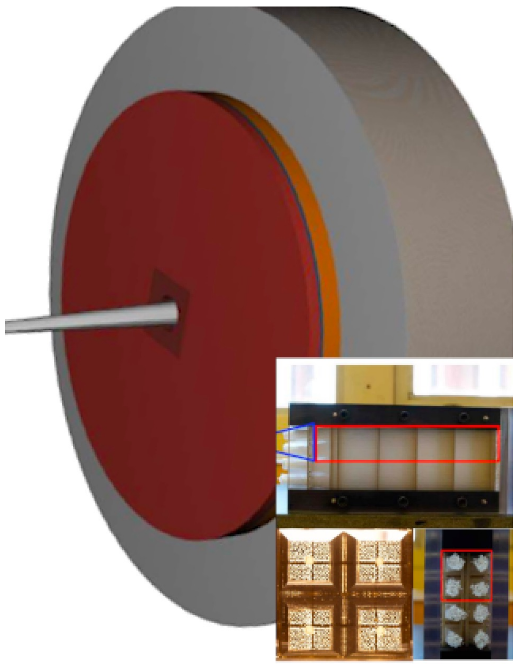

$2\%E \oplus 4-12\%/\sqrt{E} \oplus 2\%$

Endcap regions:

- **EEMC** - homogenous high resolution $PbWO_4$ crystal ECal
- **FEMC** - highly granular W-Scintilating Fiber calalorimeter

Barrel region - alternatives:

- **Sci-Glass:** homogenous, projective Sci-Glass ECal
- **Imaging:** 6 layers of 0.5x0.5mm Astro-Pix Silicon layers, interleaved with Pb-SciFi calorimeter

EIC Detector-1 Design: Hadronic Calorimeters

- Designed to complement tracking in Particle-Flow algorithm
- **OHCAL/IHCAL**
  - Fe/Scint sampling calorimeter
  - partial sPHENIX re-use & magnet flux return
- **LFHCAL**
  - Fe/Scint & W/Scint sampling calorimeter
  - Highly segmented (7 long. segments)
  - W-segment as colimator
- High granularity inserts under discussion for forward E&HCal
- Electron end-cap HCAL as neutral veto, shallow Fe/Scint calo

BHCAL

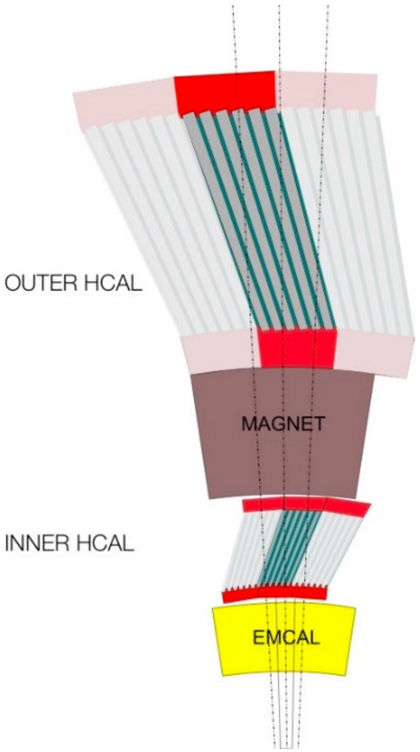

LFHCAL

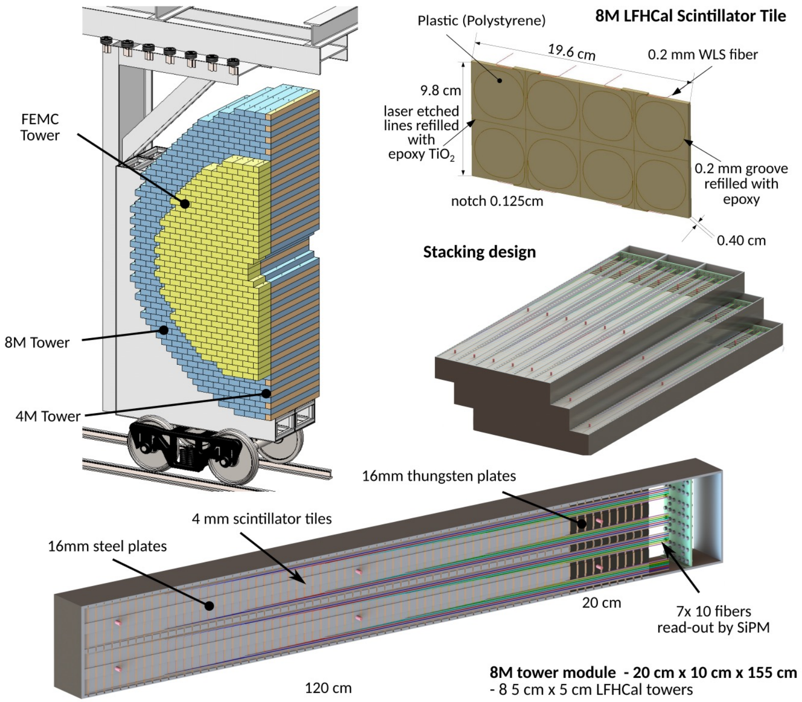

	Barrel HCal	LFHCAL
η	[-1 .. 1]	[1 .. 4]
σ_E/E	~75%/√E + 15%*	~33%/√E + 1.4%
depth	~4-5 λ_I	~7-8 λ_I

*Based on prototype beam tests and earlier experiments

EIC Detector-1 Design: Far-Forward Detectors

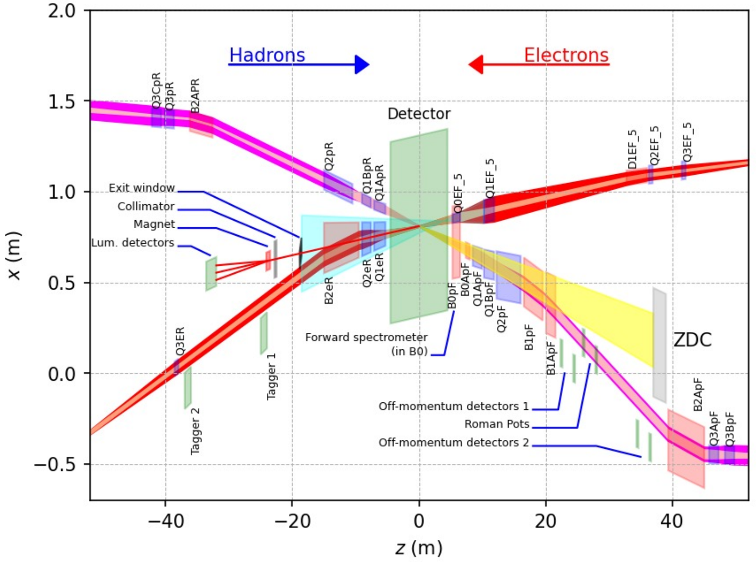

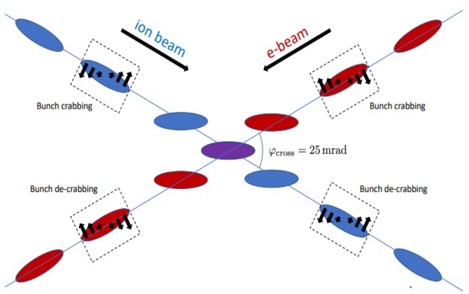

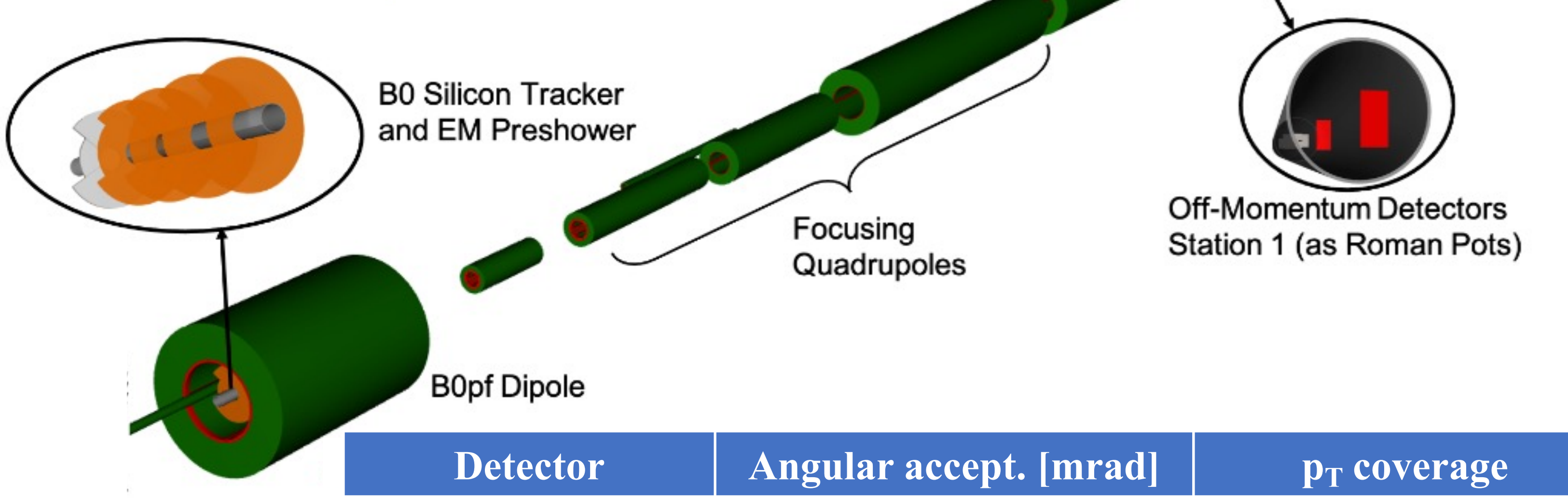

Technologies defined

- Silicon: AC-LGAD & MAPS
- ZDC:
  - ECAL (PbWO4)
  - HCAL (PbSi + PbScint)

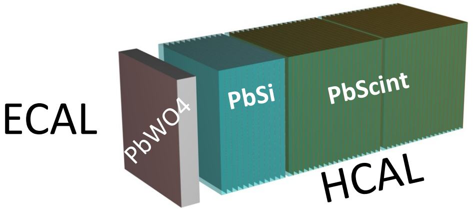

Detector	Angular accept. [mrad]	p_T coverage
ZDC @ ~30m	θ<5.5 ($\eta > 6$)	p_T<1.3 GeV
Roman Pots	0*<θ<5.0 ($\eta > 6$)	*Low p_T(t) cutoff (beam optics)
Off-Momentum Detectors	0.< θ < 5.0 ($\eta > 6$)	Low-rigidity particles from nuclear breakups
B0 forward spectrometer	$5.5 < \theta < 20.0$ (4.6< $\eta < 5.9$)	High p_T(t)

ePIC Collaboration

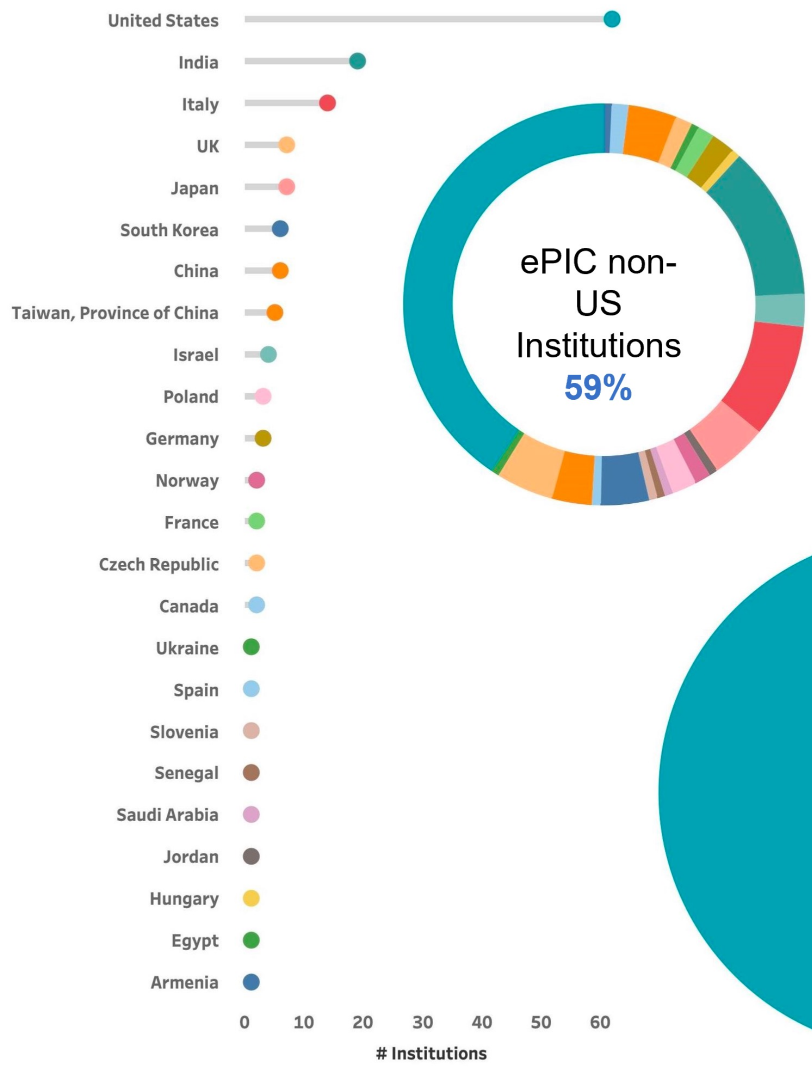

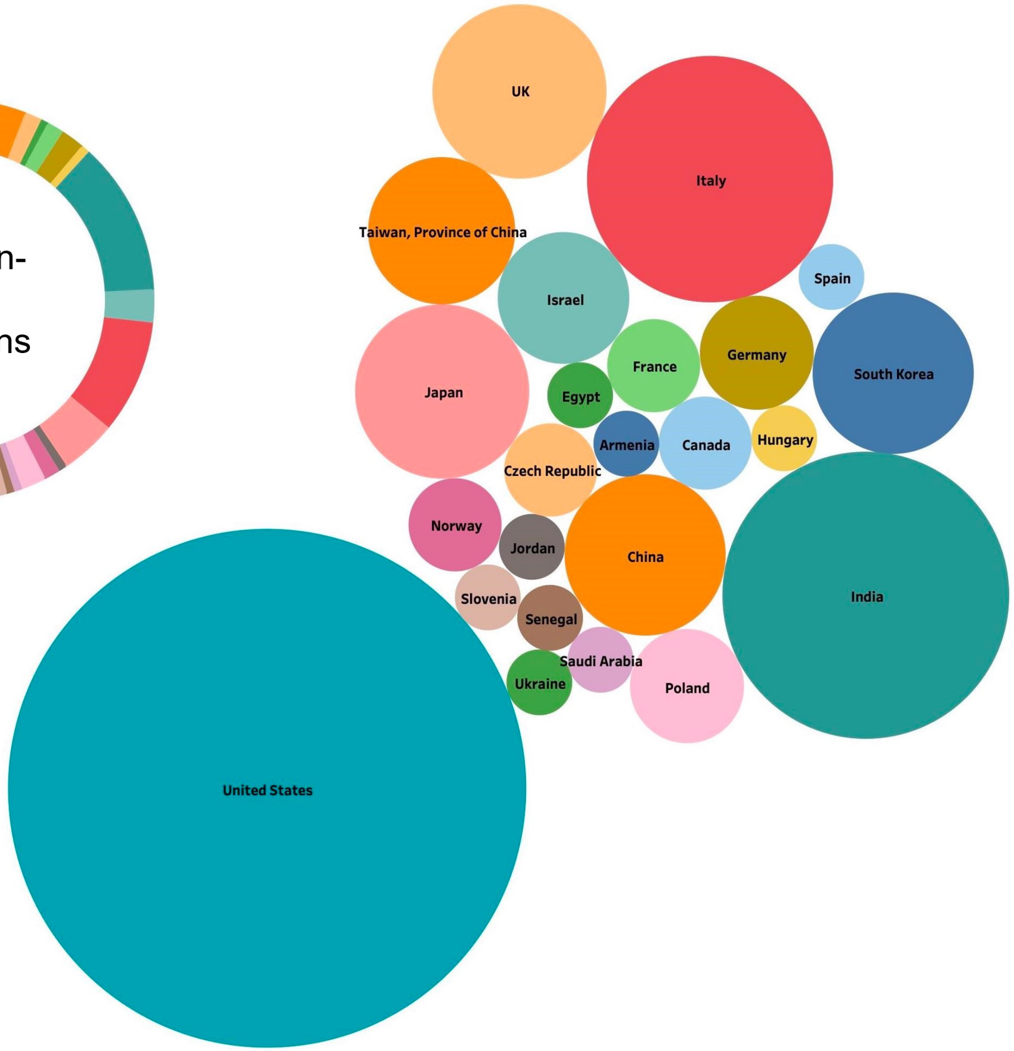

160+ institutions
24 countries

500+ participants

A truly international pursuit for a new experiment at the EIC!

EIC Schedule

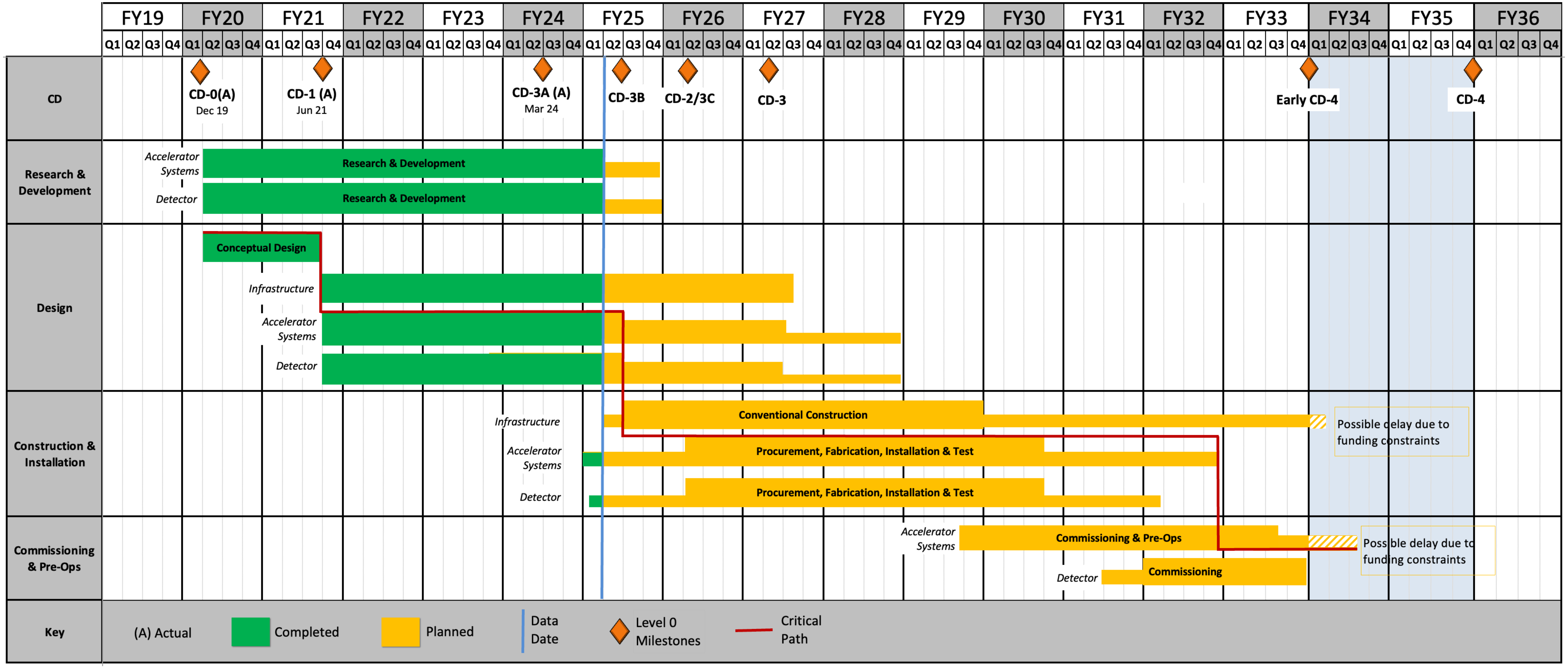

Critical Path is Accelerator Systems

Science operations start in roughly a decade

Some References

Particle Data Group Review Articles on Particle Detectors at Accelerators [link](#)

[1] Electron Ion Collider: The Next QCD Frontier - Understanding the glue that binds us all (2012), arXiv:1212.1701

[2] Reaching for the Horizon: The 2015 Long Range Plan for Nuclear Science (2015), link

[3] An Assessment of U.S.-based Electron-Ion Collider Science (2018), link

[4] Electron Ion Collider Conceptual Design Report (2021), link

[5] Science Requirements and Detector Concepts for the Electron-Ion Collider: EIC Yellow Report, link

[6] EIC Generic Detector R&D Proposals, link

[7] EIC Project Detector R&D Proposals, link

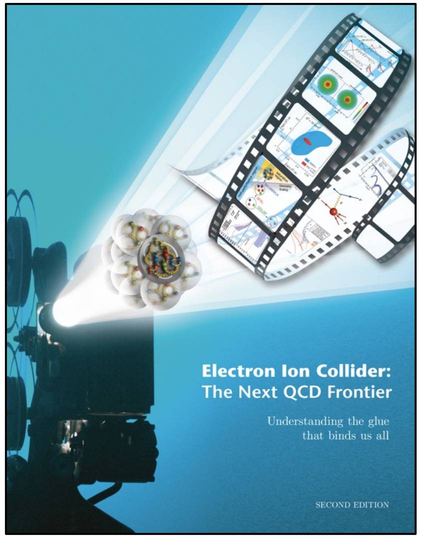

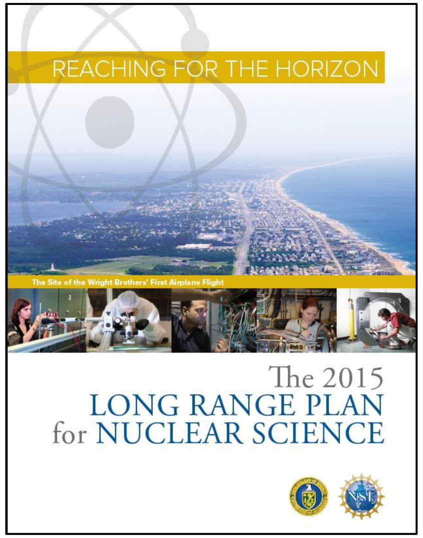

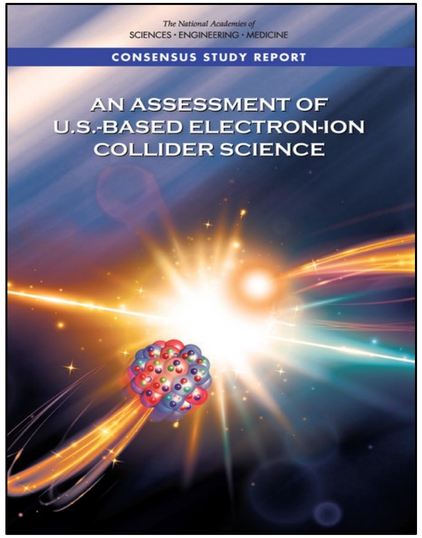

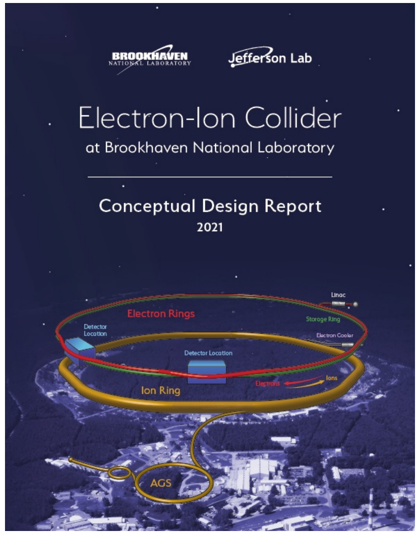

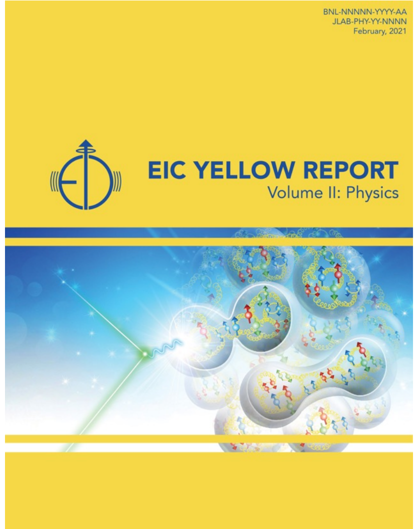

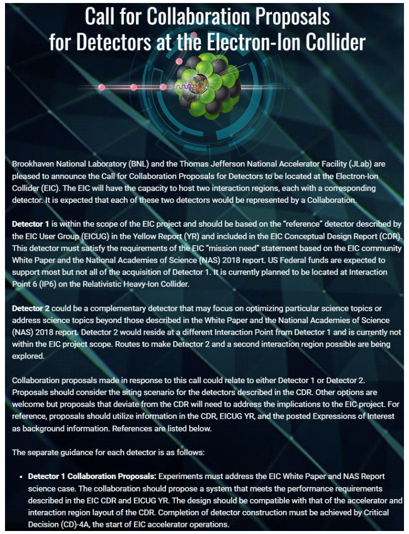

DVCS at Future Electron-Ion Colliders

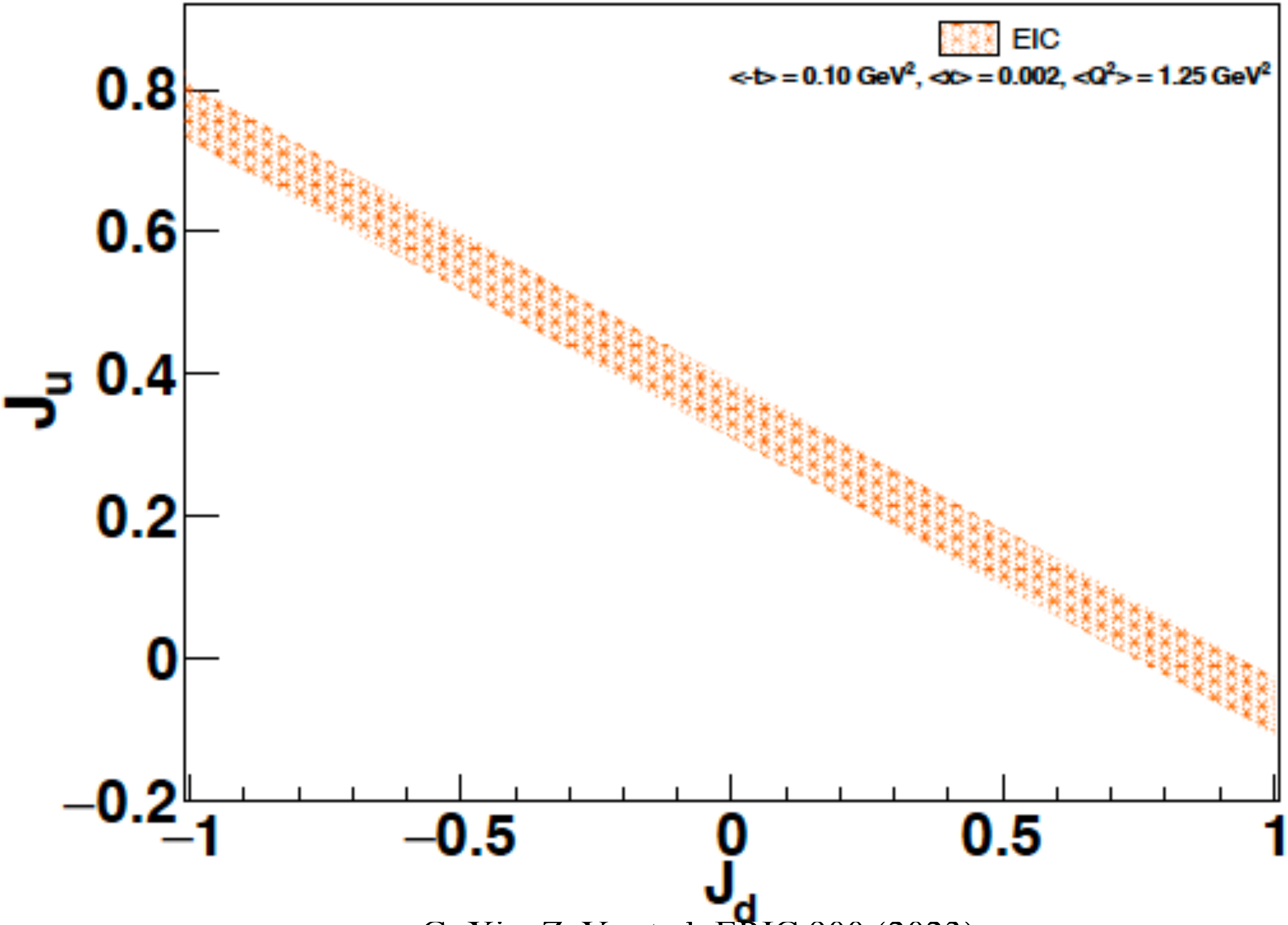

G. Xie, Z. Ye et al. EPJC 900 (2023)